Biological Conversion of Alkanes to Dicarboxylic Acids

An Investigation into Process Challenges and Optimisation in Hydrocarbon-based Bioprocesses

Peta Clair Williams

Half-thesis submitted towards fulfilment of the academic requirements for the degree of Masters of Science in Engineering in the Department of Chemical Engineering

University of Cape Town
February 2005

Abstract

The focus of this project is bioconversion of alkanes to dicarboxylic acids. Dicarboxylic acids are versatile chemical intermediates that can be used in the manufacture of perfumes, polymers, adhesives and antibiotics. The use of a hydrocarbon in a biological process, however, introduces several process challenges related to the nature of the substrate. Many of these challenges are common to all hydrocarbon fermentations, regardless of the product formed, and include flammability, volatility and inhibition of cell growth (notably at low carbon chain lengths), insolubility (notably at high carbon chain lengths) and mass transfer limitations, with respect to both oxygen and alkane substrate.

In particular, the provision of adequate oxygen transfer to the organism in hydrocarbon-based bioprocesses has been regarded as especially challenging because of the absence of oxygen in the hydrocarbon backbone. In contrast to carbohydrate-based bioprocesses in which the carbohydrate itself supplies about half of the oxygen, the metabolic requirement for oxygen in hydrocarbon-based bioprocesses has to be met entirely by the transfer of oxygen to the broth. This suggests a proportionately higher requirement for oxygen transfer under these conditions. Consequently, the oxygen transfer rate (OTR) has been mooted as a likely major process limitation, leading to a process which is transport, rather than kinetically controlled and correspondingly, a sub-optimal yield and productivity.

This thesis reviews and establishes suitable media and methods for the biological production of dicarboxylic acid from alkanes. Small scale shake flask experiments were performed to confirm that *Candida tropicalis* ATCC 20962 can be used to convert C_{12} *n*-alkane to C_{12} dicarboxylic acid. Glucose is a suitable co-substrate for the completion of the respiratory cycle of the organism, and should be added in excess of the metabolic requirements of the organism while cells grown with organic nitrogen in the form of peptone give the most sustainable dicarboxylic acid production. Poor alkane miscibility in aqueous fermentation media results in non-uniform medium composition and difficulty in obtaining representative results for process evaluation. The effect of pH on dicarboxylic acid production is also very pronounced and the medium must be maintained under alkaline conditions in order to promote acid production. Adequate mechanical or chemical dispersion techniques are required to avoid mass transfer limitation which can potentially affect oxygen transfer to the cells for growth and availability of alkane substrate for dicarboxylic acid production.

This thesis then goes on to quantify the dependence of OTR on process conditions in a cell-free system, with a view towards characterising mixing and dispersion behaviour of alkane in sparged aqueous systems and quantifying the optimum agitation and aeration rates that could be used in the biological production of dicarboxylic acids from alkanes to maximise OTR, and minimise miscibility problems and mechanical damage to cells.

Process conditions were varied at agitation rates from 200 to 1200 rpm, aeration rates from 0.5 to 1.5 vvm and alkane concentrations from 0 to 20 (v/v) % and their effect on OTR quantified through their influence on overall volumetric mass transfer coefficient (K_La) and oxygen saturation concentration (C^*).

K_La variation with alkane concentration up to 20% (v/v) was markedly different at different agitation rates. Comparatively little improvement was effected through an increase in the aeration rate across the range 0.5 to 1.5 vvm in this system when compared with that through an increase in the agitation rate across the range 200 to 1000 rpm. The greater effect of agitation when compared with aeration suggests that agitation rate is the controlling parameter for enhancement of an inadequate K_La, in both carbohydrate- and hydrocarbon-based bioprocesses. In addition, for each agitation rate employed, the results revealed a threshold aeration rate above which a further increase in aeration had a negligible effect on K_La. In general, at agitation rates below 800rpm, K_La was repressed below that of water at all alkane concentrations, while at higher agitation rates, the K_La increased initially with alkane addition, and then decreased. The optimum K_La occurred at an agitation rate of 1000 to 1200rpm an aeration rate of 1.25vvm and an alkane concentration of 5 to 10%. It is postulated that the peak in K_La results from competing influences of an increased oxygen diffusion resulting from alkane droplets acting as active oxygen transfer intermediates and an inhibition of convective oxygen transfer due to increased liquid viscosity.

The calculated increase in oxygen solubility in the liquid with increased alkane concentration resulted in a predicted increase in OTR at higher agitation rates, when compared with OTR in water at similar conditions. This will even occur under conditions where K_La depression is reported. This indicates that the maximum OTR could be reached at the same agitation and aeration rates as for maximum K_La, but with an alkane concentration of 15 to 20%. Hence, under conditions where the oxygen demand for cell growth is not satisfied, the

OTR could be increased by alkane addition to introduce more oxygen into the medium provided substrate inhibition is not induced. In addition, these optimum agitation and aeration rates would be the most suitable conditions to adequately disperse alkane to enhance the availability of substrate for the production of dicarboxylic acid.

Acknowledgements

To my supervisors for their guidance and advice:
Prof STL Harrison – University of Cape Town
Dr KG Clarke – University of Stellenbosch
Prof MS Smit – University of the Free State

To my parents for their unfailing support
To my brother, Ainsley, for looking out for me and for his technical and artistic contributions
To Andrew "Buggylugs" Markham for knowing how to talk nicely to MS-Word
To Madelyn Johnson-Robertson, Ryan Stevenson, Balasundarum, Bergert Blom, Masego Mogoro and all the other post-graduate students at the University of Cape Town and University of the Free State who made my time in the laboratory so much more bearable
To Helen Divey, Joachim Macke, Martin Williams and Marc Wust for their technical support
To Sue Jobson, Jill Stevenson and Nelli Dili - the administration staff whose contribution is so often overlooked
To Dr Roelof Coetzer of Sasol Technology for assistance with the statistical analysis
To Laura Gentile and Tessa Mackay for the food and friendship
To David Mackay for helping with the proof-reading
To "Julle by Lisanore" for the laughs
To Steven Kuo for the emotional support and philosophical debates
To Mathew Price for always turning up just when I needed him
To David Phillips for his care and patience
To my colleagues at Sasol Technology Process Development who kept hounding me to "hurry up and finish and buy a mountain bike"
To Liam for the chocolate donuts and use of his couch
And to Maverick the Chundercat for getting me out of bed when I thought I was too ill to carry on

This project was made possible by funding from Sasol (Pty) Ltd, the University of Cape Town SA College Croll Scholarship and the Department of Chemical Engineering

Table of Contents

List of Figures

List of Tables

Nomenclature

Abbreviations

DNS	glucose assay using Dinitrosalicylic acid
GC	gas chromatograph(y)
nC_i	n-alkane with i number of carbons
OTR	oxygen transfer rate
OUR	oxygen utilisation rate
syngas	synthesis gas
UFS	University of the Free State
YNB	yeast nitrogen base

Roman Symbols

A	area of plane over which diffusion/ mass transfer occurs [m^2]
a	gas-liquid interfacial area per unit volume
C_i	concentration of species i [mg/l]
C^*	saturation concentration [mg/l]
D_{AB}	mutual diffusivity of species A in species B [m^2/s]
f_i	volumetric fraction of component i
H	Henry's law constant [$atm.m^3/kg$]
J_i	flux of species i [$g/m^2.s$]
K_i	local mass transfer coefficient for phase i [m/s]
k_i	local mass transfer coefficient for phase i [m/s]
M	molecular mass [g/mol]
m	distribution factor
N	agitation [rpm]
n_i	rate of diffusion of species i [g/s]
P	pressure [Pa]
p	partial pressure [Pa]
P/V	stirrer power per liquid volume [W/m^3]
Q	volumetric gas flow rate [m^3/s]
R	universal gas constant [8.314 J/mol.K]
S	spread coefficient [N/m]
T	temperature [K]
u	superficial gas velocity [m/s]
V	fermenter volume [m^3]
X	volume fraction of alkane
y_i	gas mol fraction of component i
z	distance over which concentration gradient exists [m].

Subscripts

G/g	gas
L/l	liquid
o	oil
w	water

Greek Symbols

δ	characteristic length over which mass transfer occurs [m]
γ	surface tension [N/m]
μ	viscosity [Pa.s]
τ	probe response time [s]

1. Introduction

Successful biotechnology ventures for the production of commodity products and fine chemicals rely on an efficient process based on the availability and suitability of a cheap feedstock as well as a suitable organism. Aliphatic hydrocarbons initially became of interest as a feedstock in the early 1960's when the production of single-cell protein from hydrocarbons was proposed as an alternative food source (Rehm, 1986). Linear hydrocarbons are fast becoming a more plentiful feedstock with the expansion of gas-to-liquid and coal-to-liquid fuels technology as an alternative to crude refining. This represents a potentially increased range of substrates available for bioconversion, including odd-numbered carbons as derived from "syngas" via Fischer-Tropsch synthesis. An extensive pool of bacteria and fungi (Fukui and Tanaka, 1980; Shennan and Levi, 1974) are able to covert hydrocarbons to a considerable variety of complex value added fine chemicals and versatile chemical intermediates including amino acids, organic acids, carbohydrates, lipids, nucleic acids, vitamins, enzymes, co-enzymes and antibiotics (Fukui and Tanaka, 1980). More recently, the production of polyhydroxyalkanoates (Jung *et al.*, 2001; Kessler and Witholt, 1999; Preusting *et al.*, 1993), biosurfactants (Kosaric, 1996) and dioic acids (Chan *et al.*, 1997a, b) from alkanes has been the focus of much attention.

The focus of this project is bioconversion of alkanes to dicarboxylic acids. Dicarboxylic acids are versatile chemical intermediates that can be used in the manufacture of perfumes, polymers, adhesives and antibiotics. Most chemical methods for producing dicarboxylic acid result in mixtures of shorter chain lengths, which are less valuable. A biological process will allow longer chain dicarboxylic acids and dicarboxylic acids with an odd number of carbon atoms to be produced, as these molecules generally retain the same number of carbon atoms as the alkane feed. This is difficult with chemical processes and could afford new market opportunities. This project will evaluate the production of specifically C_{12} to C_{13} dioic acids from a C_{12} to C_{13} alkane mixture.

The use of a hydrocarbon in a microbiological process, however, introduces several process challenges related to the nature of the substrate. Many of these challenges are common to all hydrocarbon fermentations, regardless of the product formed. They include flammability, volatility and inhibition of cell growth (notably at low carbon chain lengths), insolubility (notably at high carbon chain lengths) and mass transfer limitations, with respect to both oxygen and substrate.

In particular, the provision of adequate oxygen transfer to the micro organism in hydrocarbon-based bioprocesses has been regarded as especially challenging because of the absence of oxygen in the hydrocarbon backbone. In carbohydrate-based bioprocesses the carbohydrate itself supplies about half of the oxygen (Shennan and Levi, 1974), in hydrocarbon-based bioprocesses the metabolic requirement for oxygen has to be met entirely by the transfer of molecular oxygen from the gas phase, suggesting a proportionately higher requirement for oxygen transfer under these conditions. This increased requirement has been confirmed both stoichiometrically where, for example, it has been shown that an approximately 3-fold increase in oxygen is required during growth of yeast on hydrocarbon relative to growth on carbohydrate (Darlington, 1964; Moo-Young, 1975) and experimentally, where a 2,9-fold increase in oxygen was required during yeast growth on hydrocarbon (Shennan and Levi 1974). Consequently, the oxygen transfer rate (OTR) has been mooted as a likely major process limitation, leading to a process which is transport-, rather than kinetically-, controlled and correspondingly, a sub-optimal yield and productivity.

In view of the importance of an adequate OTR in the optimisation of the hydrocarbon-based bioprocess, this work focuses on the quantification of OTR through the evaluation of the overall mass transfer coefficient (K_La) and saturation oxygen concentration (C^*) in an air-water and an air-water-alkane system. While the values of K_La and C^* generated will be different from those in a growth medium and, will depend on the reactor design and operating conditions, the trends in these values will be comparable to those in a bioprocess. Thus this system provides a convenient generic base for the evaluation of K_La and C^*, their corresponding influence on the OTR in hydrocarbon-based bioprocesses and the establishment of conditions for optimum operation of bioprocesses based on a hydrocarbon feedstock.

The aims of this project are therefore to address and quantify the following phenomena:

- Establishment of suitable media and methods for the biological production of dicarboxylic acid from alkanes using the yeast *Candida tropicalis* ATCC 20962.
- Mass transfer limitations between immiscible hydrocarbon and aqueous phases
- Increased oxygen demand for fermentation due to the absence of oxygen in alkane structure

- Establishment of optimum process conditions in terms of mass transfer or oxygen limitations in order maximise dicarboxylic acid production, while not incurring inhibition of cell growth by alkane substrate or dicarboxylic acid product.

The work commences with Chapter 2 reviewing the relevant theory relating to dicarboxylic acid production and mass transfer considerations in systems of up to four phases, vapour-liquid-liquid-solid. In Chapter 3, more practical literature on methods for dicarboxylic acid production, quantitative analysis of fermentation data and analysis of mass transfer is summarised. Chapter 4 outlines the experimental methods selected to complete this work. Chapter 5 details the results of experiments performed with live yeast to product dicarboxylic acid from alkane. Chapter 6 investigates mass transfer considerations in systems with immiscible liquid phases, and their relevance to hydrocarbon bioprocess. Finally, conclusions on the work performed and recommendations for further work are formulated.

2. Literature Review

The scope of this review is to assess key issues to gain understanding of the biological production of dicarboxylic acids and the process challenges relating to achieving optimum yield and productivity of the process. A discussion on the types of microorganisms required and a summary of their metabolism is included. Different alkane substrates and carbohydrate co-substrates are investigated, as is the effect of nutrients and oxygen supply on the productivity of the process.

As outlined in Chapter 1, C_{12} to C_{13} dioic acids have been identified as products of interest to be produced from a C_{12} to C_{13} alkane mixture. Literature addressing the biological production of C_{12} and C_{13} dioic acids is very limited. A substantial proportion of the literature available concerns the production of C_{16} dioic acid compounds from C_{16} alkane. The kinetic data for C_{16}-based biological processes must be utilised with caution, as it may not be directly applicable to a process using C_{12} and C_{13} compounds, however, some general trends are expected to be similar. Also, a genetically modified form of *Candida tropicalis* ATCC 20962 will be used for this project to produce the required dicarboxylic acids from alkanes. This means that the exact microorganisms discussed in literature will be different. However, it is envisaged that similar trends will be observed and that the data presented can be a useful tool in the understanding and eventual optimisation of long-chain dicarboxylic acid production.

The literature in the field of oxygen transfer in a biological process containing immiscible liquid phases details the use of many oil and hydrocarbon compounds as substrates for hydrocarbon-assimilating microorganisms, or as oxygen vectors for non-hydrocarbon-assimilating microorganisms. In order to benefit from the data from these sources, the hydrocarbon or oil phases must be compared on the basis of physical or transport properties, rather than chemical reaction properties. This may prove difficult, as physical data for hydrocarbons is often scarce or inconsistent. The differences between the types of organisms present must also be taken into account.

2.1 Production and Commercial Application of Dioic Acids

For over 30 years, there has been interest in research concerning value addition to alkanes via biological processes. The potential products include cell protein, lipids, co-enzymes, vitamins, antibiotics, nucleic acids, amino acids or dicarboxylic acids (Fukui and Tanaka, 1980). Dicarboxylic acids are versatile chemical intermediates that can be used in the manufacture of perfumes, polymers and adhesives (Stephen, 1991). Green *et al.* (2000) describes some uses for specific dicarboxylic acids and their salts and esters:

- Azelaic acid (C_9 dioic) is used in antibiotics for the treatment of acne. Lithium and aluminium azelate are lubricants, while alkaline or ammonium azelate salts are used in antifreeze.
- Sebacic acid (C_{10} dioic) is a component in nylon, and its dibutyl ester is used in the manufacture of food-grade plastics.
- Ethylene brassylate (C_{13} dioic) is used in perfumes.

C_9 to C_{12} dioic acids are already being produced on a large scale via chemical routes (Kirk Othmer, 1998). Dioic acids are, not usually manufactured chemically with alkane as starting material, due to the many stages and intermediates required. The starting material for the chemical production of many dioic acids consists of fatty acids that are readily available from plant or animal sources, or other petrochemical sources such as olefins or cyclic hydrocarbons. Kirk Othmer (1998) describes some processes for dioic acid production:

- Azelaic acid (C_9 dioic) is produced by ozonolysis of oleic acid (C_{18} mono-acid), with pelargonic acid (C_9 mono-acid) as a by-product.
- Sebacic acid (C_{10} dioic) is commonly produced by oxidation of castor oil or ricinoleic acid under alkaline conditions. This gives disodium sebacate and octanol or capryl (C_8 monoacid) alcohol. Disodium sebacate is then acidified to sebacic acid.
- Dodecanedioic acid (C_{12}) is produced from butadiene, with cyclododecatriene as an intermediate.
- Brassylic acid (C_{13} dioic) is usually produced via a biological process with tridecane as substrate.

As listed above, brassylic acid is already produced commercially from alkane via a biological process. It is possible to produce dioic acids of other chain-lengths in a bioprocess, provided that the appropriate alkane feedstock is

available (Uchio and Shiio, 1972a). In general, alkanes can be converted to useful products via chemical processes, but biological processes are often the preferred routes as reaction conditions are less harsh. In a chemical process, high temperatures and pressures are required to activate the hydrocarbon backbone. Selectivity and use of an appropriate catalyst is also an important concern. In comparison, biological processes are usually carried out at temperatures and pressures close to atmospheric conditions. The question to be answered is whether these biological routes to dioic acids are economically competitive with the chemical routes. This will depend on the existence of a suitable microorganism, and on optimisation of process conditions.

2.2 Hydrocarbon Assimilating Organisms

There are many kinds of microorganisms that are capable of producing dioic acids from alkanes. Chan *et al.* (1997a&b) used bacterial cells in the form of *Pseudomonas aeruginosa* and *Cryptococcus neoformans*. *Candida* and *Yarrowia* are well-known for their ability to grow on n-alkanes (Mauersberger *et al.*, 1996). However, dioic acids, which are the desired product in this case, are merely an intermediate in the degradation of n-alkanes by yeast. Most wild strains of yeast will break down dioic acids and not accumulate them sufficiently. Therefore, a mutant or genetically modified organism that is unable to assimilate dioic acids is required.

Wang *et al.* (1999) created a modified form of *Yarrowia lypolytica*. A sample of this yeast was obtained for preliminary experiments, but due to patent reasons, this yeast was not available to complete the project. Therefore, the yeasts of most interest to this project are *Candida*, as they are more readily available.

Candida maltosa, C. cloacae and *C. tropicalis* are generally considered to be amongst the best hydrocarbon (and alkane) assimilating yeasts in the genus *Candida* (Bos and de Bruyn, 1973). *C. maltosa* and *C. cloacae* were originally considered to be separate species, but more recent literature generally acknowledges that *C. cloacae, C. subtropicalis* and *C. novellus* are all synonyms for *C. maltosa*, while *C. tropicalis* is considered a separate species.

Uchio and Shiio (1972a) isolated *Candida cloacae* 310 as an example of a naturally sourced yeast than can produce dioic acids. It was noted from their experiments that the major dioic acid products accumulated had the same number of carbon atoms as the alkane substrates (with less than 15 carbon atoms) used. However, the dioic acids with 5 to 9 atoms were best accumulated as dioic acid degeneration occurred, forming dioic acid products with fewer carbon atoms than the alkane substrate used. In general, the rate of dioic acid degradation appeared to be greater for longer chains. This implies that longer chains are more difficult to manufacture with a wild-type microorganism. The most valuable dioic acids, especially those that can be used in polymer manufacture have 9 to 16 carbon atoms.

Uchio and Shiio (1972 a, b & c) therefore isolated mutants, M-1 and M-12, from *Candida cloacae* 310 to investigate improving dioic acid production, mostly of tetradecane 1,14-dicarboxylic acid (C16 dioic acid) from n-hexadecane. According to the data presented, these mutants did increase dioic acid productivity. The yeast used in this project, *Candida tropicalis* ATCC 20962, was developed by Picataggio *et al.* (1992) and tested using tridecane to product C_{13} dioic acid.

2.3 Metabolism of Hydrocarbon Assimilating Yeasts

2.3.1 Bioconversion of alkane to dioic acid

Figure 2.1 shows the diagrammatic representation of the metabolism of alkane-assimilating yeasts of the *Candida* species. Blasig *et al.* (1988) isolated some of the intermediates in the process by which alkanes are degraded by *Candida maltosa*, to characterise this pathway in more detail. *Candida maltosa* is considered to utilise long-chain alkanes mainly via monoterminal degradation. The first step in the process consists of hydroxylation of an n-alkane to a fatty alcohol catalysed by a mono-oxygenase system consisting of a cytochrome P450 and NADPH-dependent cytochrome P450 reductase, localised in the microsomal membrane fraction. The reaction requires $NADPH_2$ and O_2 in order to proceed, but is inhibited by CO.

The following stage in the alkane degradation pathway is the oxidation of the alcohol to a fatty aldehyde. This is catalysed by a fatty alcohol oxidase (FOAD) enzyme (Mauersberger *et al.*, 1996) instead of NAD(P)-dependent fatty alcohol dehydrogenase (FADH), as assumed in earlier literature. Blasig *et al.* (1988) confirms this and states that the oxidation of 1 mol of alcohol was accompanied by the use of 1 mol O_2 and the production of 1 mol H_2O_2. This is because molecular oxygen is the electron acceptor and NAD is not required for this step.

The next step, oxidation of fatty aldehydes into fatty acids, is catalysed by a membrane bound NAD-dependent dehydrogenase (FALDH) reaction (Mauersberger *et al.*, 1996). Blasig *et al.* (1988) noted that there was no O_2 consumption or H_2O_2 production in this step and concluded that fatty aldehyde dehydrogenase (FALDH) activity should catalyse this reaction.

These fatty acids can be degraded to acetyl CoA by β-oxidation as described by Fukui and Tanaka (1981). Some propionyl CoA would also be formed in the case of odd carbon numbered substrates. Alternatively, a second P450 system is involved in the ω-hydroxylation of fatty acids as the first step in diterminal oxidation to form dioic acids (Mauersberger *et al.*, 1996). Blasig *et al.* (1988) noted that this reaction was inhibited by CO and therefore that the process must be catalysed by a cytochrome P450 enzyme system. These dioic acids could then also be degraded by β-oxidation to shorter chain dioic acids and eventually acetyl CoA, which is undesired in this case.

There is however some debate around the mechanism of diterminal oxidation. Blasig *et al.* (1988) and Scheller *et al.* (1998) detected traces of 1,ω-diol. This means that the diterminal attack could occur already on the primary alcohol, and not just on the fatty acid. Scheller *et al.* (1998) found that the alternative pathway then consisted of cytochrome P450 catalysed oxidation of the 1,ω-diol to the ω-hydroxy fatty acid.

Diterminal oxidation proceeded as a minor reaction for Blasig *et al.* (1988). This is in agreement with Mauersberger *et al.* (1996) who stated that this pathway is not achieved to any remarkable extent in growing cells. However, in some mutants this diterminal oxidation can become the main pathway, thereby facilitating the industrial production of long-chain dicarboxylic acids.

This further confirms the need to utilise a genetically modified organism to induce diterminal oxidation and inhibit β-oxidation.

Most literature reports the products formed to have the same number of carbon atoms as the alkane source initially used. Also, the oxidation takes place on the terminal carbons. When alkane utilization is diverted to dicarboxylic acid production, a co-substrate is required to produce ATP. Uchio and Shiio (1972a) found that the growth rate of *Candida cloacae* M1 cells on alkane decreased notably in comparison to that of the wild type. These mutants were specifically isolated for the inability to assimilate n-alkane. This shows the necessity of a co-substrate for growth. These authors therefore compared the performance of different co-substrates. Adequate dioic acid production was obtained for strain M1 using sucrose and sorbitol as carbon source for growth. The highest rate of C_{16} dioic acid production was obtained when acetate was used as the carbon source for growth. Glucose, while producing adequate cell growth, appeared to inhibit C_{16} dioic acid production.

Various other co-substrates are described in the literature, but little further information was found on the use of different co-substrates for dioic acid production under the same conditions. Hill *et al.* (1986) used glycerol as a co-substrate for *Candida tropicalis* S76, isolated by Yi and Rehm (1982), while Jiao *et* al. (2001) used sucrose for *Candida tropicalis* CT1-12 (Tsinghua University, China). Picataggio *et al.* (1992) engineered the yeast *Candida tropicalis* ATCC 20962 and used glucose as co-substrate to produce dioic acids from alkanes. The effect of co-substrate (and hence fermentation medium) choice on dioic acid productivity is therefore an area that requires some investigation.

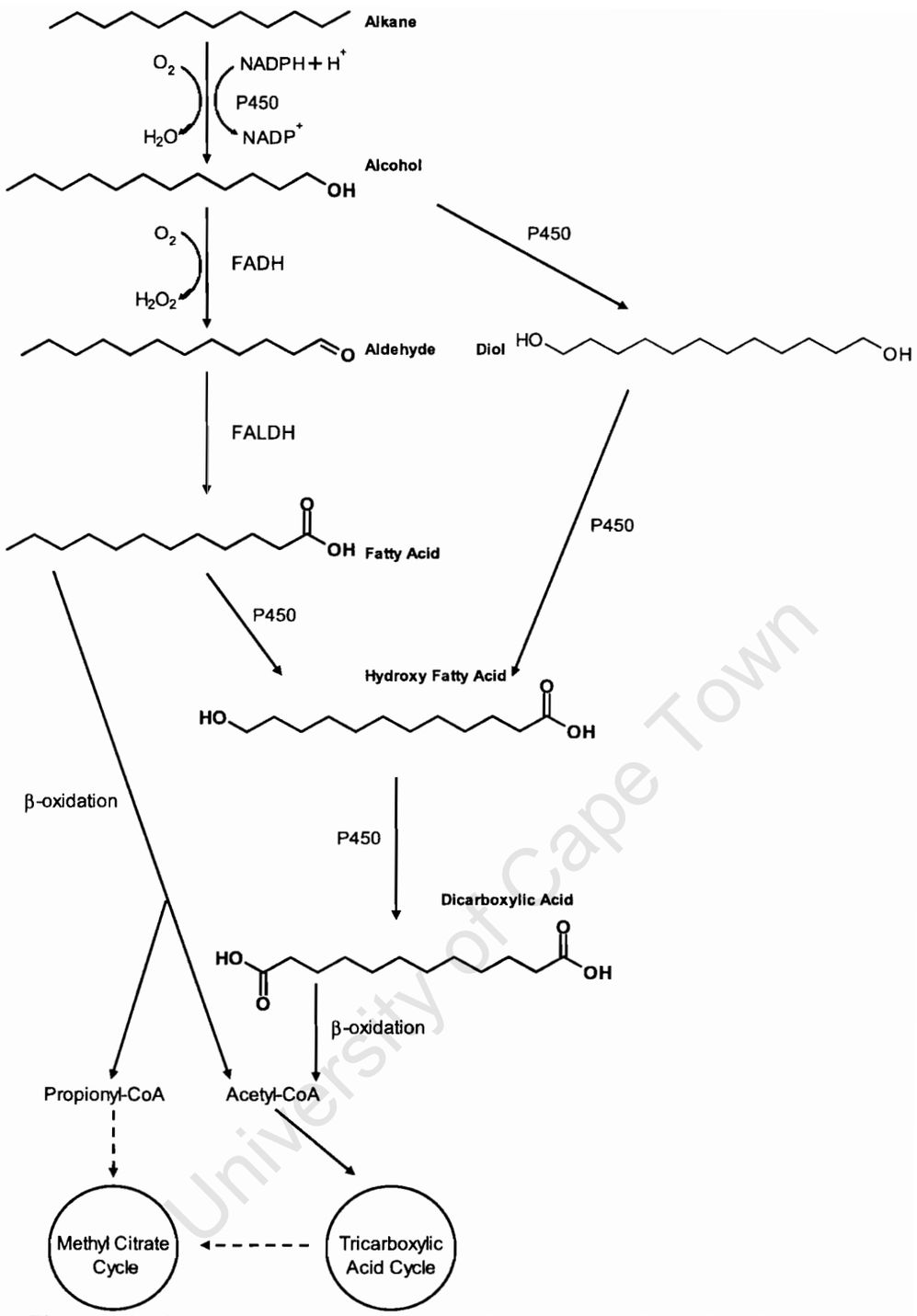

Figure 2.1: Metabolism of Alkane-assimilating yeast of the *Candida* species (adapted from Scheller *et al.*, 1998)

2.3.2 Alkane uptake

As discussed in the previous section, the choice of co-substrate affected cell growth, and in some cases, dicarboxylic acid production. Uchio and Shiio (1972a) noted specifically that glucose produced adequate cell growth but appeared to inhibit C_{16} dioic acid production. These authors concluded that the presence of glucose may repress enzymes responsible for the oxidation of n-alkane (catabolic repression). Mauersberger *et al*. (1996) noted that use of alkane as a carbon source, instead of glucose, caused both biochemical and morphological changes to the yeast cell. Hence, the role of cell structure in the mechanism for the uptake of hydrocarbons by yeasts should also be evaluated in the context of poorer dioic acid producing performance by glucose-grown cells.

In order for yeast to grow on alkanes, the hydrocarbon must be transported from the oil phase to the cell (Fukui and Tanaka, 1981). This mechanism was assumed to occur via direct contact of the cells with the alkane. Specifically, glucose-grown cells of *Candida tropicalis* seemed to have less affinity with alkane than did alkane-grown cells. Kappeli *et al*. (1978) investigated the chemical and structural alterations in *Candida tropicalis* arising from alkane growth in order to characterise this phenomenon. Hydrocarbon adsorbs preferentially to a cell surface containing a biopolymer with which it can form a hydrophile-lipophile interaction. It was found that glucose-grown cells lacked a mannan-fatty acid complex at the cell surface, resulting in a smooth surface. Alkane-grown cells had protrusions due to the arrangement of their wall polymers and hence were more favourable for hydrocarbon adsorption.

Mauersberger *et al*. (1996), describe a similar phenomenon for *C. maltosa*. The cell wall of glucose-grown cells is more hydrophilic and has lower lipid content, while alkane-grown cells have more protrusions separated by channels. It is therefore hypothesised that alkanes attach to hydrophobic outgrowths on alkane-grown cells and migrate through the channels via the plasma membrane to the endoplasmic reticulum (ER). This is the site of hydroxylation of alkanes by cytochrome P450 mono-oxygenase systems.

There is evidence to suggest that cell-alkane contact is not the only mechanism governing alkane uptake. Reddy *et al*. (1982) investigated the uptake of alkane by *Candida tropicalis* RAY14, yeast isolated by Vadalkar *et al*. (1969). The degree of cell-alkane contact depended on the degree of

emulsification of the alkane, but did not strongly affect cell growth. These authors concluded that the cells produce a solubilisation agent, most likely a protein, which stabilises submicron droplets that the cells can assimilate. Emulsification, agitation and other physical processes aid the formation of these droplets, but the specific solubilisation of the alkane by the cells appears to be the key step in alkane uptake. Some other micro organisms used in the study were found to secrete emulsification agents, in addition to solubilisation agents. Unlike the solubilisation agents, the emulsification agents did not appear to be site-specific for the cells and it was concluded that artificial agents could also be used effectively. Kappeli and Fiechter (1980) identified an alkane uptake process with *Candida tropicalis* ATCC 32113 grown on *n*-hexadecane. "Partitioning" (the transport of hexadecane from the bulk medium to the cell surface) was considered a purely physical process, not governed by enzymatic activity, while the uptake of alkane by the cells was shown to be characteristic of an active enzymatic process.

Therefore, the original conclusion by Uchio and Shiio (1972a) that glucose represses enzymes is most likely valid. It is not clear, however, if the enzymes affecting solubilisation or those affecting oxidation were affected. It would appear that it is not necessary to grow yeast on alkane in order to obtain good dioic acid production, as the presence of hydrophobic outgrowths to facilitate cell-alkane contact is not of prime importance, and dioic acid-producing mutants do not grow well on alkane (Picataggio *et al.*, 1992). What is clear, however, is that the choice of medium and co-substrate for growth is an important parameter to be considered in the optimisation of the production of dicarboxylic acid from an enzymatic standpoint. Physical conditions of the bulk fermentation fluid, such as emulsification, or agitation to disperse the alkane, can then assist the enzymatic processes.

2.4 Process Challenges in Alkane Bioprocesses

Production of dicarboxylic acids from linear alkanes by yeast will lead to some challenges for process optimisation. The most obvious challenges arise due to the nature of the liquid medium, which contains two immiscible liquid phases, aqueous and alkane. This section explores the various mass transfer implications that the presence of an immiscible alkane substrate phase can present, and the physical safety considerations for volatile alkanes in bioreactors. Thereafter potential kinetic implications in the form of substrate

and product inhibition are considered and related back to metabolism, alkane uptake and mass transfer.

2.4.1 Oxygen requirements and transfer based on carbon source

Carbohydrates contain oxygen as part of the molecular composition. Alkanes do not and so the entire oxygen requirement for an aerobic hydrocarbon bioprocess must be supplied in the form of oxygen from air. Moo-Young (1975) showed as follows that the production of yeast from hydrocarbon requires at least three times more oxygen per unit mass of cells than in the case of production from carbohydrate. Assuming the general formula for 1 mol biomass as $CH_{1.7}O_{0.5}N_{0.19}$, Moo-Young obtained the following stoichiometries for hydrocarbon-based and carbohydrate-based microbial growth respectively :

$$2CH_2 + 0.19NH_3 + 2O_2 \rightarrow CH_{1.7}O_{0.5}N_{0.19} + CO_2 + 1.5H_2O \quad (2.1)$$

$$1.68CH_2O + 0.19NH_3 + 0.68O_2 \rightarrow CH_{1.7}O_{0.5}N_{0.19} + 0.71CO_2 + 1.14H_2O \quad (2.2)$$

The critical dissolved oxygen concentration for microbial growth is typically 5 to 10% of the saturated oxygen concentration in pure water at 25°C and 1 atm (Shuler and Kargi, 1992). Below this growth is first order with respect to oxygen concentration, while above this it is independent of oxygen concentration. As mentioned previously, the key enzyme in alkane degradation by *Candida* is cytochrome P450. Mauersberger *et al.* (1996) noted that early literature stated that P450-catalysed alkane hydroxylation appeared to represent the rate-limiting step of the whole pathway, especially under conditions of oxygen limitation. In their work, Mauersberger *et al.* (1996) concluded that the cellular P450 concentration increases when the growth of *C. maltosa* on alkanes becomes oxygen-limited. Wiedmann et al. (1988) also showed that cytochrome P450 is induced when oxygen concentration is decreased. The limitation of O_2 (a co-substrate of cytochrome P450) enhances P450 formation in response to alkane accumulation inside the cells due to hydroxylation being restricted by O_2 limitation. Therefore an adequate oxygen transfer rate (OTR) is required in order to avoid oxygen limitation. This oxygen transfer requirement becomes greatly increased in alkane bioprocesses, when compared with carbohydrate

bioprocesses. It will therefore be advantageous to determine which process conditions can be modified to overcome this.

It will be shown mathematically in Section 2.5 that OTR can be improved by increasing oxygen solubility in the medium, and this solubility can be affected by changing the composition of the medium. The solubility of oxygen in hydrocarbons and fluorocarbons is 6 to 10 times higher than the solubility of oxygen in water. As a result, several authors have added perfluorocarbons (Mattiasson and Adlercreutz, 1983; McMillan and Wang, 1987) or alkanes (Ho *et al.,* 1990) to fermentation media to increase oxygen solubility, and hence OTR. These substances are known as oxygen vectors. These studies suggest that the increased oxygen transfer requirements due to the absence of oxygen in the hydrocarbon backbone can be met by adding increased amounts of hydrocarbon to the medium, up to a threshold value where the hydrocarbon becomes toxic to the yeast cells.

2.4.2 Flammability of hydrocarbons

The use of hydrocarbons in bioprocesses can result in hazardous working conditions due to their flammability. The bioreactor is sparged with air and hence ignition potential must be considered. The hydrocarbons used as substrate for the bioprocess in this project are *n*-dodecane and *n*-tridecane, classed as "long-chain" alkanes. They are liquid at room temperature and have boiling points and auto-ignition temperatures above 200°C. The physical data for the alkanes are listed in Table 2.1.

The temperature for fermentation is generally about 30°C, well below the flash point or the auto-ignition temperatures. However, only a 0.6% concentration of dodecane in dry air is required for explosion. The vapour pressures are about 0.1% of atmospheric pressure of 760mmHg. Therefore the air stream must be maintained to the reactor in excess to ensure that any alkane vapour present is diluted as much as possible. The condenser on the outlet air stream from the bioreactor must be active at all times to maintain a low temperature and this air stream must be ventilated to the atmosphere. The main hazard listed with respect to human health for these alkanes is respiratory damage and irritation.

Table 2.1: Physical Data of Feed n-Alkanes

Alkane	*n*-dodecane (C_{12})	*n*-tridecane (C_{13})
Melting Point	-9.6 °C	-5 °C
Boiling Point	216.2 °C	234 °C
Vapour Pressure	1mmHg @ 47.8 °C	1mmHg @ 59 °C
Flash Point	71 °C	102 °C
Explosion Limits	0.6%	
Auto-ignition Temperature	205 °C	
Specific Gravity	0.75	0.75

2.4.3 Liquid-liquid mass transfer

There are other mass transfer concerns in an alkane bioprocess. Schmid *et al.* (1998) studied the growth of *Pseudomonas oleovorans* on octane and concluded that, since alkane and cells are in immiscible phases, liquid-liquid mass transfer limitation may result. The process will then no longer be kinetically controlled. In this case, the cells did not have a high affinity for the alkane. This affinity can vary depending on type of the cell and the structure of the cell wall, as discussed in the context of alkane uptake in Section 2.3.2. In other words, the process may become limited by the physical partitioning of the alkane from the bulk fermentation medium to the cell, and not by the enzymatic solubilisation of the alkane, as described in Section 2.3.2. This means that the liquid-liquid interfacial area is an important parameter in evaluating the effect of liquid-liquid mass transfer limitation. Increasing agitation increases dispersion of two immiscible phases. The mixture may not become entirely homogeneous, but the alkane will form small droplets within the aqueous phase, therefore increasing the interfacial area per unit volume (Shuler and Kargi, 1992). This is discussed further in Section 2.5. It can therefore be concluded that substrate mass transfer area is an important factor in alkane fermentations.

2.4.4 Substrate inhibition

In addition, the bulk amount of alkane present is important. Kappeli and Fiechter (1980) concluded that growth of C. *tropicalis* on hexadecane is limited by alkane uptake when the ratio of alkane to cells drops below a threshold value. Wiedmann *et al.* (1988) concluded that hexadecane induced cytochrome P450 in *C. maltosa*. This is the enzyme that catalyses

hydroxylation. This suggests that adding alkane in excess of the metabolic requirement is advisable. This would also have a positive effect on the OTR, by increasing oxygen solubility in the fermentation medium. However, cases of substrate inhibition in alkane processes are documented. Schmid *et al.* (1998) studied the growth of the bacteria *Pseudomonas oleovorans* on octane. It was found that the octane caused cell disintegration unless it was diluted in a longer chain carrier solvent, thus indicating substrate inhibition for bacterial growth on short chain alkanes. There is no information readily available on substrate inhibition by longer alkanes such as hexadecane, and on inhibition of growth of yeasts (as opposed to bacteria).

It is postulated that low solubility of long chain alkanes will have a greater impact than substrate inhibition by alkane is most likely not significant for longer alkanes. It is not clear which will dominate yeast processes using medium chain length C_{12} to C_{13} alkanes. It is postulated that there is threshold value of alkane concentration, above which substrate inhibition is a factor. Caution must be employed when excess alkanes are added to the medium to increase OTR, as there is likely to be an optimum value to maximise OTR, before incurring significant substrate inhibition. While the use of longer alkanes may allow this threshold concentration to be higher than in the case of shorter chain alkanes, longer alkanes are less miscible in aqueous systems. Additional energy input to the process will be required in order to achieve consistent alkane distribution through the medium. This will most likely need to take the form of a mechanical input.

2.4.5 Product Inhibition

Another important kinetic factor to consider in bioprocesses is product inhibition. Scheller *et al.* (1998) showed that C_{16} dicarboxylic acid is a competitive inhibitor for C_{16} alkane binding. The system consisted of purified recombinant cytochrome P450 and the corresponding NADPH-cytochrome P450 reductase from *C. maltosa* reconstituted into an active alkane monooxygenase system. The authors proposed that the product inhibition may control P450 activity to the rate of transport of intermediates out of the endoplasmic reticulum. A K_i value of 74μM was calculated.

Chan *et al.* (1997 a, b) noticed similar behaviour by the C_{15} dicarboxylic acid in *Cryptococcus* and *Pseudomonas* cells. Continuous culture operation prevents excessive product accumulation and this was employed successfully

in the cultivation of the *Pseudomonas* cells where yields four times higher than in a batch process were obtained.

Chan *et al.* (1997b) employed a number of methods to reduce product inhibition in batch cultivation of immobilized *Cryptococcus* cells. The C_{15} dicarboxylic acid formed was removed every 50-hour period by centrifuging. The cell pellets were reused at least 5 times with fresh medium. An alternative method was employed in a continuous process. Effluent from an immobilized cells column was passed through an Amberlite XAD-2 resin column and then recycled back to the reactor. The dicarboxylic acid was eluted from the Amberlite column with an acetone-water mixture. This method of *in situ* removal could possibly be employed in a batch process.

2.4.6 Summary of process challenges

It is evident that the optimisation of an alkane bioprocess is not trivial. Gas-liquid mass transfer, in the context of oxygen transfer rate, is the most apparent potential limiting factor. The presence of liquid alkane with high oxygen solubility may resolve this, but conversely, may cause hydrodynamic problems due to immiscible phase dispersion and physical alkane-cell contact considerations. In addition, compromise of process kinetics in the form of substrate inhibition cannot be ruled out. Hence, issues of medium composition, system geometry and mechanical inputs must therefore be investigated in detail, in the context of mass transfer in multiple-phase dynamic systems, with a view to creating models for bioprocesses with immiscible liquid phases. Such models can then assist in optimisation of bioprocesses, such as the conversion of alkanes to dicarboxylic acids, by indicating which process conditions can be changed with the greatest effect.

2.5 Oxygen Transfer Considerations in Two-Phase Partitioning Bioreactors

There are numerous industrial processes that involve oxygen transfer between a gaseous medium and a homogeneous liquid medium. Such systems have been modelled extensively and much data is available for the purpose of engineering design of such processes (Treybal, 1980). In many

cases, however, the liquid medium may consist of two immiscible liquids, or an emulsion thereof. Examples of such systems include wastewater treatment processes where organic solvents have contaminated water (Hassan and Robinson, 1977). In the bioconversion of hydrocarbons by microorganisms, such as in the production of dioic acids, there exist two immiscible liquid phases, as well as solid particles in the form of cells. The introduction of additional solid or liquid phases has implications for mass transfer. The additional phases must be accounted for in proposing a mass transfer mechanism, and the main resistance to mass transfer must be identified in order to effectively design and optimise such processes.

This section will investigate mass transfer in multiple phase systems, beginning with the well-known model used to quantify gas-liquid mass transfer, in the context of oxygen transfer rate from an air-bubble to a Newtonian liquid. Following from this, various fundamental phase-interactions and surface chemistry issues will be investigated and compared with existing literature for multiple phase systems, in order to propose possible mass transfer pathways in gas-liquid-liquid-solid processes.

2.5.1 Theory of Gas-liquid Mass Transfer applied to Oxygen Transfer in Bioprocesses

Mass transfer involves the transport of material from regions of high concentration to regions of low concentration. In a bioprocess, the concentration of oxygen in air bubbles is higher than the concentration of oxygen in the liquid fermentation medium. This concentration difference acts as a driving force to encourage the transfer of oxygen from the gas phase to the liquid phase. In a stagnant fluid within a single homogenous fluid phase, mass transfer takes place through molecular diffusion. Doran (1997) defines molecular diffusion as the movement of molecules in a mixture from a region of high concentration to a region of low concentration. However, in the case of a turbulent flow regime, such as is generally found in a stirred bioreactor, convective mass transfer also takes place as a result of the movement of the bulk fluid. These convective currents increase the overall rate of mass transfer.

Fick's first law of molecular diffusion is based on the following principles:

1. Mass transfer by molecular diffusion occurs because of a concentration gradient and the species diffuses in the direction of decreasing concentration.
2. The mass transfer of the species occurs as a flux across an area normal to the direction of diffusion.

The rate of mass transfer in Fick's first law of diffusion is therefore expressed as a proportionality between a flux and a gradient:

$$J_A = -D_{AB} \cdot \frac{dC_A}{dz} \tag{2.3}$$

where J_A = flux of species A

D_{AB} = mutual diffusivity of species A in species B

C_A = concentration of species A

z = distance over which concentration gradient exists.

Hence, the mass transfer rate by diffusion across a plane becomes

$$n_A = -D_{AB} \cdot A \cdot \frac{dC_A}{dz} \tag{2.4}$$

where n_A = rate of diffusion of species A

A = area of plane over which diffusion occurs.

Mass transfer between two phases is often modelled by "Two-Film Theory" (Doran, 1997). The theory is based on the assumption that a stagnant boundary layer forms at the interface between two phases, on both sides of the interface. The turbulence in the fluid phase dies out at the phase boundary, leaving this stagnant layer. It is assumed that there is negligible resistance to mass transfer at the interface itself as the phases are in equilibrium at the phase boundary. An additional assumption is made that the concentration profiles are independent of time, or that the system is at steady state. The resistance to mass transfer occurs in the stagnant boundary layer as mass transfer in this layer can occur only through molecular diffusion. An increase in turbulence of the bulk phase can reduce the width of this stagnant boundary layer, and hence increase the overall rate of mass transfer. This is how convective mass transfer contributes positively to the overall rate of mass transfer, as a result of its effect on interfacial boundary layers. A

diagrammatic representation of Two-Film theory in a gas-liquid system is shown in Figure 2.2.

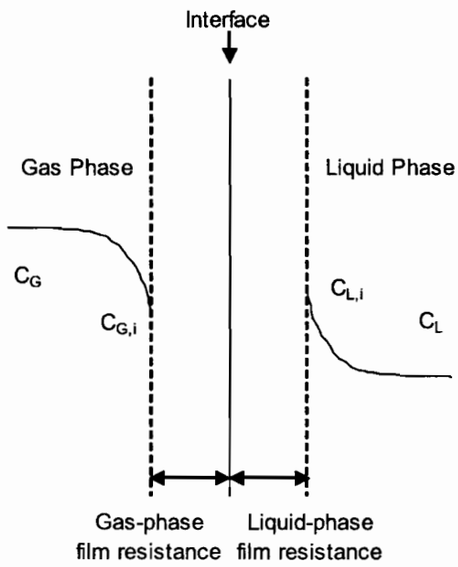

Figure 2.2: Concentration Profiles at a Gas-Liquid Interface

Mass transfer of a component such as oxygen from air to an aqueous liquid medium can be modelled using two-film theory. The concentration of oxygen in air will be higher than that in an aqueous medium, and so oxygen will be transferred from the gas phase to the liquid phase. The concentration of oxygen in the bulk gas is given by C_G, while $C_{G,i}$ is the interfacial gas-phase oxygen concentration. Similarly, the concentration of oxygen in the bulk liquid is given by C_L, while $C_{L,i}$ is the interfacial liquid-phase oxygen concentration. These concentration profiles are shown in Figure 2.2. In order to formulate a mathematical expression for mass transfer through the gas-phase film, equation 2.4 can therefore be rewritten, assuming that the rate of mass transfer in a fluid is considered directly proportional to the driving force for the transfer process (as given by the concentration gradient) and the area available for the transfer to take place:

$$n = k_G A(C_G - C_{G,i}) \tag{2.5}$$

where k_G = gas-phase mass transfer proportionality coefficient

A = interfacial area for mass transfer.

Similarly, the rate of mass transfer of oxygen through the liquid-phase film is given by

$$n = k_L A(C_{L,i} - C_L) \tag{2.6}$$

where k_L = liquid-phase mass transfer proportionality coefficient.

Hence, combining equation 2.4 and with an equation of the form of 2.5 or 2.6, we obtain the approximation

$$k \cdot \Delta C = -D_{AB} \cdot \frac{\Delta C}{\Delta z} \tag{2.7}$$

This gives rise to the dimensionless Nusselt number for mass transfer

$$Nu_{AB} = \frac{k.\delta}{D_{AB}} \tag{2.8}$$

where δ = characteristic length over which mass transfer occurs.

The mass transfer proportionality constant is therefore considered inversely proportional to the length over which mass transfer occurs. Applying this to "Two-Film Theory", the rate of mass transfer increases as the stagnant boundary layer narrows.

"Two-Film Theory" assumes that the phases are in equilibrium at the interface. The equilibrium concentration of oxygen in the gas phase can be approximated as a linear function of equilibrium liquid concentration as follows:

$$C_{G,i} = mC_{L,i} \tag{2.9}$$

where m = distribution factor.

Substituting (2.9) into (2.5) and rearranging:

$$\frac{n}{k_G A} = (C_G - mC_{L,i}) \tag{2.10}$$

And similarly, substituting (2.9) into (2.6) and rearranging:

$$\frac{n}{k_L A} = (\frac{C_{G,i}}{m} - C_L) \tag{2.11}$$

Dividing (2.5) by m and rearranging:

$$\frac{n}{mk_G A} = \left(\frac{C_G}{m} - \frac{C_{G,i}}{m}\right) \tag{2.12}$$

Multiplying (2.6) by m and rearranging:

$$\frac{m \cdot n}{k_L A} = (mC_{L,i} - mC_L) \tag{2.13}$$

On adding (2.10) to (2.13) and (2.11) to (2.12), we obtain

$$n\left(\frac{1}{k_G A} + \frac{m}{k_L A}\right) = (C_G - mC_L) \tag{2.14}$$

and

$$n\left(\frac{1}{mk_G A} + \frac{1}{k_L A}\right) = \left(\frac{C_G}{m} - C_L\right) \tag{2.15}$$

(2.14) and (2.15) are in the general form

mass transfer rate / overall mass transfer coefficient = concentration gradient

based on the bulk oxygen concentration in each phase.

Hence, the overall gas-phase mass transfer coefficient, K_G is given by

$$\frac{1}{K_G A} = \frac{1}{k_G A} + \frac{m}{k_L A} \tag{2.16}$$

and similarly, the overall liquid-phase mass transfer coefficient, K_L is given by

$$\frac{1}{K_L A} = \frac{1}{mk_G A} + \frac{1}{k_L A} \tag{2.17}$$

Therefore, (2.14) and (2.15), respectively, can be rewritten as follows:

$$n = K_G A(C_G - mC_L) \tag{2.18}$$

and

$$n = K_L A\left(\frac{C_G}{m} - C_L\right) \tag{2.19}$$

Equations (2.18) and (2.19) both represent the rate of oxygen transfer from the gas phase to the liquid phase. Further substitutions can be made using

(2.9). mC_L can be replaced by C_G*, the gas-phase oxygen concentration in equilibrium with C_L, to give

$$n = K_L A(C_G - C_G^*) \tag{2.20}$$

Similarly, according to (2.9), C_G/m is equal to C_L*, the liquid-phase oxygen concentration in equilibrium with C_G, which gives

$$n = K_L A(C_L^* - C_L) \tag{2.21}$$

When the gas is sparingly soluble in the liquid, such as in the case of oxygen in an aqueous system, it is assumed that most of the resistance to mass transfer occurs in the stagnant liquid film surrounding the air bubbles. This means that k_L is very small, and k_G is much larger. Therefore, equation (2.17) can be simplified to $K_L a \approx k_L a$.

In bioreactors, the mass transfer parameters are conventionally defined on a volumetric basis as follows:

$$OTR = K_L a(C^* - C) \tag{2.22a}$$

or

$$OTR = k_L a(C^* - C) \tag{2.22b}$$

where OTR = oxygen transfer rate $\left[\frac{mass}{volume \cdot time}\right]$

a = gas-liquid interfacial area per unit volume $\left[\frac{area}{volume}\right]$

C* = saturation concentration of oxygen in liquid phase $\left[\frac{mass}{volume}\right]$

C = concentration of oxygen in liquid phase.

2.5.1.1 Factors affecting mass transfer coefficient ($k_L a$)

It was stated previously that an increase in turbulence of the bulk phase reduces the width of the stagnant boundary layer, and hence increases the overall rate of mass transfer. Increasing agitation and aeration, or reducing the viscosity of the liquid medium, can increase turbulence in the liquid. This is represented by a numerical increase in the value of k_L (the dominating mass

transfer coefficient) and was shown mathematically in equations 2.8 and 2.9. Increased aeration and agitation will also increase gas hold-up, while increased agitation will decrease bubble size through mechanical shear. These factors will increase a. In addition, viscosity changes will affect bubble formation and have an effect on the size of the bubble, and hence a. It is therefore clear that k_L and a are affected by the same variables, though not always in the same manner. It has therefore become common practice to define a composite variable, K_La, as the overall volumetric mass transfer coefficient to represent the mass transfer capability of a bioreactor system.

Treybal (1980) reports diffusivity as increasing with temperature, and hence k_La is also affected by system temperature changes. A correlation relating changes in k_La to changes in temperature and viscosity is shown in Aiba *et al.* (1965):

$$\frac{k_La(T_1)}{k_La(T_2)} = \sqrt{\frac{T_1\mu_2}{T_2\mu_1}} \tag{2.23}$$

where $k_La(T)$ = overall volumetric mass transfer coefficient at temperature T

T = absolute temperature [Kelvin]

μ = liquid viscosity.

The drawback of this equation, however, is that it was developed for a biological activated-sludge treatment process, where oxygen transfer was only due to bubble aeration. It is not clear how this would change when agitation is also a factor.

2.5.1.2 Factors affecting oxygen solubility (C)*

As with diffusivity and mass transfer coefficient, temperature can also affect oxygen solubility in liquids. The saturation concentration of 1 atm oxygen in pure water between 0°C and 36°C is given by the following correlation (Doran, 1997):

$$C^* = 14.161 - 0.3943T + 0.00771T^2 - 0.0000646T^3 \tag{2.24}$$

where C^* = oxygen solubility [mg/l]

T = temperature [°C].

The oxygen solubility in water decreases with an increase in temperature, and equates to 41.4 mg/l at 25°C and 38.4 mg/l at 30°C at a partial pressure of 1 atm O_2. The effect of pressure on solubility in dilute solutions can then be calculated by Henry's Law (Welty *et al.*, 1984):

$$p_A = H \cdot C_A \tag{2.25}$$

where p_A = partial pressure of component A

H = Henry's law constant

C_A = equilibrium concentration of component A in the liquid phase.

Therefore, the saturation concentration of oxygen in water under 1 atm air, can be calculated, assuming that air contains 21 mol% oxygen. Using Dalton's law

$$p_A = y_A P \tag{2.26}$$

where y_A = mol fraction of component A

P = system pressure.

and taking the Henry's law constant at 30°C to be 26.1 atm.m^3.kg^{-1} (Doran, 1997), the saturation concentration of oxygen in water at 30°C equates to 8.05 mg/l under 1 atm air.

In aqueous systems the addition of solutes can affect the solubility of oxygen. This is of importance in bioprocesses, as fermentation media contain ingredients such as electrolytes, salts, acids and sugars. These soluble ingredients can decrease the oxygen saturation concentration, compared with that in pure water, by 5 to 25% at typical fermentation concentrations. Authors such as Baburin *et al.* (1981) and Schumpe *et al.* (1982) have developed empirical relationships to predict the change in saturation oxygen concentration upon addition of solutes to water.

In alkane-based bioprocesses, the saturation concentration of oxygen in alkanes is also of interest. Literature data for C^* of oxygen in alkane is shown in Table 2.2. There are some discrepancies in the exact saturation concentration of oxygen in *n*-alkanes, but the values reported by most authors are of a similar order of magnitude, especially for compounds such as octane

(n-C_8 alkane) for which there is much comparative data, all differing by no more than 15%. For the larger alkane molecules, there is less data available, and the differences between the reported data values are larger. Makranczy *et al.* (1976) lists the solubility oxygen in dodecane (n-C_{12} alkane) as approximately 260mg/l at 25°C and 1 atm, while a more recent work by Hesse *et al.* (1996) lists it as 324 mg/l, 25% larger. Blanc and Batiste (1970) list the equivalent solubility of oxygen in dodecane as approximately 305mg/l at 30°C. This value would be expected to be lower than the values at 25°C, due to the effect of temperature on gas solubility in liquids. In general, all 3 authors report a decrease in solubility with an increase in carbon number, except for the data for nonane and undecane (n-C_9 and n-C_{11} alkane) reported by Blanc and Batiste (1970). Considering that this is the earliest work on such a comprehensive range of alkanes, this apparent discrepancy could be due to purity of the alkane, as odd-numbered hydrocarbon-producing processes tended to be rare in the past. In summary, however, it is clear that oxygen is significantly more soluble in alkane than water, by a factor of at least 6 (when compared with dodecane).

2.5.1.3 Factors affecting oxygen transfer rate (OTR)

Increasing k_La or C^* can thus increase OTR. While k_La is affected by turbulence, as discussed above, both k_La and C^* can be affected by changing the temperature or the composition of the medium. Medium composition, specifically, has an effect on bubble formation. It is therefore important to investigate effect of all system parameters on the behaviour and formation of bubbles. Aeration level, agitation level and the physical configuration of the air spargers and impellers used have complex effects on fluid dynamics and bulk mixing in a bioreactor. This is an important consideration in mass transfer, as illustrated by "Two-Film Theory", and will be elaborated on in Section 2.5.2. In addition, Section 2.5.2 will also introduce theory of fluid dynamic behaviour in a system where the liquid medium is composed of two immiscible liquid phases, and not merely a pure liquid phase or a bulk liquid phase containing miscible solutes.

Table 2.2: Comparison of Data for Solubility of Oxygen in Alkanes

Author	**Year**	**T**	**P**	*n*-C_8	*n*-C_9	*n*-C_{10}	*n*-C_{11}	*n*-C_{12}	*n*-C_{13}	*n*-C_{14}	*n*-C_{15}	*n*-C_{16}	*n*-C_{17}	*n*-C_{18}
		°C	atm	0.703	0.718	0.73	0.74	0.749	0.75	0.763	0.77	0.773	0.775	0.777
				Solubility (mg/l)										
Ju & Ho	1989	22	1									340		
Ho *et al.*	1990	25	1									322		
Makranczy *et al.*	1976	25	1	371	337	302	276	260	234	222	199	190		
Blanc & Batiste	1970	30	1	389	395	316	349	305	283	269	263	255	240	230
Wilcock *et al.*	1978	10	1	426		363								
		25	1	428		361								
		40	1	428		359								
Thomsen,Gjaldbæk	1963	25		412										
Hesse *et al.*	1996	25	1	405	383	358	344	324	300	292	281	271		

T - temperature

P - pressure

2.5.2 Bioreactor fluid dynamics

In Section 2.5.1, the conventional understanding of mass transfer from a gas to liquid was presented. However, for the purposes of this project an understanding of the dynamic fluid behaviour of dispersed solid phase and an additional immiscible liquid phase is required, in addition to the gas and aqueous phases. The following section therefore outlines some surface chemistry considerations that affect the behaviour at the interfaces between these various phases, or affect the distribution of these phases. Bulk fluid considerations, such as the effect of mechanical agitation, aeration and bioreactor geometry, also play an important role in determining the fluid dynamics of the system. However, much of the data available on these topics is for pure liquids or pure water. Fermentation media, however, are not pure liquids. Therefore, the effect of both soluble and insoluble additions to the liquid phases must be investigated in detail, in order to better relate the information to behaviour in a real bioprocess containing a non-pure liquid phase.

2.5.2.1 Aeration, bubble formation and the influence of miscible solutes

Air is generally introduced into a bioprocess by a sparger with an outlet situated at the bottom of the bioreactor, both in the case of an agitated bioreactor with impeller(s), or an airlift bioreactor with no impellers. There is much research available investigating the effects of mass transfer from gas to liquid from a single bubble rising through a column of liquid, which can provide an understanding of the fluid dynamics and bubble formation occurring in aerated bioprocesses. Paaschen and Lubbert (1997) investigated oxygen transfer from a single oxygen bubble rising through a bubble column containing water. Fluorescent dye was used to show the location of dissolved oxygen in the water. It was found that the oxygen accumulated in the bubble wake. The oxygen concentration was higher along the edges of the bubble wake, than in the main volume of the wake. It was concluded that the dissolved oxygen flows along the borders of the bubble wake. It then enters the main volume of the wake from underneath the bubble, mixed with liquid from the bulk fluid, which has a lower oxygen concentration. This fluid is then released from the wake to the bulk fluid. The rate of oxygen transfer to the liquid is therefore highly dependent on the residence time of liquid in the bubble wake. Paaschen and Lubbert (1997) found that mass transfer in the bubble column did not depend heavily on bubble size, but rather on the presence of neighbouring bubbles. It was concluded that the presence of other bubbles disturbed the concentration boundary layer and actually

enhanced mass transfer through increased turbulence. This is consistent with "Two-Film" Theory discussed in Section 2.5.1, and implies that an increase in aeration will increase oxygen transfer: macroscopically through the presence of increased total oxygen supply, and microscopically by increasing the effectiveness of oxygen transfer for each individual bubble.

Bubble-bubble interaction is therefore a very important aspect to consider when modelling the fluid behaviour of liquid-gas systems, especially in the context of the bioprocess industry where fermentation broths are often sparged with a multitude of bubbles in quick succession. Bubbles formed in any pure liquids, whether polar on non-polar, will coalesce (merge). Coalescence is inhibited by the addition of surface-active impurities (Hassan and Robinson, 1977).

A surfactant molecule adsorbs at the liquid/gas interface due to the fact that it is comprised of polar and non-polar groups. This increases the strength of the gas/liquid interface, thus reducing coalescence. The presence of a surfactant at this interface is therefore responsible for foam formation (Leja, 1982). Many micro organisms secrete species such as polypeptides during fermentation (Bailey and Ollis, 1986). These may behave like surfactants and cause foaming, especially in aerated bioreactors.

Surfactants affect mass transfer due to the interaction at the gas-liquid interface. Aiba *et al.* (1965) show that the addition of a small amount of surfactant, sodium lauryl sulphate results a sharp decrease in k_La. As more surfactant is added, k_La reaches a minimum value, and then increases slightly again (but without recovering its initial value at zero surfactant concentration). This phenomenon is due to conflicting effects of the surfactant on k_L and a respectively.

k_L is decreased sharply with surfactant addition, up to a critical concentration where surfactant addition no longer has an effect. This is due to surface saturation, whereby there is sufficient surfactant to cover the entire gas-liquid interface. According to surface-drag theory (Aiba *et al.,* 1965), the surfactant absorbed at the air-liquid interface is not necessarily retarding oxygen diffusion from the gas phase to the liquid phase. Instead, the surfactant serves to dampen any movement of the interface by making it more rigid, thus reducing turbulence, and hence k_L. On the other hand, the addition of surfactant reduces bubble size, and hence increases interfacial area, a. This

accounts for the minimum in the curve of k_La as a function of surfactant concentration.

Due to the conflicting effects on both k_L and a, foaming is not necessarily advantageous for improving mass transfer. While smaller bubbles will rise more slowly and increase gas hold-up (Keitel and Onken, 1982), the overall k_La is still lower in the presence of surfactant, due to the additional resistance that the surface-active molecules provide at the interface. Machon *et al.* (1997) also noted that increased gas hold-up due to small bubbles in aqueous-electrolyte solutions was not sufficient to increase overall k_La. In practical applications, foaming causes difficulties in maintaining asepsis in the fermentation vessels. As a result, it is common practice to add chemical antifoams during bioconversion processes to counteract the surfactant products of the bioprocess.

The change in bubble size on the addition of solutes was originally attributed to a change in surface tension and the resulting effect on coalescence, however there is some debate regarding this. The mechanism of coalescence is not well understood. According to Zieminski *et al.* (1967) coalescence is caused when two bubbles collide and the liquid film (lamella) between them ruptures. The rate at which this occurs is related to the rate of drainage of the continuous phase (liquid) between the bubbles. The rate of drainage, film viscosity and thickness are affected by the adsorption of a surfactant at the gas/liquid interface. Coalescence is therefore decreased by the addition of a surfactant as its polar groups will attract and bind more water to the film surrounding the bubble. This will slow the rate of drainage and hence the rate of coalescence. Pure liquids do not foam because they cannot form membranes around the bubbles to reduce drainage of water from the lamellae (Kitchener and Cooper, 1959). Due to such explanations, bubble size was commonly predicted by the Weber number (Keitel and Onken, 1982), which took into account the balance between inertial force and surface tension. Machon *et al.* (1997) compared bubble sizes in aqueous solutions containing alcohols or electrolytes to give surface tensions greater than and less than that of water, respectively. The authors found no correlation between surface tension and bubble size, and could not use the Weber number to correlate their results. They therefore concluded that more parameters, such as surface charges, needed to be taken into account. Keitel and Onken (1982) noted that the inhibition of coalescence could not be explained by surface potential alone. It is therefore clear that a number of parameters affect bubble formation and size.

Zieminski *et al.* (1967) investigated the effect of dicarboxylic acids on bubble size and interfacial area in a bubble column. They concluded that bubble size decreased with an increase in acid concentration or carbon number. While the mechanism is unclear, this result is of interest for predicting bubble behaviour in bioprocesses producing dicarboxylic acids.

In addition to the chemical properties of the liquid, bubbles are also affected by the presence of mechanical agitation (Aiba *et al.,* 1965). The turbulence introduced by the impeller will change the motion of the bubbles, and cause them to deform. Therefore, as an alternative to the Weber number approach, bubble size can be considered to be dependent on a dynamic equilibrium between breakage and coalescence, with the exact relationship between coalescence and interfacial properties (such as surface tension or surface charges) requiring further study (Machon *et al.*, 1997). The effect of mechanical agitation is discussed further in Sections 2.5.2.2 and 2.5.2.3.

2.5.2.2 Agitation and droplet formation due to the presence of immiscible liquid components

In the bioconversion of alkanes to dicarboxylic acids, the fermentation medium contains an aqueous phase including water-soluble carbohydrates and salts, as well as alkane. The alkane phase is less dense than the aqueous phase, partitioning into and upper phase unless the liquid is agitated. Agitation needs to be sufficient to disperse the liquid phases uniformly, but not excessive so as to result in shear damage to the microorganisms in the process. There has been much investigation to determine the minimum agitation speed for complete dispersion.

Armenante & Abu-Hakmeh (1994) defined N_{cgd} as the minimum agitation for "complete gassed dispersion" of an organic liquid phase, in this case 10% mineral oil, in a gassed aqueous system. This minimum agitation speed is not necessarily a fixed value. N_{cgd} was not affected by liquid height in the tank and sampling position. N_{cgd} was reduced by 20% as air flow rate increased from 0.0 to 0.44 vvm. N_{cgd} was strongly affected by impeller geometry. For example, N_{cgd} in a system agitated with a disk turbine is half that required on agitation of an identical system with a curved-blade turbine. N_{cgd} also increased by approximately 175% as impeller diameter was reduced from 0.35 of tank diameter to 0.22 of tank diameter, but was not affected significantly by impeller clearance off the bottom of the vessel. The effect of oil fraction on N_{cgd} was not explored.

While impeller clearance and sampling point seem not to affect droplet dispersion, Daglas and Stamatoudis (2000) found that impeller vertical position has an effect on kerosene droplet size in distilled water. The vertical position of the sampling point also affects the observed Sauter mean droplet diameter. The authors concluded that the Sauter mean droplet diameter increased at low agitation rates and as the distance from sampling point to impeller increased. This indicated that the observed increase in drop size was largely dependent on lower mechanical breakage rate, allowing for increased coalescence. Contributions by gravity forces, such as rising/settling velocities for droplets of different sizes, could not be excluded.

Earlier work by Calabrese *et al.* (1986) would seem to separate the effects of mechanical breakage and coalescence. The authors state that coalescence is negligible in dilute suspensions with a dispersed phase viscosity less than 0.5 Pa.s, but acknowledge that drop sizes are determined by mechanical breakage in the impeller region. They also conclude that Sauter diameter should decrease as the ratio of impeller diameter to tank diameter decreases, since the droplets would be exposed to greater localised mechanical turbulence. Calabrese *et al.* (1986) then extrapolate their results to predict the behaviour in non-dilute solutions. In such cases, it was assumed that coalescence would be significant, as there is increased probability of droplet collision, and the localised mechanical turbulence per droplet is decreased. Recalling the work by Armenante & Abu-Hakmeh (1994), the minimum agitation for "complete gassed dispersion", N_{cgd}, increases as the ratio of impeller diameter to tank diameter decreases, due to less overall mechanical turbulence in the tank. Therefore, dispersion and drop size are both affected by agitation, but in a different manner. Droplet size is seemingly determined by the microscopic turbulence in the impeller zone, while droplet dispersion is determined by the macroscopic influence of the impeller on the tank as a whole.

The coalescence of droplets (and hence the size of droplets) is also related to surface tension by some authors. A factor known as "spread coefficient" is defined for oil in aqueous systems (Hassan and Robinson, 1977):

$$S_{ow} = \gamma_{gw} - \gamma_{go} - \gamma_{ow} \qquad (2.27)$$

where S_{ow} = spread coefficient of oil in water

γ_{gw} = gas-water surface tension

γ_{go} = gas-oil surface tension

γ_{ow} = oil-water interfacial tension.

If S_{ow} is positive, the oil will spread at the gas-water interface, but if S_{ow} is negative, then the oil will form discrete droplets. The data for surface tension concerning alkanes shows some discrepancies. The values reported by various authors are summarised in Table 2.3.

Table 2.3: Interfacial surface tension and spread coefficients in alkane-water systems

Author	Year	Temperature	Alkane	Air-Water	Alkane-Water	Alkane-Air	
				γ_{gw}	γ_{ow}	γ_{go}	S_{ow}
		°C		mN/m	mN/m	mN/m	mN/m
Jasper & Kring*	1955	30	*n*-C_{12}			24.5	
"		30	*n*-C_{13}			25.1	
Linek & Benes	1976	30	C_{11} - C_{18}	71.2	48.7	26.1	-3.6
Hassan & Robinson	1977	30	*n*-C_{12}	71.3	49.3	24.6	-2.6
"			*n*-C_{16}	71.3	53.2	27.4	-9.3
Rols *et al.*	1990	25	*n*-C_{12}	72	46.8	24.6	0.6
Freitas & Quina	2000	20	*n*-C_{12}	72.75	52.4	25.3	-4.9
"		20	*n*-C_{13}	72.75	53.3	26.6	-7.2

*data included for comparison only – measured under nitrogen, not air

While the absolute values reported for interfacial/surface tensions do not differ by a large degree, the difference becomes significant when applied to equation 2.27. The spread coefficient for *n*-dodecane is calculated as negative by most authors, thus indicating that the alkane should form discrete droplets within an aqueous system. Rols *et al.* (1990) report that the spread coefficient of *n*-dodecane is positive. The actual value obtained is very close to zero. Considering the discrepancies in the effect of surface tension on bubble coalescence (see Section 2.5.2.1), the data for spread coefficients and droplet coalescence of alkanes also warrants thorough scrutiny and further research, as in the case of oxygen solubility in alkane.

2.5.2.3 Effect of impeller and sparger configuration

Sections 2.5.2.1 and 2.5.2.2 have outlined the importance of aeration or agitation alone on mixing in bioreactors. However, the combined effects of these two parameters are of interest as most aerobic bioprocesses will employ both methods for media dispersion. This section therefore

investigates the situation when agitation and aeration are combined, or multiple impellers are employed.

Impeller vertical position has an effect on oil droplet size in water (Daglas and Stamatoudis, 2000), in the case of a single impeller. Multiple impellers also have a profound effect on mixing behaviour. Abrardi *et al.* (1990) defined several hydrodynamic regimes occurring around Rushton impellers, comparing mono- and dual-impeller aerated systems. For the bottom impeller, or in the case of a single impeller, the authors defined flooding, loading and complete dispersion. When a second impeller was added, N_{cgd} decreased. Only two hydrodynamic configurations for the upper impeller were observed, namely, ineffective and effective dispersion. In the former, the bubbles are only dispersed above the upper impeller, but in a rather unstable manner. No stable loading zone was observed. The latter condition was considered to occur when bubbles are well dispersed and re-circulate underneath the impeller. The impellers were spaced 2 diameters apart, which had previously been considered sufficiently far apart for the impellers not to influence each other.

Cronin *et al.* (1994) compared mixing time in systems with single and multiple Rushton impellers. They used a colorimetric method to determine the extent of mixing. "Mixing time" was defined as the time for complete (uniform) dispersion. These authors concluded that impellers spaced two or more diameters apart in water (with no aeration) resulted in compartmentalised mixing zones around each impeller. As the distance between the impellers decreased, mixing time increased (i.e. less effective mixing was observed). The authors concluded that, while the two mixing zones were interfering with each other and improving mass transfer, the bottom zone mixed first, while the upper zone remained compartmentalised for longer. Thus the overall mixing time increased. Whitton *et al.* (1997) also performed mixing studies with a colorimetric technique similar to Cronin *et al.* (1994). They concluded that the most effective impeller configuration used a Rushton (radial) turbine as the bottom impeller, with downward pumping (axial) impellers above it. This produced better results than Rushton impellers alone under un-gassed conditions, due to increased exchange flows between compartmentalised impeller mixing zones. Under gassed conditions, there was no marked benefit of employing axial impellers.

The results obtained when aeration was introduced were more difficult to correlate and authors concluded that the interaction between air bubbles and

mechanically induced agitation zones is very complex. Abrardi *et al.* (1990) and Whitton *et al.* (1997) found that mixing time increases with the introduction of aeration, and Cronin *et al.* (1994) confirm this in the cases where the impellers are not flooded. As gas flow increased, the deviation from expected results increased (Cronin *et al.*, 1994).

It is therefore clear that the effects of agitation and aeration on mixing are linked. Many authors have derived correlations expressing k_La as a function of agitation and aeration parameters (Calderbank and Moo-Young, 1961; Robinson and Wilke, 1973, Wong and Shiuan, 1986). Doran (1997) reports the following expression for stirred bioreactors containing non-coalescing non-viscous media:

$$k_L a = \delta \left(\frac{P}{V}\right)^{\alpha} u_G^{\beta} \qquad (2.28)$$

where P/V = stirrer power per liquid volume [W/m^3]

u_G = superficial gas velocity (volumetric gas flowrate/vessel cross-sectional area) [m/s]

and δ, α and β were empirical constants with the values 2.0x10^{-3}, 0.7 and 0.2 respectively.

Other authors such as Aiba *et al.* (1965) report relationships of a similar form, but with different coefficient and exponent values. According to Moo-Young and Blanch (1981), the values of α and β vary between 0.4-0.42 and 0.35-0.5 respectively in water, and 0.52-0.74 and 0.26-0.62 in electrolyte solutions. These are empirical system-dependent values and are a function of system geometry and fluid properties such as coalescence. Equation 2.28 specifically does not take into account any non-Newtonian fluid behaviour, or the presence of the immiscible liquid phase. Therefore, for the purposes of alkane fermentation, such correlations cannot apply, as the liquid phase consists of two immiscible liquids (Hassan and Robinson, 1977). It is therefore important to modify the correlations and models developed for mass transfer in gas-liquid systems, by incorporating the effect of adding a second liquid phase.

2.5.3 Theory of gas-liquid-liquid mass transfer

The purpose of this section is to expand the mass transfer theory developed for gas-liquid systems to predict the behaviour of gas-liquid-liquid systems. When thermodynamic equilibrium is reached, the amount of gas dissolved in a mixture of oil and water is considered to be the same as the total gas dissolved in the equivalent amounts of oil and water, measured separately (Linek and Benes, 1976). Authors such as Ju and Ho (1989) proposed a volumetric relationship for C^* in a mixture of immiscible liquid components and confirmed this experimentally in penicillin fermentations (Ho *et al.*, 1990):

$$C^*_{overall} = \sum f_i . C^*_i \qquad (2.29)$$

where f_i = volumetric fraction of component *i*.

It is also important to account for the processes affecting mass transfer until equilibrium is attained, or in other words, the rate of mass transfer. In bioprocesses, OTR is typically defined in equation 2.22a. Hassan and Robinson (1977) defined K_La^* as the air-aqueous mass transfer coefficient for a three-phase system containing an immiscible hydrocarbon liquid phase in water. K_La^* was affected by the type and volume fraction of hydrocarbon used. Linek and Benes (1976) performed detailed investigation of the mass transfer mechanism in oil-water emulsions. In an attempt to isolate of the main resistance to mass transfer, the authors performed experiments with a well-defined gas-liquid contact area, thus allowing separate measurement of k_L and a for various phase boundaries.

In developing a model for mass transfer in a gas-water-hydrocarbon system, the first assumption is that the liquid phases are immiscible, thus the effect of hydrocarbon as a solute can be ignored. Mączyński *et al.* (2003) list the solubility of dodecane in water at 298.15K as a mole fraction of 6.0×10^{-11}. This can be considered negligible. Linek and Benes (1976) proposed four possible scenarios for the mechanism of gas transfer into an oil water emulsion. Firstly, they divided the scenarios into two kinds of emulsions: oil/water (oil dispersed in a continuous aqueous phase) and water/oil (water dispersed in a continuous oil phase). Each type of emulsion was then divided into two gas transfer scenarios: gas-to-continuous-to-dispersed phase and parallel transfer from the gas phase to both liquid phases. These scenarios are represented in Figure 2.3.

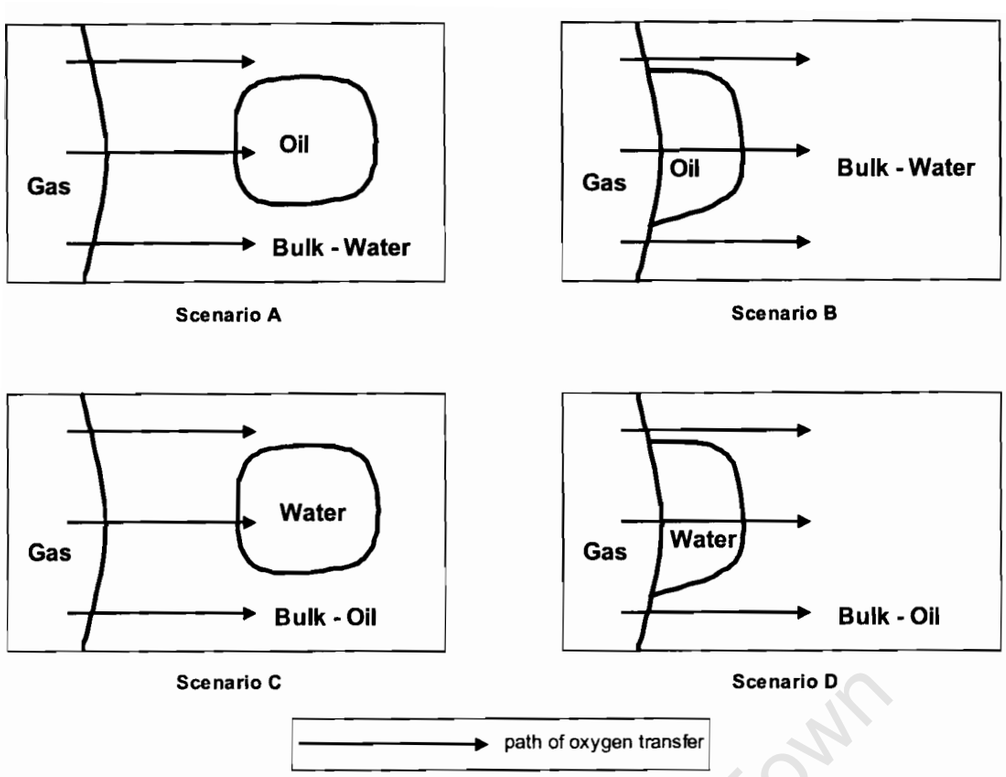

Figure 2.3: Possible gas transfer mechanisms into oil-water mixtures proposed by Linek and Benes (1976)

In order to predict which scenario is likely to arise, the volume fraction and spread coefficient of the oil are required. As discussed in Section 2.5.2.2, an oil phase with a negative spread coefficient will form discrete droplets. As seen in Table 2.3, most authors list n-C_{11-18} alkanes as having negative spread coefficients. Linek and Benes (1976) predict the transition from oil/water to water/oil emulsion as approximately 20-volume% n-alkane in 0.5M Na_2SO_4 aqueous solutions. Therefore, in mixtures containing less than 20% n-C_{12-13} alkane in water, as is of interest for this project, Scenarios A or B are most likely to occur.

Linek and Benes (1976) define $k_L{}^w$ as the mass transfer coefficient of oxygen (at the gas-water interface). The measured values of $k_L{}^w$ were not affected by alkane addition. Hence, the authors concluded that no direct contact between gas and negative spread coefficient oil phase exists in an oil/water emulsion. This would indicate that Scenario A is likely to predominate. However, Rols and Goma (1989) report that, in the case of a negative spread coefficient, the

oil forms a droplet floating on the bubble surface, which would seem to indicate the predominance of Scenario B.

Yamane and Yoshida (1970) showed that a small oil droplet reached oxygen equilibrium rapidly when placed in aqueous liquid. They concluded that the main resistance to oxygen absorption in the oil/water emulsion in an agitated system is in water film around gas bubbles. Mimura *et al.* (1969) assumed that the oxygen transfer rate from oil to water is faster than from air to oil. Therefore, assuming that oil droplets are impinged on the gas bubble surface, oil can act as an oxygen vector to facilitate overall air-to-water transfer.

The different findings of Linek and Benes (1976) who report $k_L{}^w$ as constant, and Hassan and Robinson(1977) and Rols *et al.* (1990) who report a change in K_La or k_La respectively as alkane is added, can be attributed to a change in a as a result of alkane addition. The alkane droplets affect the surface available for mass transfer from gas to liquid and therefore affect the bulk volumetric mass transfer coefficient observed. The trends in the change of overall volumetric mass transfer coefficient upon alkane addition are not consistent. Hassan and Robinson report a decrease in K_La as n-dodecane was added to distilled water. On n-dodecane addition to 0.15M Na_2SO_4 aqueous solution, K_La decreased, increased and then returned to its initial value as n-dodecane fraction varied from 0 to 10 volume %. In addition, these trends were different to those observed in similar experiments with n-hexadecane. Rols *et al.* (1990) observed k_La to pass through a maximum as n-dodecane was added to a glucose-based fermentation medium, up to 30-volume %. It is therefore apparent that K_La is dependent on the type of hydrocarbon added, the volume fraction of hydrocarbon, and the ionic strength of the medium that affects the alkane concentration at the interface.

The effect of alkane droplets on mass transfer in any given system is therefore not readily predicted. If droplets are highly mobile due to mechanical agitation and experience many collisions with air bubbles, the rate of mass transfer could be increased due to localised disturbances at the gas-liquid interface. Alternatively, if droplets are static and impinged on the bubble surface, they may increase the gas-liquid interfacial boundary layers and therefore reduce the measured oxygen transfer coefficient. The overall mass transfer coefficient and resulting oxygen transfer rate in a gas-liquid-liquid system is therefore likely to be determined by conflicting enhancement and retardation systems, most probably unique to the geometry of the system and the physical properties of the liquid present.

Even if $K_L a$ is reduced by the addition of alkane, addition of alkane can result in an increase in saturation concentration of the mixture, as the result of the high oxygen solubility in alkane (see Table 2.2). As a result, higher OTR values could be achieved (see Section 2.5.1.3). Oxygen transfer limitation due to lack of oxygen in the hydrocarbon backbone, and concomitant increase O_2 utilisation rates required, was identified as a potential process challenge to overcome in the biological conversion of alkanes to dicarboxylic acids (see Section 2.4). On the other hand hydrocarbons are recommended as oxygen vectors for overcoming microbial oxygen limitations in fermentations. The feasibility for overcoming oxygen transfer problems with the use of alkane will be explored in Section 2.6, by comparing literature findings with the interfacial interaction theory compiled in this document.

2.6 Theory of Gas-liquid-liquid-cell Mass Transfer in Fermentation of Hydrocarbon Assimilating Yeasts

In fermentation with live cells, the rate of change of dissolved oxygen in the medium is not dependent only on the oxygen transfer rate (OTR), but also on the oxygen utilisation rate (OUR) of the cells. Equation 2.22a can therefore be expanded to

$$\frac{dC}{dt} = OTR - OUR = K_L a(C^* - C) - OUR \tag{2.30}$$

If OUR is greater than OTR, oxygen limitation will arise. As discussed in Section 2.4, alkane fermentation has a higher oxygen mass transfer requirement when compared with carbohydrate fermentation, as there is no oxygen in the carbon source. It is therefore more likely that oxygen limitation can result.

In contrast, Ju *et al.* (1990) increased cell growth in penicillin fermentations by adding *n*-hexadecane. They attributed this to increased oxygen solubility in the fermentation medium due to the high solubility of oxygen in alkane. The oxygen solubility, C^*, in a mixture of immiscible liquid components can be

calculated according to the volumetric relationship (equation 2.31) proposed by Ju and Ho (1988). However, this equation does not take the location of the second liquid phase into account and will compute the same result for the same water/alkane ratio, irrespective of whether Scenario A or Scenario B predominates (Figure 2.3).

$$C^*_{overall} = \sum f_i . C^*_i \qquad (2.31)$$

where f_i = volumetric fraction of component i.

However, this equation does not take the location of the second liquid phase into account and will compute the same result for the same water/alkane ratio, irrespective of whether Scenario A or Scenario B predominates (Figure 2.3).

In recent years, there has been renewed interest in the use of hydrocarbon oxygen vectors in non-hydrocarbon assimilating biological processes. Jia *et al.* (1997) used *n*-dodecane to enhance biomass production of *Saccharomyces cerevisae*. Galindo *et al.* (2000) and Cordova-Aguilar (2001) worked with air-oil-aqueous-solid systems to simulate 4-phase fermentation broths so as to gain insight into the mass transfer mechanisms occurring. Both sets of researchers used castor oil with a positive spread coefficient as the oxygen vector. Galindo *et al.* (2000) showed photographically that the oil droplets spread to encapsulate the air bubbles. This agrees with Section 2.5.2.2 where literature stated that oil with a positive spread coefficient would spread at the gas-liquid interface. Oil with a negative spread coefficient is expected to form discrete droplets. It is possible that these droplets would also impinge on the bubble surface. Rols *et al.* (1990) observed *n*-dodecane droplet at the surface of air bubbles, giving credence to the idea that negative spread coefficient oils can behave in this way. Upon addition of surfactant, the spread coefficient increased (to a large positive number), thus enhancing spreading of the oil around the air bubble. The authors then proposed a path for oxygen transfer in *Aerobacter aerogenes* system consisting of gas-vector-water-cell. However, the proposal of this pathway was based on the assumption that *A. aerogenes* is only hydrophobic to a limited extent and that the cell would take up oxygen from the aqueous phase. This scenario may change in the case of a more hydrophobic organism, such as hydrocarbon-assimilating *Candida tropicalis* used in the biological conversion of alkanes to dicarboxylic acids.

Mimura *et al.* (1973) noted that hydrocarbon-assimilating yeasts attach to droplets of oil, and these "flocs" of cells and oil then adsorb onto the surface of

air bubbles. As a result, the measured value of K_La decreases since the cells essentially block the transfer of oxygen from the gas to the bulk (aqueous) liquid phase. However, the growth rate of cells did not appear to be oxygen limited, and hence it was suggested that the cells in fact take up oxygen directly from the hydrocarbon by chemical adsorption. Upon addition of antifoam, surface modification of the air bubbles prevents the cells from adhering to the bubble surface. These become dispersed in the fermentation liquid. The measured value of K_La increases. It was not clear how this affected cell growth. In general, without the presence of antifoam, these "flocs" were formed during the exponential growth phase of the fermentation. As the hydrocarbon was exhausted, the cells became dispersed in the fermentation medium. Yoshida *et al.* (1977) observed similar behaviour. Lower values of $(k_La)_{gw}$ and $(k_La)_{ow}$ and a higher value of $(k_La)_{go}$ were observed during the growth phase of *Candida rugosa* (where the subscripts g, o and w refer to interfaces of gas, oil and water respectively). In the lag and stationary phases, the cells were dispersed. During cell growth, the measured rate of oxygen uptake from the hydrocarbon phase was greater than that from the aqueous phase, most likely facilitated by the higher gas-oil oxygen transfer coefficient, $(k_La)_{go}$. Mimura *et al.* (1973) proposed a possible path for oxygen transfer in submerged hydrocarbon fermentation with yeast, in which the cells take up oxygen via direct adsorption from the common liquid film, and not from the bulk liquid phase, as shown in Figure 2.4.

The amount of hydrocarbon added can also play an important role. The hydrocarbon must be present in sufficient quantity to satisfy the metabolic requirements of the organism. Hydrocarbon availability in excess of this requirement may allow for easier oxygen adsorption by the cells, straight from the hydrocarbon phase. However, caution must be employed, as excess hydrocarbon could be toxic to the cells or result in substrate inhibition.

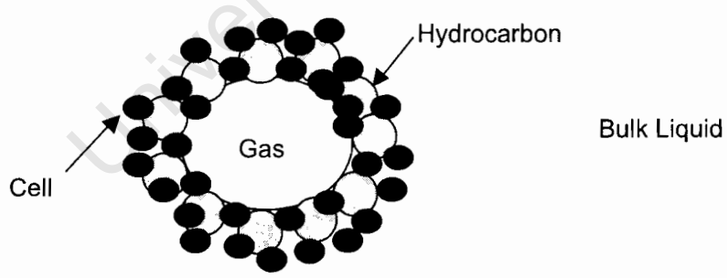

Figure 2.4: Mass transfer of Oxygen to Cells in Hydrocarbon "Flocs" on the Air Bubble Surface

Another point of concern in fermentation is the effect of additives, such as antifoams. While Mimura *et al.* (1973) observed that antifoam caused cell dispersion, it was not clear if this had adverse effects on the ability of *Candida* cells to absorb oxygen from the hydrocarbon "flocs" during the growth phase. Uchio and Shiio (1972c) noted that the addition of antifoam stimulated the production of dicarboxylic acid in *Candida cloacae*. It must be noted that dicarboxylic acid production was induced in this case during the stationary phase, after the cell growth phase. It is therefore possible that this reduced product accumulation near the cells and therefore reduced product inhibition.

2.7 Hypotheses

It is therefore clear that there are many parameters that require optimisation in the successful bioconversion of alkanes to dicarboxylic acids. Judicious choice of fermentation parameters may enable the supply of an adequate OTR, while minimising the adverse effects of shear damage and toxicity to yeast cells. In order to expedite the prediction of such parameters, investigation of both cell behaviour and fluid dynamics and mixing will be required. The following hypotheses are proposed:

- *Candida tropicalis* ATCC 20962, a genetically modified hydrocarbon-assimilating yeast, can be used to convert a C_{12-13} *n*-alkane cut to C_{12-13} dioic acid. The β-oxidation pathway has been blocked in order to allow accumulation of dicarboxylic acid as an intermediate product in the metabolism of alkanes. Glucose is a suitable co-substrate for the completion of the respiratory cycle of the organism, but optimisation of other medium components, such as nitrogen source, will require further investigation.
- A key concern in the biological conversion of alkanes to dicarboxylic acids is that of oxygen transfer in a system containing immiscible liquid phases. Oxygen transfer in a simplified air-aqueous-alkane system can yield insight into the mass transfer pathways occurring in a fermentation containing immiscible phases. It is likely that alkane droplets will impinge on the gas bubble surface, and that the alkane can act as an oxygen vector to facilitate overall air to water transfer. The mass transfer coefficient observed will be dependent on the type of hydrocarbon added, the volume fraction of hydrocarbon, and the ionic

strength of the medium, as this will affect the spreading of the alkane droplets and hence the surface area available for mass transfer. In addition, the overall mass transfer coefficient in an air-aqueous-alkane system is likely to be determined by the effect of turbulence induced by mechanical agitation and aeration on the boundary layer interfacial properties. This will most probably be unique to the geometry of the system and the physical properties of the liquid present. Even if mass transfer coefficient is reduced to some extent by the addition of alkane, addition of alkane can result in an increase in saturation concentration of the mixture and higher OTR values can still be achieved.

- In the biological conversion of alkanes to dicarboxylic acids, alkane could act as an oxygen vector and improve oxygen transfer to the cells. It is likely that cells take up oxygen via direct adsorption from the common liquid film at the air-alkane interface, and not from the bulk aqueous phase. Careful selection of fermentation parameters could balance the advantage gained by using an oxygen vector with that gained by mixing. Increasing agitation may result in increased shear damage to the cells, while excess hydrocarbon could be toxic to the cells or result in substrate inhibition.

3. Review of Analysis of Yeast Behaviour during the Production of Dicarboxylic Acids and Experimental Techniques for Oxygen Transfer Measurement

In Chapter 2, the concept of production of dicarboxylic acids via alkane fermentation was introduced. In order to produce these dicarboxylic acids, alkane-assimilating yeast is required. This yeast requires a growth medium containing alkane and a carbohydrate co-substrate, as well as a variety of other nutrients essential for healthy cells. In addition, various process challenges were discussed, most of which arose due to mixing or mass transfer problems surrounding the presence of an immiscible hydrocarbon phase in an otherwise aqueous medium. The purpose of this chapter is to explore the options surrounding cultivation of hydrocarbon assimilating yeasts, as well as specialised equipment and analytical techniques that will be required to measure yeast behaviour in hydrocarbon fermentation.

3.1 Analysis of Yeast Behaviour in Different Media

The type of medium used for cell culture is of vital importance for obtaining optimum cell growth, and where relevant, product secretion. The medium needs to contain a carbon source, a nitrogen source, trace vitamins and minerals, and buffer salts to maintain the correct pH. The macronutrient composition of some media used by authors to culture *Candida* species are compared in Table 3.1. The UFS (University of the Free State) medium was used for growth and maintenance of a wild-type *Candida maltosa* species that did not produce dicarboxylic acid, while the other media presented were used for dicarboxylic acid production from alkane.

3.2 Process Conditions in Similar Dicarboxylic Bioprocesses

Most bioprocesses presented in Table 3.1 are carried out at atmospheric pressure and a temperature of about 30°C. Medium pH is also of vital importance in dicarboxylic acid fermentations, due to the acidic nature of the product. Most studies presented in Table 3.1 used various sulphate, nitrate and phosphate salts to facilitate buffering capacity. In addition, different pHs

were used for cell growth phase and dicarboxylic acid production phase. Uchio and Shiio (1972c) used a pH of 6.5 for the growth phase. The pH was then raised slightly to 7.75 by adding NaOH to achieve the level optimum for dioic acid production from the alkane. Picataggio *et al.* (1992), Hill *et al.* (1986) and Jiao *et al.* (2001) raised the pH in a similar manner to induce dicarboxylic acid production by *Candida*.

Table 3.1: Comparison of Media Types and Fermentation Conditions for Candida

Author	UFS	Hill *et al.*	Jiao *et al.*	Picataggio *et al.*	Uchio & Shiio
Year		1986	2001	1992	1972 (c)
Organism	*C. maltosa*	*C. tropicalis*	*C. tropicalis*	*C. tropicalis*	*C. cloacae*
Volume (l)		6.5	22	15	0.3
Agitation (rpm)		600	-	1300	1400
Aeration (vvm)		1	-	1	0.5
Temperature (°C)	25	32	30	30	30
Carbon Source	Glucose	Glycerol Polypropylene Glycol	Sucrose	Glucose	Sucrose
Nitrogen Source	Peptone Yeast Extract	Peptone Yeast Extract Corn Steep Liquor	Urea Yeast Extract	YNB Yeast Extract	NH4 Acetate
Salts		$(NH4)_2SO_4$ NH_4NO_3 $Na_2HPO_4.H_2O$ $MgSO_4.7H_2O$ KCl MnCl2 ZnSO4 $FeSO_4.7H_2O$	$(NH4)_2SO_4$ KH_2PO_4	$(NH4)_2SO_4$ KH_2PO_4 K_2HPO_4	$(NH_3)_2HPO_4$ KH_2PO_4 $MnSO_4.nH_2O$ $ZnSO_4.7H_2O$ $FeSO_4.7H_2O$ $MgSO_4.7H_2O$
Vitamins			B1		Biotin
Growth Phase Time (h)	24-48	20	20	18	16 - 40
Growth pH	6	6.5	6.5	6.5	6.5
Dioic Acid Production pH		8	8	8.3	7.75
C:N (excluding alkane)	6.5	-	8.3	13.75	1.5
Alkane Addition		6% for Growth	At pH Change	At pH Change	Growth Phase
Alkane		C11-16	C13	C13	C11-18
Volume %		1.0-16	10 - 15	0.5-3.0	10
Dioic Acid Product		C11-16	C13	C13	C11-18
Dioic Acid Yield (g/l)		36 - 64	22	120	13 - 50

Hill *et al.* (1986) added 6% of the total alkane for the growth phase, and the remaining 94% at the time of pH change. Uchio and Shiio (1972c) added all their alkane substrate at the beginning of the growth phase, whereas the other authors added all alkane on raising the pH, after the growth phase. This could account for the low C:N (carbon: nitrogen) ratio of the medium used by Uchio and Shiio (1972c). C:N ratio was calculated excluding alkane, but in the case of Uchio and Shiio, the alkane was present during the growth phase, providing additional carbon.

Most authors used multiple-stage inocula in their preparation for fermentation. Picataggio *et al.* (1992), Hill *et al.* (1986) and Uchio and Shiio (1972c) inoculated a loop full of cells into a small vessel with medium and grew this up for about 24 hours. The contents of the small vessel were then added

aseptically to a large vessel of medium. The volume added from the small vessel comprised 10%, 8% and 5% of the medium volume in the large vessel, for the three research groups respectively. The cells were then grown up again in the large vessel, before the pH was raised to induce dicarboxylic acid production. Picataggio *et al.* (1992) raised pH after 18 hours of growth, while Hill *et al.* (1986) waited 20 hours. Uchio and Shiio (1972c) waited between 16 and 40 hours.

3.3 Sampling and Recording of Bioprocess Information

In order to monitor the bioprocess, it is important to sample at regular intervals and analyse these samples. Probes can measure dissolved oxygen, temperature and pH and readings can be logged by the bioreactor indicator/controllers. However, some important information can only be obtained by physically sampling the fermentation medium. Important information for monitoring a dicarboxylic acid biotransformation includes analysis of cell biomass production, alkane utilisation and dicarboxylic acid production. However, some deviations from conventional analytical techniques are required, due to the presence of immiscible liquid phases.

3.3.1 Analysis of biomass production

Solid particles can be separated from liquid via filtration or centrifugation. Laboratory analysis of cell biomass in fermentations employs these basic techniques, but an organic solvent is required to dissolve the alkane, especially given that the cells are proposed to adhere to the alkane, as outlined in Section 2.6. Jiao *et al.* (2001) centrifuged the sample, using ethanol, *n*-butanol, chloroform and water to wash the alkane from the cells, in order to facilitate good liquid-cell separation.

3.3.2 Analysis of substrate utilisation and product formation

The alkanes, intermediates, and dicarboxylic acid products can be analysed by Gas Chromatography (GC). Both slightly polar and non-polar columns can be suitable for this purpose, but different temperature programming will be required. When using a Flame Ionization Detector (FID), the amount of any compound present can be determined by referencing the peak size from

internal standard (as used by Chan and Kuo, 1997), or by creating a standard calibration curve (as done by Uchio and Shiio, 1972a). For either method, the residence times of the compounds of interest must be known. If GC-MS (mass spectroscopy) is used, unknown compounds can also be identified.

In general, it is best to view the methyl ester derivatives of the intermediates (consisting of alcohols, carboxylic acids, hydroxycarboxylic acids and diols) and the dicarboxylic acids. Therefore, a methylating agent is required. Uchio and Shiio (1972a) used diazomethane to methylate their dicarboxylic acid samples, but this is highly toxic and decomposes quickly. A possible alternative is to use BF_3/14% in methanol for preparing methyl esters, as used by Green *et al.* (2000).

Extraction of alkanes and dicarboxylic acids from the fermentation medium is not trivial, as alkane is in an organic phase, while dicarboxylic acid can be present in the aqueous phase or extracted with a suitable organic solvent. Chan and Kuo (1997) and Uchio and Shiio (1972a) used fairly similar methods to achieve the extraction. Firstly, the sample pH was raised from 7.5 to allow dissolution of the dicarboxylic acids into the aqueous phase. (At this stage, the cells were also extracted, if they had not been removed in an earlier step). Then, an organic solvent, such as ether, was added, and the pH lowered, causing the dicarboxylic acids to move from the aqueous phase to the organic phase. The organic phase, containing both the alkanes and the dicarboxylic acid, could be separated. An esterifying agent was added to the organic solution before injection into a suitable GC for quantitative analysis of both alkanes and dicarboxylic acids.

3.4 Oxygen Transfer Measurement in Fermentations

There are a number of methods for measuring oxygen transfer in biological reactors. Some methods can be applied during fermentation, but it is often useful to apply these methods to non-fermentative systems that simulate certain aspects of fermentation as process conditions can be changed over a larger range, without affecting the biomass. In this section, use of the "Sulphite", "Oxygen Balance" and "Gassing Out" Methods for measurement of oxygen transfer will be discussed, as well as the advantages and problems that can occur with each method.

3.4.1 Sulphite method

The "Sulphite" method is derived from the use of a gas-liquid reaction to consume O_2 (Bailey and Ollis, 1986). It is only suitable for measurement of oxygen transfer in a non-fermentative system. Sodium sulphite is added and the following reaction occurs in the presence of oxygen and a metal catalyst such a Co^{2+} or Cu^{2+}:

$$Na_2SO_3 + ½O_2 \rightarrow Na_2SO_4 \qquad (3.1)$$

With reference to equation 2.22 a, it is assumed that $C=0$ since all oxygen present is consumed instantaneously by the chemical reaction. Hence OTR equals the product of K_La and C^*, and this is equal to the rate of the chemical reaction and OUR is restricted by OTR. If C^* is known, and the reaction rate can be measured, K_La can be determined.

This method is not without drawbacks. While the reaction could occur in the film surrounding the bubbles, and therefore not adequately represent the transfer of oxygen to the bulk liquid, it is possible that it could represent the manner in which more hydrophobic cells take up oxygen, as discussed in Section 2.6. However, the rate constant for the reaction depends on many other factors, such as the catalyst, the ionic strength of the medium, and the pH, all of which could affect the accuracy of the method.

3.4.2 Oxygen balance method

The Oxygen Balance Method (or Steady State Method) is used to measure oxygen transfer in a steady-state fermentative system by means of a mass balance (Doran, 1997). Applying fundamental mass balance principles at steady state, the difference between the oxygen flow into the reactor and the oxygen flow out of the reactor, must equal the oxygen utilisation rate (OUR) of the process. Therefore, according to Bailey and Ollis (1986):

$$OUR = [Q_{gas\text{-}in} \cdot p_{O2\text{-}in} - Q_{gas\text{-}out} \cdot p_{O2\text{-}out}]/VRT \qquad (3.2)$$

where Q = volumetric gas flow rate

p_{O2} = oxygen partial pressure

V = bioreactor volume

R = universal gas constant

T = system temperature.

OUR can be determined from analysis of the flow rate and oxygen concentration of the streams coming into and exiting the bioreactor. From the steady state assumption applied to equation 2.30, it follows that $OUR=OTR$, and hence $OUR=K_La(C^*-C)$. C^* can be determined from literature, and C can be measured by means of a submerged oxygen probe in the bioreactor, and hence k_La can be determined.

This method requires uniform mixing throughout the bioreactor, and accurately calibrated gas analysis equipment, both inside the liquid of the bioreactor, and on the gas streams entering and exiting the bioreactor. As a result, the "Oxygen Balance" method is often passed over in favour of the "Gassing Out" Method, as the latter requires only a submerged oxygen probe and can be applied to both fermentative and non-fermentative systems.

3.4.3 Gassing out method

The "Gassing Out" method is also known as the "Unsteady State" method (Shuler and Kargi, 1992) or the "Dynamic" method (Bailey and Ollis. 1986). The method makes use of a polarographic oxygen probe to measure dissolved oxygen concentration in the fermentation medium. The oxygen concentration of the medium is first lowered. This can be achieved either by sparging with nitrogen in a non-fermentative system (gassing out), or by stopping the oxygen flow and allowing the microorganisms to deplete the oxygen in a fermentative system. In the case of a fermentative system, the rate of oxygen depletion will equal OUR, but caution must be employed as the dissolved oxygen does not drop below the critical value to prevent oxygen limiting conditions. In a non-fermentative system, OUR is taken as zero, as discussed in Section 2.6.

The next step is then to re-start the air (or oxygen) flow and measure the change in oxygen concentration with time. An expression for the rate of change of oxygen concentration equals was derived in Section 2.6:

$$\frac{dC}{dt} = OTR - OUR = K_L a(C^* - C) - OUR \qquad (2.25)$$

Since C and t are measured variables, and OUR and C^* are known constants, $K_L a$ (and hence OTR) can be determined.

The "Gassing Out" method, while relatively simple to implement, is not without its pitfalls. The main cause for concern surrounds the use of polarographic oxygen electrodes and electrode response time. Probe response delay arises due to the time taken for oxygen to diffuse across the probe membrane to the cathode, where the oxygen is reduced and produces a current proportional to the partial pressure of dissolved oxygen (or the dissolved oxygen tension). In general, the rate of reaction at the cathode is so fast that it is limited by the rate of diffusion of oxygen to the cathode (Ruchti *et al.,* 1981). In general, however, probe response time, τ_e, can be considered negligible if the following criterion is satisfied (Badino *et al.*, 2000):

$$\tau_e = 1/k_e << 1/k_L a \qquad (3.3)$$

τ_e is defined as the time taken for the probe to reach 63% of oxygen saturation as a response to a step input.

The response time delay also becomes important during "gassing out" with nitrogen. The dissolved oxygen in the medium may fall slightly lower than the dissolved oxygen reading on the probe (Tribe *et al,* 1995), which can result in oxygen limitation of microorganisms. In addition, reproducibility of mass transfer data obtained is often a problem due to the fact that measurements are taken at unsteady state. Therefore, it is best to measure the rate of change between 2 consistent steady states. An example of this would involve sparging with nitrogen until a steady state of zero oxygen content is attained, and then sparging with air and measuring the rate of change until a new steady state of oxygen saturation is achieved. This is of course more difficult in a fermentative system, as the oxygen level must not drop below the critical value.

In addition, it must be considered that the electrodes are not measuring oxygen concentration, but rather oxygen partial pressure (Johnson *et al.*, 1964). Polarographic oxygen electrodes can therefore not be used to determine saturation concentration.

The final point of concern regards the use of submerged oxygen probes in 3-phase gas-liquid-liquid systems, due to the fact that the liquid phases are immiscible. Hassan and Robinson (1977) note that dissolved oxygen tension is the same in all 3 phases at equilibrium. However, during the unsteady-state "Gassing Out" method, this is unlikely to be the case, but the probe is most likely to respond to the dissolved oxygen tension of the bulk aqueous phase. Therefore, the probe is measuring overall oxygen transfer from the gas phase to the aqueous liquid, including both the component of oxygen transferred directly from the gas to the aqueous phase, and the component of oxygen transferred from the gas to the aqueous phase, via alkane oxygen vectors. It is therefore appropriate to use this method for determination of $K_L a$ and OTR in alkane bioprocesses.

3.5 Development of Experimental Methods

It is clear that are were certain practical issues that would require resolution before conducting research towards finding a viable procedure for converting alkanes to dicarboxylic acids in a biological process. Customised experimental techniques using the information presented in this chapter need to be developed in order to study media optimization with respect to cell growth and dicarboxylic acid production, and for the study of mass transfer in a typical bioreactor in order to determine if the oxygen demand of the organism could be satisfied. Any experimental program would also need to link to the issue of mass transfer in the context of alkane dispersion, and how this is related to mixing phenomena, fluid dynamics and air-aqueous-alkane-cell contact, as discussed in Section 2.6. The formulation and compilation of suitable experimental techniques is presented in Chapter 4.

4. Experimental Methods

An experimental program was developed in order to investigate the factors hypothesised to affect successful conversion of alkanes to dicarboxylic acids. Investigation of the hypotheses proposed in Section 2.7 required the study of media optimization with respect to cell growth and dicarboxylic acid production, and development of a method for quantifying mass transfer in a typical bioreactor, specifically to determine if the oxygen demand of the organism could be satisfied, either through mechanically induced turbulence or the use of alkane as an oxygen vector. Following on from Chapter 3, it becomes clear that there are a number of practical issues that need to be resolved in order to quantify the necessary experimental observations. The experimental program therefore needed to be divided into two distinct aspects.

The one aspect involved the shake flask culture of yeast to determine the growth patterns and dicarboxylic acid production capabilities various media, by varying pH, nitrogen source and carbohydrate level.

The second aspect of the experimental program was that of mass transfer, which was investigated in a cell-free system. A cell-free system was used in order to obtain more reproducible measurements of K_La and C*, their corresponding influence on the OTR in hydrocarbon-based bioprocesses, as any variation due to cell behaviour was eliminated. Such a system provides a convenient generic base for the evaluation and the establishment of conditions for optimum operation of bioprocesses based on a hydrocarbon feedstock.

4.1 Bioconversion of Alkanes by Candida tropicalis for Dioic Acid Production

4.1.1 Microorganism

The organism used was a genetically modified dicarboxylic acid producing yeast. The specific strain used, *Candida tropicalis* ATCC 20962, was developed by Picataggio *et al.* (1992).

4.1.2 Media

Media used for storage and maintenance of stock cultures are detailed in Appendix I. Several media were used for shake flask experiments. These were based largely on the UFS medium and the Picataggio *et al.* (1992) medium as outlined in Table 3.1, since both of these were glucose- and yeast extract-based media, but with different nitrogen sources for comparison. The former contained organic nitrogen in the form of peptone, while the latter contained inorganic nitrogen in the form of Difco® YNB.

The cheaper YP (Yeast Peptone) from UFS consisted of the following:

- Peptone 10g/l
- Yeast Extract 10g/l
- Carbon Source 40g/l (glucose)

A more expensive YNB medium based on work by Picataggio *et al.* (1992) was also used:

- Difco® YNB (with amino acids) 6.7g/l
- Yeast Extract 3 g/l
- $(NH_4)_2SO_4$ 3 g/l
- K_2HPO_4 1 g/l
- KH_2PO_4 1 g/l
- Glucose 75 g/l

The bulk component in YNB is ammonium sulphate (Appendix I), which acts as a nitrogen source. In most experiments, YNB medium was used for pre-culture, while the main culture media were modified from this basis in order to investigate the role of carbon and nitrogen sources. The YNB medium was modified as shown in Table 4.1 for medium comparison experiments.

Media was autoclaved at 115°C for 20 min. The initial pH of the media (after sterilisation) was set to 6.5. Alkane and heat labile compounds (as contained in YNB) were filter sterilised and not heat sterilised.

Table 4.1: Modifications to YNB Medium for Comparative Studies

	Medium 1	Medium 2	Medium 3	Medium 4	Medium 5
	(g/l)				
YNB	6.7	6.7	-	6.7	-
Peptone	-	-	9.64	-	9.64
Yeast Extract	3	3	3	16	16
Glucose	75	40	75	75	75
$(NH4)_2SO_4$	3	3	3	3	3
KH_2PO_4	1	1	1	1	1
K_2HPO_4	1	1	1	1	1
C:N	13.75	7.53	13.75	7.53	7.53

*The carbon and nitrogen contribution of YNB, yeast extract and peptone towards carbon: nitrogen ratio (C:N) was calculated according to detailed chemical composition provided by the supplier (see Appendix I).

4.1.3 Alkane substrate sources

Pure dodecane (≥98% purity) was obtained from Fluka. The mixed C_{12-13} alkane obtained from Sasol Ltd contained 38% *n*-dodecane and 51% *n*-tridecane.

4.1.4 Shake flask experiments

A single-stage inoculum was employed for all shake flask experiments. A loop of cells taken from the stock culture maintained as solid medium (Appendix I) was used to inoculate a shake flask of either YP or YNB medium and grown overnight. This pre-culture was then inoculated aseptically into the main culture.

4.1.5 Analysis

The following analyses were developed from generally accepted laboratory practices at the University of Cape Town and the University of the Free State,

combined with the techniques presented in Section 3.3, and were used to analyse the progress of shake flask experiments.

4.1.5.1 Optical density

Optical density measurements were performed as an indication of cell growth. Specifically, readings were taken immediately before and immediately after substrate addition in order to examine any effect of substrate on turbidity.

The samples were prepared for turbidity analysis as follows:

In an Eppendorf, 500µl of sample was added to 200µl of cyclohexane, to dissolve residual alkane, and 100µl of 5M NaOH, to promote dissociation of the dioic acid in the aqueous phase. This was vortexed for 5 min and then centrifuged for 10 min at 60000 $m.s^{-2}$. The supernatant was discarded and the pellet re-suspended in 500µl of physiological salt (0.9% NaCl) solution.

The spectrophotometer tare was set with a sample of 0.9% NaCl solution. The absorbance of a well-agitated sample at 620nm was determined. This sample was diluted by a recorded factor until the absorbance reading was below 0.8, as absorbance readings are linear with respect to cell concentration in the range of 0 to 0.8. The effect of budding on turbidity measurements has not yet been established.

4.1.5.2 Cell dry mass

4ml of agitated sample was added into each of 3 test tubes. The sample was filtered using filter papers with a pore size of 0.45µm pre-weighed to 4 decimal places. The supernatant was collected and retained for the glucose assay (Section 4.1.4.5). The cells remaining on the filter paper were washed 3 times with an organic solvent to remove residual alkane, as described in Section 3.3.1,. The first wash consisted of 4ml distilled water, 2ml of cyclohexane and 400µl of 5M NaOH. The second wash consisted of 6ml of distilled water and the third wash consisted of 20ml distilled water. The filter papers were then placed in an 80°C oven for 48 hours, before being weighed again to 4 decimal places.

4.1.5.3 Cell viability

Samples for cell counting were also taken from the flasks used for biomass measurements and viewed under an Olympus BX40 System microscope. The cells were counted using a haemocytometer. A grid is visible and the numbers of cells in various squares on the grid were counted. If there are too many cells to count, the solution should be diluted by a known factor. Then, if the area of the squares and the depth of the chamber are known, the cell concentration can be calculated by

$$concentration = \frac{cells}{area \cdot depth} \cdot dilution \qquad 4.1$$

Cells were also photographed with an Olympus U-TVO-5XC Soft Imaging System.

4.1.5.4 Alkane utilisation and dioic acid formation

This method was developed by the University of the Free State, but employs a similar technique to those used by Kuo (1997), Green *et al.*(2000) and Uchio and Shiio (1972a), as discussed in Section 3.3.2. The method employs an acidifying step to remove the dioic acids from the aqueous phase, and ether (containing known quantities of internal standards) as a solvent to extract the alkanes and the dioic acids.

Aliquots (500µl) of the fermentation broth samples were placed into Eppendorf tubes. These were then acidified to pH3 with 1M HCl (usually about 50µl is required).

Internal standards of 500mg of undecanol and 500mg of C14 carboxylic acid were dissolved in 50ml of tertiary butyl methyl ether. 300µl of this mixture was then added to the acidified samples in order to extract the alkanes and the dioic acids (and most intermediates). The Eppendorfs were vortexed for 5 min and centrifuged for 10 min at 60000 $m.s^{-2}$. The top organic layer was extracted and placed into a new Eppendorf tube. The extraction process was then repeated and the extracts pooled.

The combined extracts (50µl) were removed and methylated with trimethylsulphonium hydroxide (TMSH) (50µl). This mixture was agitated and 2µl injected into the GC.

The GC was set up as follows:

Column:	HP-Wax Bonded Polyethylene Glycol (or equivalent)
	Macro bore 30m x 530µm x 1µm
Head Pressure:	3.6 psi
Split:	5:1
Carrier Gas:	N_2 38.4 ml/min
Detector:	350°C
Flame Gas:	H_2 at 35ml/min
	Air at 380 ml/min
Oven:	120°C held for 5 min
	Increment 10°C/min to 260°C
	Held for 7 min

The retention times for important compounds are as follows:

n-Dodecane (C12)	-	1.9 min
n-Tridecane	-	2.2 min
Undecanol	-	9.6 min
C14 carboxylic acid methyl ester		- 11.6 min
Dodecane dioic acid methyl ester		- 16.4min

In cases of higher acid concentration methylation was sometimes incomplete and a large peak was observed at 23 min. In this case, a further 50µl tertiary butyl methyl ether (without internal standards) and 50 µl TMSH were added and the sample injected a second time.

The standard curves used for quantitative calibration of the GC peaks obtained are available in Appendix II.

4.1.5.5 *Analysis of carbohydrate usage*

The glucose concentration was determined using the reducing sugar method, DNS (Dinitrosalicylic Acid) Assay, based on the method by Miller (1959).

DNS reagent consists of the following:

10.6 g 3,5 Dinitrosalicylic acid

19.8 g NaOH

306 g Rochelle salts (Na K Tartrate)

7.6 g Phenol

8.3 g Na-metabisulphite

1416 ml Distilled water

The first 3 reagents were dissolved completely in water before adding the other constituents and dissolving them in turn. The phenol was melted at 50 ℃.

The pH of the solution was adjusted by placing a 3 ml sample in a test tube and adding a drop of phenolphthalein. 0.1 M HCl was added drop-wise to reach neutrality (pink). If the pH was correct, 5 to 6 ml of the 0.1 M HCl solution was required. If the solution turned pink with the addition of less than 5ml HCl, 2g NaOH was added to the DNS reagent for every 1ml of HCl below this limit. The titration was repeated until 5 to 6 ml HCl was required.

To perform the analysis, 200 µl sample (collected as in Section 4.1.4.2) was added to 600 µl DNS reagent in triplicate. The mixture was boiled rapidly in a water bath for exactly 5 min and cooled on ice. 3200 µl distilled water was then added and the absorbance was read at 510 nm against a blank of distilled water. The analysis was conducted in triplicate. A standard curve was used for quantitative calibration and is shown in Appendix II.

4.2 *Investigation of Mass Transfer in a Cell-Free System*

In Chapter 2 we derived an expression for OTR relating it to concentration gradient and interfacial area by means of an overall volumetric liquid-phase

mass transfer coefficient, K_L. The following formula is used to model this process:

$$OTR = K_L a(C^* - C) \tag{2.22a}$$

where OTR = oxygen transfer rate $\left[\frac{mass}{volume \cdot time}\right]$

a = gas-liquid interfacial area per unit volume $\left[\frac{area}{volume}\right]$

C^* = weighted average saturation concentration of oxygen in liquid phase as calculated by equation 2.31 $\left[\frac{mass}{volume}\right]$

C = actual concentration of oxygen in liquid phase.

As discussed in Chapter 2, increasing K_L, a or C^* can therefore increase OTR. There are a variety of factors that affect these variables. Increased aeration and agitation increase gas hold-up and decrease bubble size, thereby increasing *a*. Decreased viscosity of the liquid medium can reduce stagnant boundary layers and improve mass transfer through K_L. These factors are however interrelated as the properties of the fluid also affect bubble formation (and hence a), while turbulence can also affect boundary layer formation (and hence K_L). Correlations for mass-transfer coefficients are therefore often given as a combined parameter, $K_L a$.

4.2.1 Measurement of $K_L a$

The method chosen for $K_L a$ measurement is known as the "Unsteady-state gassing Out" method, as discussed in Section 3.4.3. This method was chosen as it is suitable for a cell-free system and the purpose of the mass transfer experiments was to provide insight into oxygen transfer in a system containing immiscible liquid phases, by means of a simplified air-aqueous-alkane system. This method was chosen over the "Sulphite Method" described in Section 3.4.1 as the "Sulphite Method" measures the rate of a chemical oxidation reaction and assumes that this is limited only by the rate of oxygen transfer. This introduces some error into the method as the reaction

rate can also be affected by other factors, such as the catalyst used. The "Gassing Out" method measures dissolved oxygen tension in the bulk medium directly. Since $OTR = dC/dt$, by integrating equation 2.22a, the following relationship is obtained:

$$ln(1-C/C^*) = -K_La \cdot t \qquad (4.2)$$

A plot of $ln(1-C/C^*)$ as a function of time, t, will have a slope equal to $-K_La$. K_La values can be obtained by measuring the rate of change of the dissolved oxygen concentration, for a specific set of process conditions (aeration, agitation and alkane concentration).

Experimental work was performed in a bench-scale bioreactor to study the mass transfer coefficients and the oxygen transfer rates attainable in a mixture of water and Sasol C_{12} to C_{13} alkane cut. No yeast is required at this stage. The process conditions, alkane concentration in water, agitation rate and aeration rate, were varied across the range shown in Table 4.2. All possible combinations of these variables were used. The experiments were performed in a 5-litre New Brunswick bioreactor. The actual working volume used was 4.25 litres to provide the specific geometry shown in Figure 4.1.

Table 4.2: Table of Process Conditions used to gather Mass Transfer Data

Alkane Concentrations	**Agitation Rates**	**Aeration Rates**
(volume % in water)	(rpm)	(vvm)
0	200	0.5
2.5	400	0.75
5	600	1.0
10	800	1.25
15	1000	1.5
20	1200	

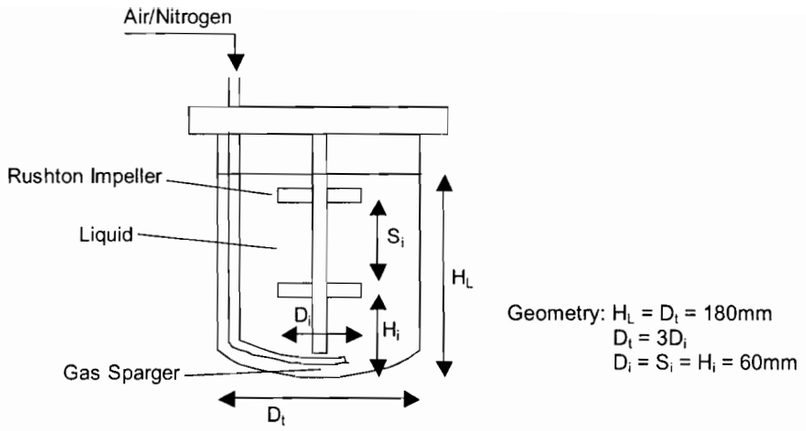

Figure 4.1: Geometry of Experimental System

The unsteady state "Gassing Out Method" was used to calculate the K_La of the water/alkane mixtures in order to quantify the effect of the process conditions on K_La, and hence OTR, as in equation 2.22a. A submerged polarographic dissolved oxygen electrode was used to measure dissolved oxygen as a percentage of saturation (%DO). The dissolved oxygen sensor used was a Mettler Toledo/Ingold® Inpro® 6000 Series with a 12mm T-96 Teflon membrane, as Teflon membranes are more durable in hydrocarbon than Silicon membranes. Before use, the electrode was connected to a power source for 6 hours in order to polarize completely. The probe was then calibrated. To do this, the liquid medium was agitated and sparged with nitrogen until a minimum voltage reading was obtained. This reading was then taken as 0% dissolved oxygen. Thereafter, the liquid medium is sparged with air at a suitable agitation and aeration rate. The liquid was considered saturated with oxygen when equilibrium was reached and the voltage reading no longer changed with time. This voltage reading was taken as 100% dissolved oxygen, which corresponds to a saturated oxygen concentration of 8.05mg/l (C^*) in water at atmospheric conditions and 30°C.

After calibration, the "Gassing Out Method" was employed at all combinations of the process conditions shown in Table 4.2. The liquid medium was sparged with nitrogen until 0% DO was reached. For the purposes of experimental reproducibility, it was important to ensure that the system was at steady state at this point, with agitation and gas flow maintained at the desired rate. A 3-way valve was then used to switch the nitrogen flow instantaneously

to air, and the increase in %DO was monitored with respect to time, until 100% DO was reached. The nitrogen and air flowrates were equal on a volumetric basis in order to minimize any pressure changes during the transition, as pressure influences the saturation concentration of gases in liquids. The entire process was also controlled at a temperature of 30.0°C, as temperature also influences saturation oxygen concentration and K_La through liquid viscosity.

4.2.2 Estimation of OTR

Solubility (C^*) of oxygen can be affected by changing the composition of the medium. Makranczy *et al.* (1976) lists the solubility of oxygen in C_{12} to C_{13} n-alkanes as approximately 250 mg/l at 30°C and 1 atm (oxygen pressure). This value was used in calculation of C* for alkanes in order to ensure that the OTR would not be overestimated, as it was the lowest reported value (Table 2.2). The solubility of oxygen in water was taken as 38.4 mg/l at 30°C and 1 atm (oxygen pressure) (Doran, 1992). It can therefore be noted that oxygen is 6 times more soluble in this alkane than in water under these conditions.

C^* in a mixture of immiscible liquid components can be calculated according to the volumetric relationship proposed by Ju and Ho (1988) as discussed in Section 2.5.3, given by the following formula:

$$C^*_{overall} = \sum f_i . C^*_i \qquad (2.29)$$

where f_i = volumetric fraction of component i.

The maximum OTR at any set of operating conditions occurs when dissolved oxygen concentration equals zero, and so equation 2.22a reduces to

$$OTR_{max} = K_La \, . \, C^* \qquad (4.3)$$

4.2.3 Evaluation of probe measurement reproducibility

Previous laboratory experience at the University of Cape Town had indicated that silicon membranes became damaged when used in hydrocarbon for extended periods of time. Therefore, a decision was made to use Teflon membranes. The probe was serviced according to the Mettler Toledo User

Manual at regular intervals to ensure consistent operation, as depleted electrolyte or a fouled membrane can induce delayed response time. The electrode was rinsed with deionised water and allowed to dry, while the membrane was also soaked and rinsed with deionised water and allowed to dry. If there appeared to be any damage or viscous build-up on the membrane, it was replaced. The probe was then reassembled and refilled with fresh electrolyte solution. The probe was then calibrated in water and the performance evaluated at various process conditions to ensure reproducibility. The reproducibility of various probe tests at 30°C, 1200rpm and 1.5 vvm is shown in Figure 4.2. The response shown corresponds to a K_La value of $0.047s^{-1} \pm 0.001s^{-1}$ at these conditions.

The 63% probe response time, τ_e, to a step input for an Ingold® 12mm oxygen electrode is 9.6s (Montes *et al.*, 1999). Therefore, in order to satisfy

$$\tau_e = 1/k_e << 1/k_La \tag{3.3}$$

probe response time is sufficient if K_La is much less than $0.1s^{-1}$. Montes *et al.* (1999) and Galaction *et al.* (2004) therefore assumed that the response time of Inpro® 6000 Series dissolved oxygen electrodes is sufficiently fast and does not affect the accuracy of the results obtained.

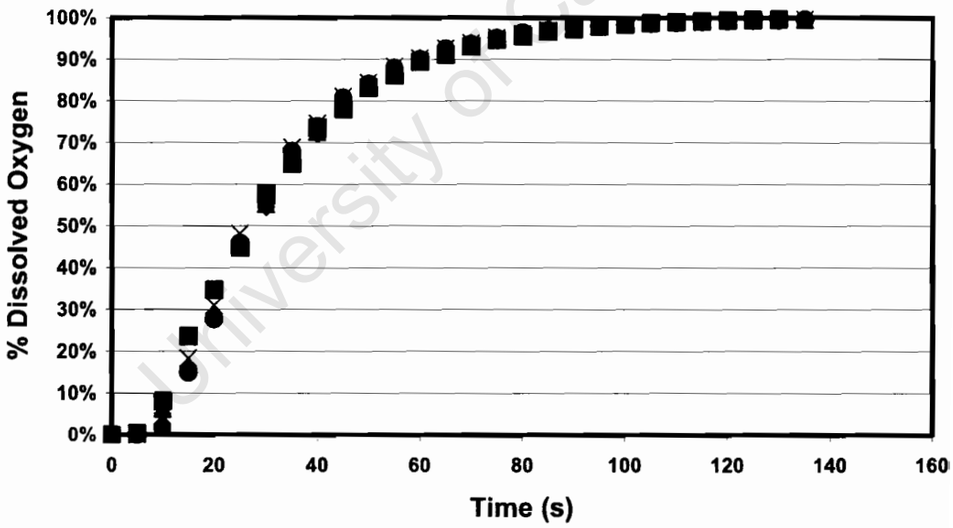

Figure 4.2 Plot of electrode response vs. time to examine reproducibility

♦ 6 May '03; ■ 1 Jun '03; ▲ 18 Jun '03; ● 23 Jun '03; x 14 Jun '03

4.2.4 Development of mathematical correlation to estimate K_La

A correlation for K_La as a function of agitation, aeration and alkane concentration was developed by non-linear regression. A non-linear form of equation was selected and the regression coefficients were determined using R 1.9.1, a language and environment for statistical computing and graphics (software available online from The Comprehensive R Archive Network, 2004). The source code used for the regression can be viewed in Appendix V.

4.3 Summary of Experimental Work for the Project

Chapter 5 will present the results of shake flask experiments from the study of the effect of media on *Candida tropicalis* growth and production of dicarboxylic acid. Chapter 6 will present the results of mass transfer experiments in a cell-free system, and quantify OTR through its effect on K_La and C*.

5. Results and Discussion I: Bioconversion of Alkane by *Candida tropicalis*

This chapter outlines the results of shake flask experiments using *Candida tropicalis* cells to determine the growth patterns and dicarboxylic acid production capabilities of the yeast. Growth and dicarboxylic acid production was examined in various kinds of media with different nitrogen sources and levels of carbohydrate in order to optimise conditions for producing dicarboxylic acid.

5.1 Preliminary Investigation into Dicarboxylic Acid Production in Small Shake Flasks with YP Medium

A set of preliminary shake flask experiments was performed in small flasks with the *Candida tropicalis* ATCC 20962 strain, developed by Picataggio *et al.* (1992). The objective of this set of experiments was to confirm that the yeast could assimilate alkane and produce dicarboxylic acid, and to determine if pH control and other medium additions may be required. These experiments examine the effect of Tween as an emulsifier in the medium and to evaluate the optimum time for addition of the alkane substrate to initiate dioic acid formation. Further, this set of experiments also to compares the level of dicarboxylic acid production on different alkane substrates. The Sasol C_{12-13} alkane cut and chemically pure dodecane were compared.

In the first set of experiments, YP medium (described in Section 4.1) was used for both the pre-culture and the main culture media. This medium was selected as it used a cheap nitrogen source (peptone) and contained a low glucose concentration, 10g/l. It would therefore give some indication of the potential to produce dicarboxylic acid on a cheap medium. A loop of yeast cells was used to inoculate the pre-culture, which was grown in a shaker at 25^{o}C for 24 hours. This pre-culture (250µl) was used to inoculate 3 500ml flasks each containing 25ml of medium to which the Sasol C_{12-13} cut was later added (1% inoculum). The alkane fraction was added to 3 vol% (22.5 g/l), comprising 8.5 g/l dodecane and 11.5 g/l tridecane.

- Flask A contained 0.01% Tween 80 and was shaken for 48 hours at 25^{o}C before Sasol C_{12-13} alkane cut was added as substrate.

- Flask B contained no Tween 80 and was shaken for 48 hours at 25°C before Sasol C_{12-13} alkane cut was added as substrate.
- Flask C contained 0.01% Tween 80 and was shaken for only 24 hours at 25°C before Sasol C_{12-13} alkane cut was added as substrate.

In the same way, 250µl of this pre-culture was used to inoculate 3 different 500ml flasks containing 25ml of medium to which dodecane was later added at a level of 3 vol% (22.5 g/l):

- Flask AA contained 0.01% Tween 80 and was shaken for 48 hours at 25°C before dodecane was added as substrate.
- Flask BB contained no Tween 80 and was shaken for 48 hours at 25°C before dodecane was added as substrate.
- Flask CC contained 0.01% Tween 80 and was shaken for only 24 hours at 25°C before dodecane was added as substrate.

Due to the small volume used, only samples for turbidity and GC analysis were taken regularly from each flask. Biomass measurements were taken at the time of alkane addition. The biomass concentrations recorded are shown in Table 5.1. Dodecanedioic acid yield, based on initial level of dodecane substrate added is summarised in Table 5.2. Tridecanedioic acid standard was not available and therefore it could not be analysed quantitatively.

Table 5.1: Biomass Levels of Candida tropicalis in YP medium

Growth Time	**24 hours**	**48 hours**	**48 hours**
	With Tween 80	With Tween 80	No Tween 80
	(Flasks C, CC)	(Flasks A, AA)	(Flasks B, BB)
Cell Dry Weight (g/l)	13.3 ± 0.1	15.0 ± 0.4	13.1 ± 0.4

The detailed results obtained for the turbidity, alkane and dicarboxylic acid concentration are shown in Figure 5.1. Time zero indicates alkane addition.

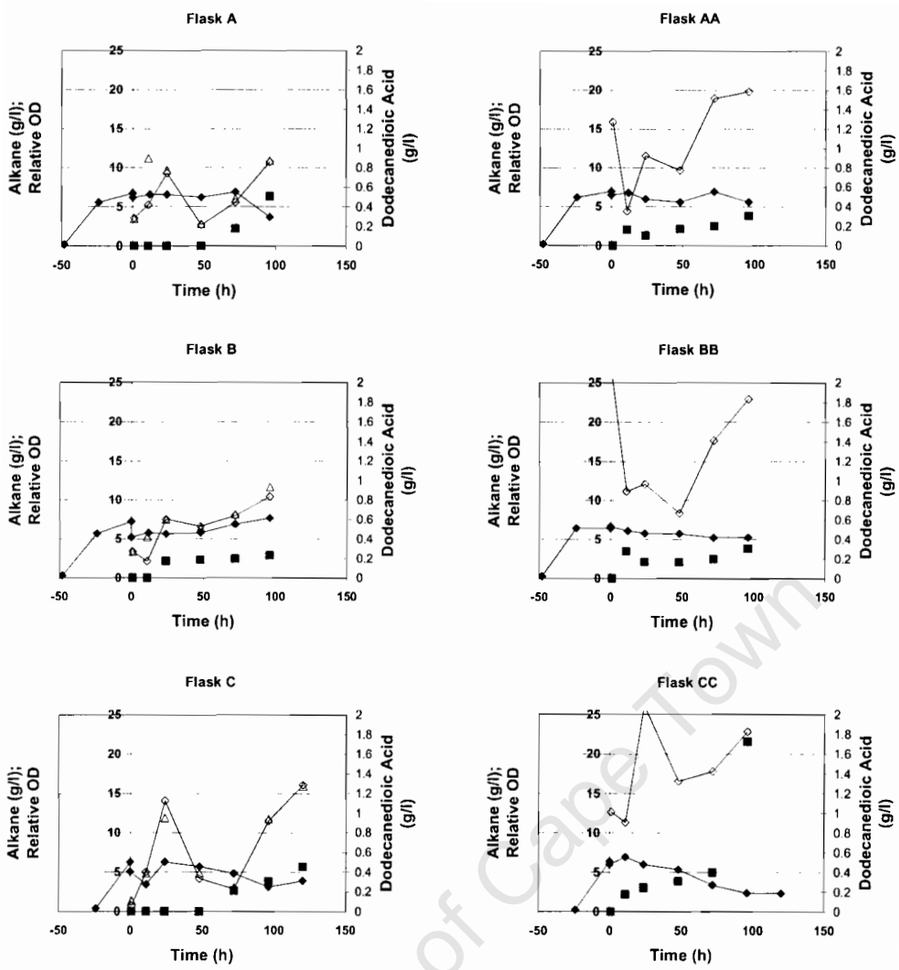

Figure 5.1: Dicarboxylic acid production by Candida tropicalis in shake flasks in YP medium

--◆-- Optical Density; --◇-- Dodecane; △ Tridecane; ■ Dodecanedioic Acid

In these experiments, the pH was not raised after substrate addition, as is suggested in the literature. Therefore, 72 hours after substrate addition, the pH in all flasks was raised to pH 8, from a pH of approximately 5 to investigate if the level of dodecanedioic acid present would increase. The variation of dodecanedioic acid with time for all the flasks is shown in Figure 5.2. After this point, the level of dodecanedioic acid present increased. The most

dramatic increase in the level of dodecanedioic acid was in the case of Flask CC, where dodecane was added after 24 hours. It is unclear at this stage whether this is due to the fact that higher pH promotes the secretion of dicarboxylic acid (Lin *et al.,* 2000), or if the higher pH merely ensures that the dicarboxylic acid present is dissolved adequately in the aqueous solution to facilitate representative sampling, as discussed in Section 3.3. It could be a combination of these effects. The results indicate that adding hydrocarbon only is not sufficient for extracellular dicarboxylic acid accumulation. The pH should be increased, as discussed in Section 3.2.

Table 5.2: Dodecanedioic Acid Yields in YP Medium

Flask	**A**	**B**	**C**	**AA**	**BB**	**CC**
Growth Time	**48 hours**	**48 hours**	**24 hours**	**48 hours**	**48 hours**	**24 hours**
	With Tween 80	No Tween 80	With Tween 80	With Tween 80	No Tween 80	With Tween 80
Alkane	Sasol cut	Sasol cut	Sasol cut	Dodecane	Dodecane	Dodecane
Dioic Acid Product before pH change (g/l)	0.18	0.19	0.21	0.20	0.20	0.40
Final Dioic Acid Product (g/l)	0.50	0.23	0.45	0.31	0.31	1.7
Yield (g C12 acid /g dodecane added)	5.9%	2.7%	5.3%	1.4%	1.4%	7.7%

There is limited dicarboxylic acid production in all flasks, and the alkane is not depleted. Flasks A and C show delayed production while the other flasks produce directly on alkane addition. Flask CC, containing an emulsifier and with pure dodecane added after 24 hours of cell growth, shows the highest yield of dioic acid. The data confirms that the cells can produce dicarboxylic acid under a variety of conditions. Analysis of total dicarboxylic acid production (if tridecanedioic acid standard were available) could yield more information, as authors such as Shiio and Uchio (1971) indicate that different molecular weight alkane substrates give very different dicarboxylic acid levels.

In the case of the *Candida cloacae* used in that case, lower molecular weight alkane substrates showed a higher conversion to dicarboxylic acid.

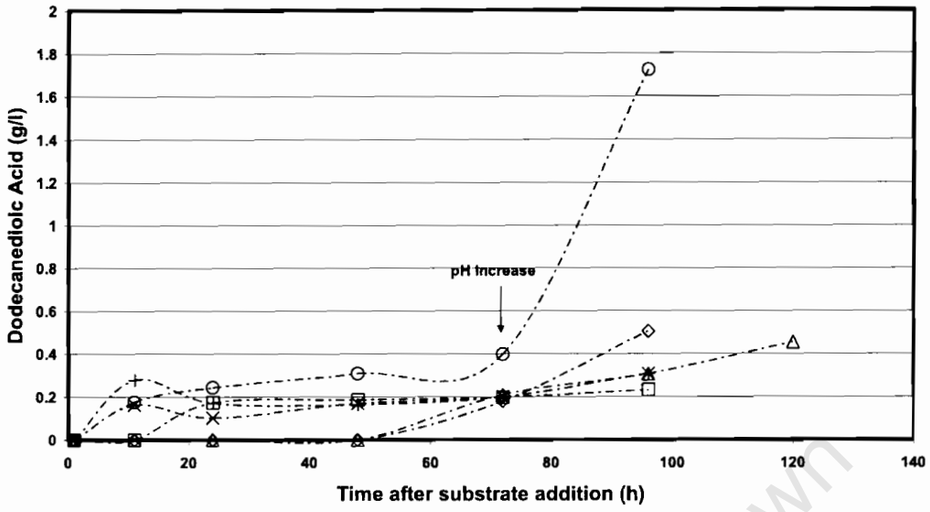

Figure 5.2: Comparison of Dicarboxylic Acid Production in Different Flasks containing YP medium

Flask A: ◇ 0.01% Tween 80, Sasol cut addition at 48 hours growth

Flask B: □ 0.00% Tween 80, Sasol cut addition at 48 hours growth

Flask C: △ 0.01% Tween 80, Sasol cut addition at 24 hours growth

Flask AA: x 0.01% Tween 80, dodecane addition at 48 hours growth

Flask BB: + 0.00% Tween 80, dodecane addition at 48 hours growth

Flask CC: O 0.01% Tween 80, dodecane addition at 24 hours growth

Dicarboxylic acid production was higher where alkane was added after 24 hours of growth, rather than after 48 hour of growth, with the exception of Flask A. Little biomass was produced between 24 and 48 hours, and hence the cells are entering the stationary growth phase. Addition of the alkane substrate to actively growing cells as an optimum condition for producing more dicarboxylic acid seems to be in keeping with as the studies of Picataggio *et al.* (1992), Uchio & Shiio (1971-1972), Jiao *et al.* (2001) and Green *et al.* (2000). All these researchers used *Candida* to produce

dicarboxylic acids and initiated the acid production stage between 16 and 24 hours after inoculation. It is therefore proposed that dicarboxylic acid production is mixed growth associated.

GC results were also processed in an attempt to quantify alkane uptake, but the results were erratic and did not follow any expected trends, as shown in Figures 5.3 and 5.4. Potential inaccuracies in the measurement of alkane and dicarboxylic acid may result from the extraction method of the alkane from all the liquid phases present in the media (described in Section 3.2), non-representative sampling, alkane uptake by the cells or an emulsifying agent (Reddy *et al.,* 1982). An emulsification agent could allow more accurate sampling of alkane in a specific flask, but it may take some time to form. Some samples show alkane levels exceeding the maximum level of alkane added, confirming that sampling was not representative. Phase separation was observed to some degree in the flasks, but the fluid appeared to homogenise with sufficient agitation. Clearly, the level of agitation applied immediately prior to sampling was not sufficient.

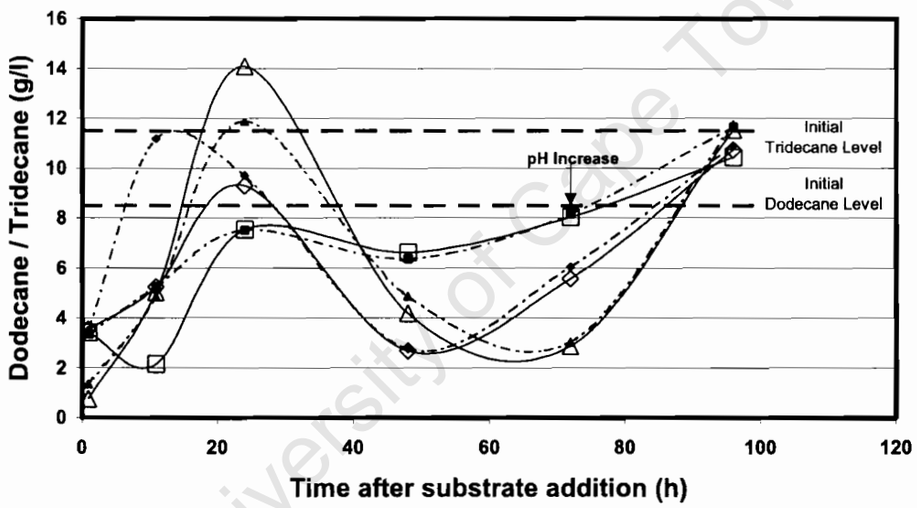

Figure 5.3: Dodecane and Tridecane fluctuation during bioconversion with Sasol alkane cut as substrate in YP medium

Flask A: --◇-- Dodecane; ◆ Tridecane

Flask B: --□-- Dodecane; ■ Tridecane

Flask C: --△-- Dodecane; ▲ Tridecane

It is interesting to note that in Figure 5.3, the measured levels of dodecane and tridecane fluctuate in a similar manner, further supporting inconsistent sampling of the alkane liquid phase, and aqueous liquid phase. It is however surprising that the tridecane concentrations are similar to the dodecane concentrations, considering that more tridecane was added initially. Perhaps tridecane is utilised preferentially. Future experiments should include quantification of conversion to tridecanedioic acid in order to confirm this.

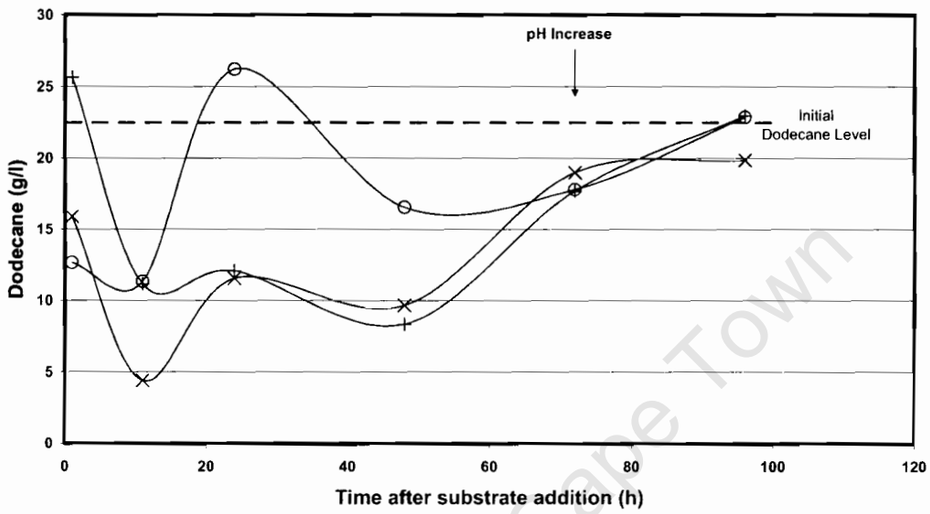

Figure 5.4: Dodecane fluctuation during bioconversion with pure dodecane as substrate in YP medium

Flask AA: --X-- Dodecane

Flask BB: --+-- Dodecane

Flask CC: --O-- Dodecane

5.2 Preliminary Investigation into Dicarboxylic Acid Production in Small Shake Flasks with YNB Medium

Due to the poor dicarboxylic acid productivity observed in the shake flask experiments described in Section 5.1, a set of experiments was conducted duplicating the conditions described by Picataggio *et al.* (1992). These

authors were responsible for creating the strain ATCC 20962 of *Candida tropicalis*. The YNB medium described in Section 4.1.2 was used for both the pre-culture and the main culture media. No Tween 80 was used. The pre-culture was grown in a shaker at 25°C for 24 hours. 2.5 ml of this pre-culture medium was used to inoculate flasks containing 22.5ml of medium (10% inoculum). These flasks were incubated on a shaker for 18 hours at pH 5 and 25°C. Thereafter, the pH was raised to 8 and dodecane was added to a concentration of 3 mass % (30g/l). The pH was raised again using 5M NaOH to pH 8 immediately before sampling at 24-hour intervals following alkane addition. At 24 and 48 hours after alkane addition, the pH required raising through 3 pH units. From 72 hours after substrate addition onwards, the pH only needed to be raised through 1 pH unit. The results of experiment are shown in Figure 5.5.

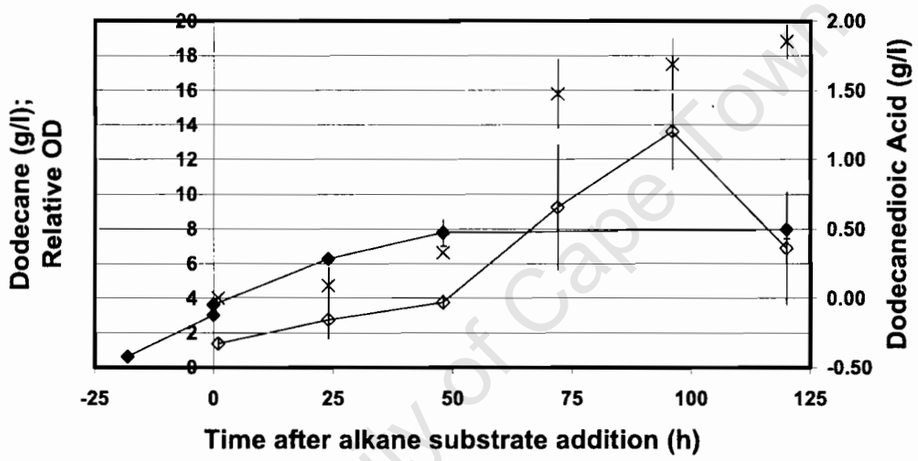

Figure 5.5: Dicarboxylic Acid Production by Candida tropicalis in YNB medium

--◆-- Optical Density; --◇-- Dodecane; x Dodecanedioic Acid

The final concentration of dicarboxylic acid produced was 1.8 g/l, representing a mass yield of 0.062±0.004 g dicarboxylic acid/g alkane added. This 6% yield is the same order of magnitude as those obtained on YP medium reported in Section 5.1. However, higher levels of dioic acid were present earlier in the experiment with YNB medium, most likely due to more effective pH control.

The alkane concentrations reported in Figure 5.5 remained inconsistent with expectation. Theoretically, the initial level should be 30g/l, and should decrease thereafter as alkane is assimilated. Instead, the alkane level appears to increase to a maximum level of 14 g/l, and then decreases. The same miscibility problems encountered in Section 5.1 appear to occur here too and experimental technique required refining.

Comparison of the preliminary shake flask experiments in YP and YNB medium illustrates that *Candida tropicalis* ATCC 20962 will yield dicarboxylic acid in both media despite different glucose concentrations (40 vs. 75 g/l) and different nitrogen sources (organic nitrogen vs. ammonium sulphate). It would also appear preferable to add alkane substrate during active growth, i.e. after 24 hours of growth, or less.

5.3 Effect of Nitrogen Source and Carbon: Nitrogen Ratio on Cell Growth

Picataggio *et al.* (1992) used the YNB medium discussed in Section 4.1. However, YNB is very costly as a nitrogen source. It was therefore considered judicious to compare the growth of *Candida tropicalis* on other similar media to investigate the possibility of decreasing cost in this regard, since the results of Section 5.1 indicate that it is possible to produce dicarboxylic acid with a peptone-based medium.

The results of Section 5.1 and 5.2 also indicate that pH control is important. Since this Picataggio's YNB medium contains appropriate salts to facilitate buffering capacity, it medium was used as a starting point to prepare other media for comparison, as discussed in Section 4.1. These media are therefore suitable for shake flask experiments to determine the effect of nitrogen source, glucose concentration and carbon to nitrogen ratio (C:N) on growth.

Four sets of flasks were cultivated (in duplicate) for this experiment, using Medium 1, 2, 3 and 4, as outlined in Section 4.1. Table 5.3 summarises the differences between the media used.

Table 5.3: Comparison of Media Composition of Flasks 1 to 4

	Flask 1	**Flask 2**	**Flask 3**	**Flask 4**
	Medium 1	Medium 2	Medium 3	Medium 4
Carbohydrate	Glucose 75g/l	Glucose 40g/l	Glucose 75g/l	Glucose 75g/l
Nitrogen source	YNB 6.7g/l	YNB 6.7g/l	Peptone 9.64g/l	YNB 6.7g/l
C/N source	Yeast Extract 3g/l	Yeast Extract 3g/l	Yeast Extract 3g/l	Yeast Extract 16g/l
C:N ratio	14	7.5	14	7.5

The YNB medium described in Section 4.1 was used as pre-culture medium. Following inoculation of 100ml pre-culture medium, this was then grown in a shaker at 30^{o}C for 24 hours at 120rpm. After this period of time, the flask contained 26 g/l glucose and 5.5 g/l biomass. A 10 ml aliquot of this pre-culture was used to inoculate the 4 sets of duplicate flasks, each containing 100ml of medium in a 1-litre flask. These flasks were then incubated on the shaker at 30^{o}C for 96 hours. Samples were taken every 4.5 hours to determine cell dry weight and turbidity. The pH was also measured. The changes in cell mass, glucose, pH and turbidity for the four flasks are shown in Figure 5.6.

As can be seen in Figure 5.6, Flask 4 yielded the highest level of biomass (over 7 g/l). This is expected, as it was the richest medium, containing the highest levels of both glucose and nitrogen through yeast extract. Flask 2 had the same initial carbon to nitrogen ratio (C:N of 7.5), but yielded a lower level of biomass, in accordance with the lower level of carbohydrate and nitrogen. It can also be seen that the glucose in Flask 2 was exhausted after only 13.5 hours, compared with 18 hours in Flask 4. The cell mass in Flask 2 continued to increase slightly, even with no glucose present. This can indicate diauxic growth (Bailey and Ollis, 1986), whereby the cells metabolise carbon from another source, possibly for carbon compounds in the yeast extract. In the other flasks, glucose only became exhausted after 18 hours or more, after the end of the growth phase.

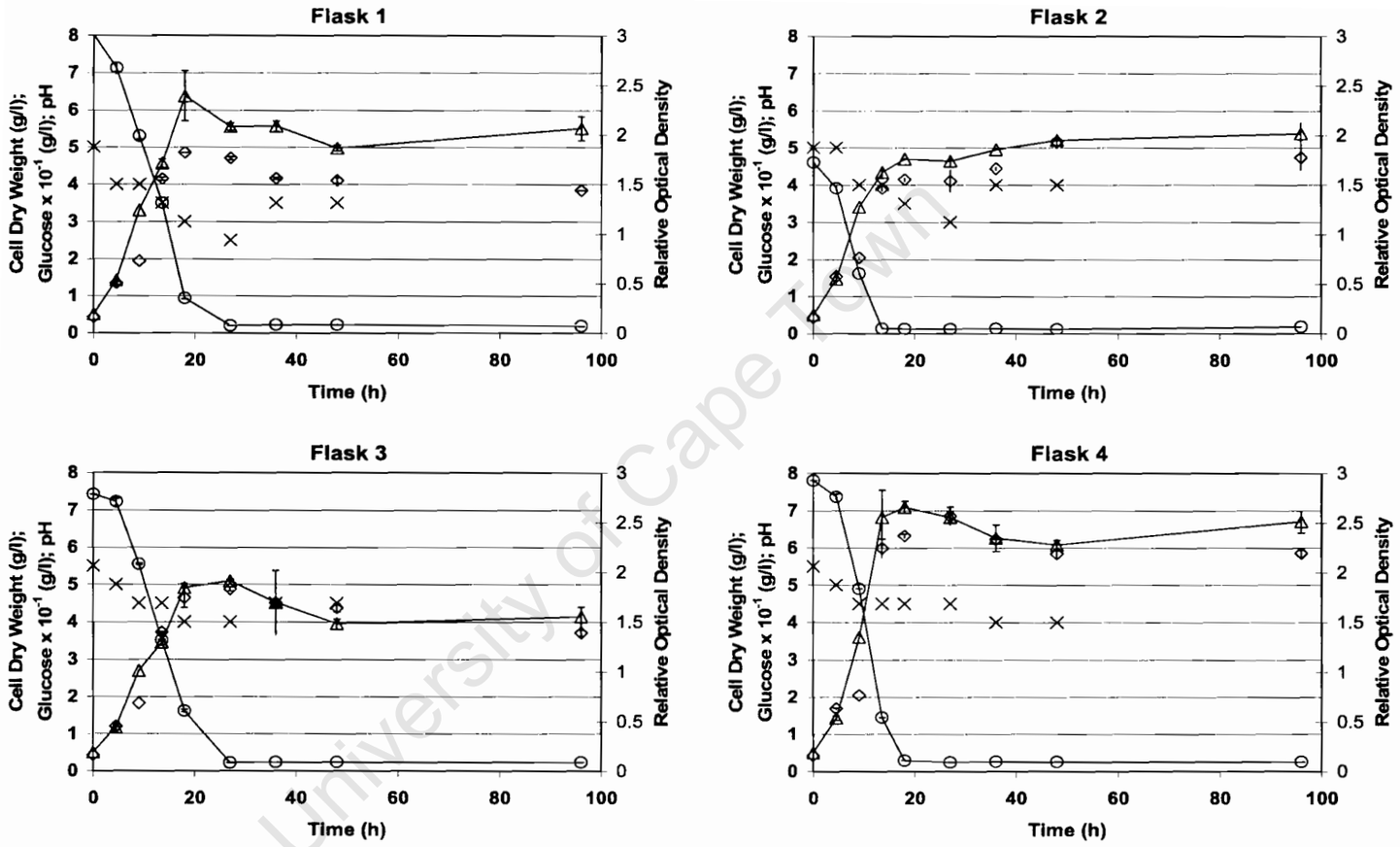

Figure 5.6: Growth of Candida tropicalis in shake flasks in different media

--△-- Cell Dry Weight; --O-- Glucose; ◇ Optical Density; x pH

Flasks 1 and 3 had the same initial carbon to nitrogen ratio of 14, with the source of nitrogen varying. Flasks 1 and 3 reach their maximum cell mass at 18 hours, but Flask 1 contained 1.5 fold more biomass than Flask 3. Flask 1 contained YNB (inorganic nitrogen) as its main nitrogen source, while Flask 3 contained peptone (organic nitrogen). It is interesting to note, however, that Flasks 1 and 3 have the same C:N ratio of 13.75. Picataggio *et al.* (1992) added alkane substrate after 18 hours of cell growth. This would coincide with the end of the exponential growth phase in their medium, used in Flask 1.

In order to investigate the growth pattern of the cells, the cell dry weight data in Figure 5.2 was re-plotted on a logarithmic scale in Figure 5.7. Due to the initial linearity in the curves of ln(dry biomass) as a function of time (Figure 5.3), it can be concluded that the lag phase negligible. This may be attributed to using a high inoculum (10 vol%) of actively growing yeast from a pre-culture flask.

It can be assumed that the exponential growth is first order, due to the presence of excess nutrients, and can be described by the Malthus equation (Shuler and Kargi, 1992):

$$\frac{dX}{dt} = \mu X \tag{5.1}$$

which can be integrated to

$$\ln\left(\frac{X}{X_0}\right) = \mu t \tag{5.2}$$

where X = cell concentration at time t

X_0 = cell concentration at time t_0

μ = specific growth rate

The specific growth rate is therefore given by the slope of the logarithm of cell dry weight as a function of time during the exponential growth phase, as shown in Figure 5.7. The values of growth rate obtained from the slopes of the curves are summarised in Table 5.4.

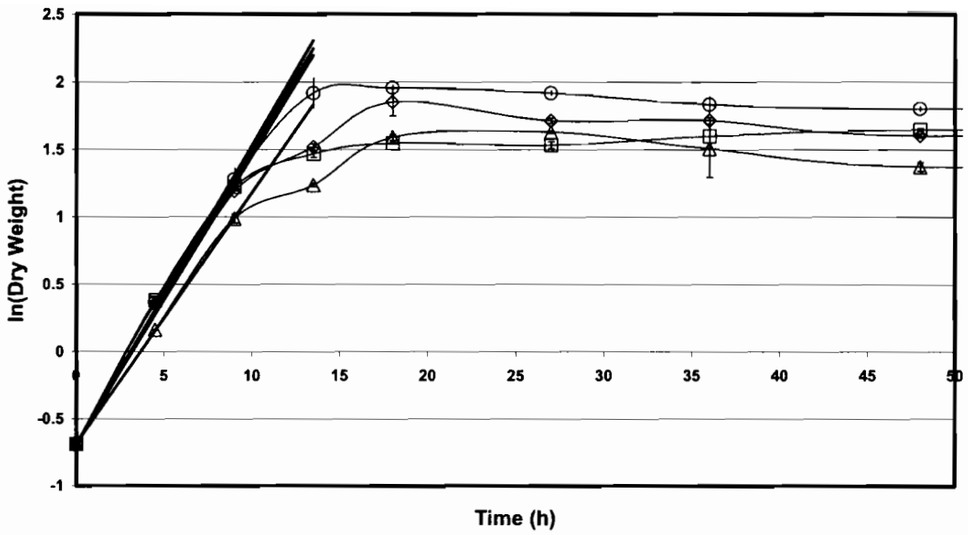

Figure 5.7: Logarithmic Growth curve for Candida tropicalis

Flask 1: -◇-; **Flask 2**: -□-; **Flask 3**: -△-; **Flask 4**: -○-

Table 5.4: Growth rates in Flasks 1 to 4

	Flask 1	**Flask 2**	**Flask 3**	**Flask 4**
	Medium 1	Medium 2	Medium 3	Medium 4
Specific Growth Rate (h^{-1})	0.21	0.22	0.19	0.22
R^2 of linear fit	0.995	0.995	0.999	0.998

Upon consideration of the error in the biomass measurements presented in Figure 5.7, the values for specific growth rate for Flasks 1, 2 and 4 presented in Table 5.4 are not significantly different. However, Flasks 1, 2 and 4 (containing inorganic and organic nitrogen) grew faster than Flask 3 (containing only organic nitrogen). This could indicate that inorganic nitrogen is in a form that cells can utilize more easily. Flask 2 exhibited the same growth rate as Flasks 1 and 4 until glucose limitation was reached. These flask all contained inorganic nitrogen. This result is expected as growth should be zero order with respect to nutrient concentration where substrate is not limiting.

In Figure 5.8, the correlation between the turbidity measurement and cell dry weight was investigated. A linear correlation is apparent, as indicated on the

graph (y=0.3335x). However, the points show a fairly wide scatter with half the datum points deviating by more than 5% from the value predicted by the linear best-fit. In addition, there is a large difference in the trends observed for the different flasks, which means that it would be necessary to redo the calibration curve for OD as a function of cell dry weight every time medium composition was changed. It was therefore decided that for future experiments, cell dry weight and cell counts would be used as a quantitative measure of cell growth.

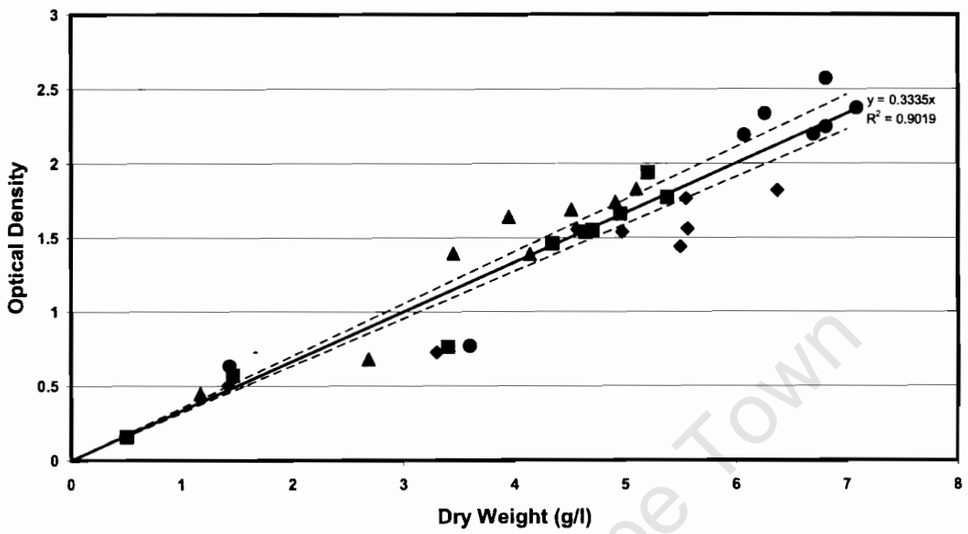

Figure 5.8: Plot to determine correlation between optical density and cell dry weight

Flask 1: ◆; **Flask 2**: ■; **Flask 3**: ▲; **Flask 4**: ●

5.4 Dioic Acid Production in Large Shake flasks in Various Media

The effect of the type of nitrogen source, concentration of carbon source and C:N ratio on growth was examined in Section 5.3. Here, the effect of these variables on dicarboxylic acid production is considered as the fastest growing cells or largest amount of biomass may not necessarily result in the best production of dicarboxylic acids by yeast.

YNB medium described in Section 4.1 was used for all the pre-culture media. A loop of *Candida tropicalis* cells was used to inoculate 100ml of pre-culture

medium. This was incubated in a shaker at 30°C for 24 hours at 120rpm. After this time, the inoculum contained 6.8 g/l glucose and 7 g/l cell biomass (compared with 26 g/l glucose and 5.5 g/l biomass in the inoculum in Section 4.3). 10 ml of this pre-culture medium was used to inoculate each of the 4 sets of duplicate flasks, each containing 100ml of medium in a 1-litre flask. The media use in the 4 sets of duplicate flasks is detailed in Table 5.5.

Table 5.5: Comparison of Media Composition of Flasks 1A, 3A, 4A and 5A

	Flask 1A	**Flask 3A**	**Flask 4A**	**Flask 5A**
	Medium 1	Medium 3	Medium 4	Medium 5
Carbohydrate	Glucose 75g/l	Glucose 75g/l	Glucose 75g/l	Glucose 75g/l
N source	YNB 6.7g/l	Peptone 9.64g/l	YNB 6.7g/l	Peptone 9.64g/l
C/N source	Yeast Extract 3g/l	Yeast Extract 3g/l	Yeast Extract 16g/l	Yeast Extract 16g/l
C:N ratio	13.75	13.75	7.53	7.53

Flask 2 containing the medium with reduced glucose and nitrogen concentration was not repeated owing to nutrient limitation. Instead, Medium 5 was introduced, in which YNB was replaced with peptone and high levels of glucose were maintained while reducing the C:N ratio by addition of yeast extract.

The initial pH of the flasks was between 5 and 6. These flasks were incubated on the shaker for 18 hours. Samples were taken to determine cell dry weight, glucose consumption and cell number. Thereafter, the pH was raised to pH 8 using 5M NaOH and dodecane was added to a level of 2.5 vol% (18g/l). Sampling continued after this, and samples were also taken for GC analysis to determine alkane and dicarboxylic acid levels. pH was checked at 36 hour intervals. The changes in cell dry weight, cell number, glucose and pH are shown in Figure 5.9, with the time of substrate addition shown as time zero. Alkane and dicarboxylic acid results are given in Figure 5.11. Table 5.6 compares the biomass results from the cell growth experiments in Section 5.3 with the biomass results of the dicarboxylic acid production experiments from this Section.

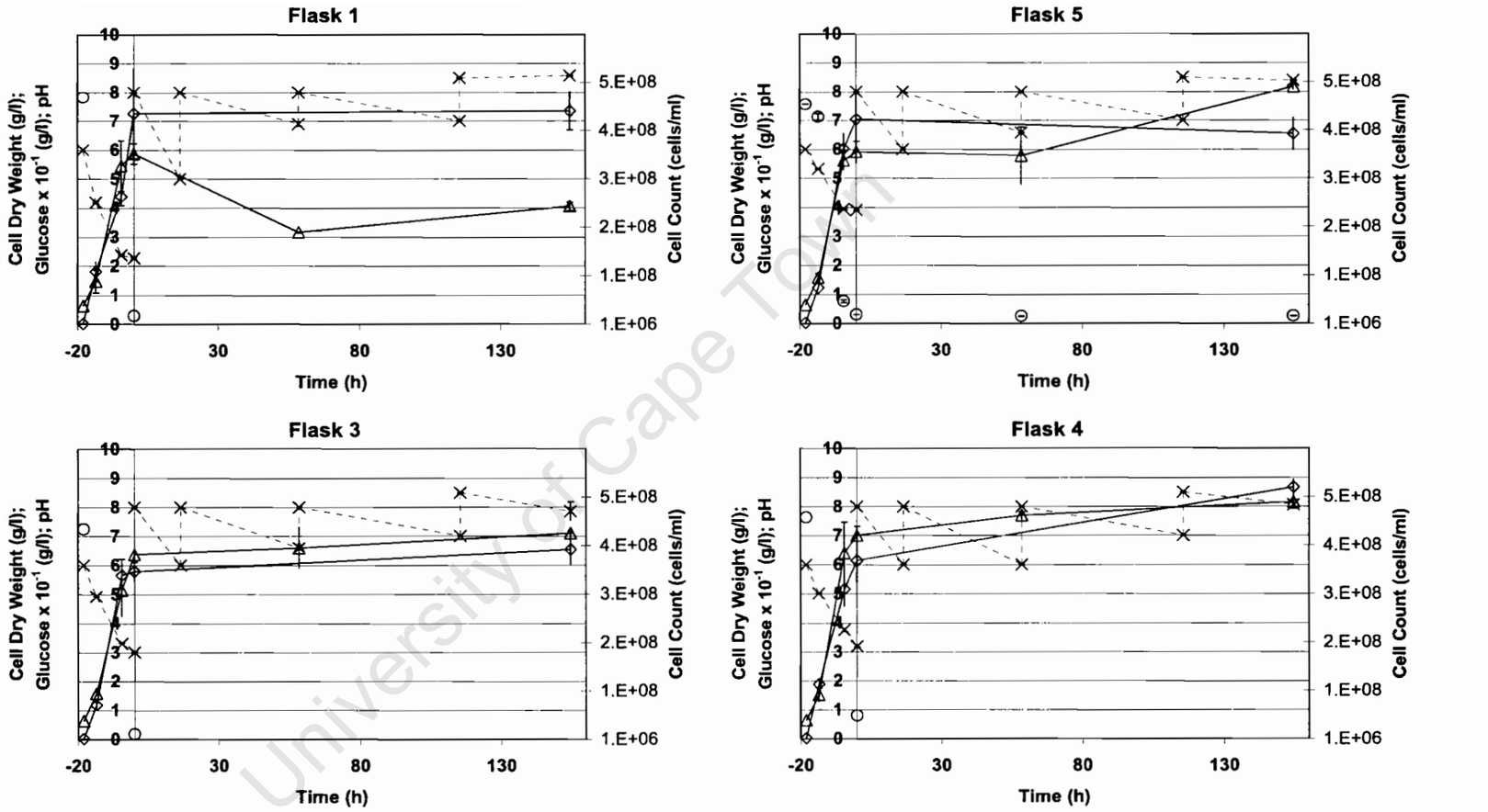

Figure 5.9: Growth of Candida tropicalis in shake flasks in high-glucose media

--△-- Cell Dry Weight; --O-- Glucose; ◇ Cell Count; x pH

Table 5.6: Comparison of Biomass Production in Different Experimental Sets

	Flask 1	Flask 2	Flask 3	Flask 4	Flask 5A
Biomass after 18h (g/l)	6.2	4.7	5.0	7.0	
	Flask 1A		**Flask 3A**	**Flask 4A**	**Flask 5A**
Biomass after 18h (g/l)	6.0		6.2	7.0	5.8

In all the flasks the pH and glucose concentration decreased until dodecane substrate was added at time zero. After substrate addition, the pH was raised to pH 8. This was repeated at 12, 60 and 120 hours after substrate addition. In accordance with Section 5.3, Flask 4A containing Medium 4 yielded the highest level of biomass (7 g/l) at the end of the exponential growth phase (time zero). This medium contained an inorganic nitrogen source (YNB) and high levels of yeast extract. Flask 1A yielded approximately 6 g/l of biomass, and is consistent with the yield in Flask 1 of Section 5.3 of 6.2 g/l.

Flasks 3A and 5A (containing Medium 3 and Medium 5 respectively) yielded approximately the same level of cell dry weight (6 g/l). Both these media contained organic nitrogen (as peptone) with Medium 3 containing a low level of yeast extract and Medium 5 a high level of yeast extract. It could have been expected than Medium 5 should produce more biomass than Medium 3, as seen in the comparisons between Medium 1 and Medium 4. The biomass production of Flask 3A appears inconsistent with that of Flask 3, but Flask 3A contained a higher initial biomass concentration.

The logarithmic growth curves used to determine specific growth rates in Flasks 1A, 3A, 4A and 5A are shown in Figure 5.10. As seen in Figure 5.7, the curves in Figure 5.10 increase linearly initially, indicating the duration of the exponential growth phase. The specific growth rates during exponential growth from the slope of each curve are summarised in Table 5.7, and compared with the data in Table 5.4.

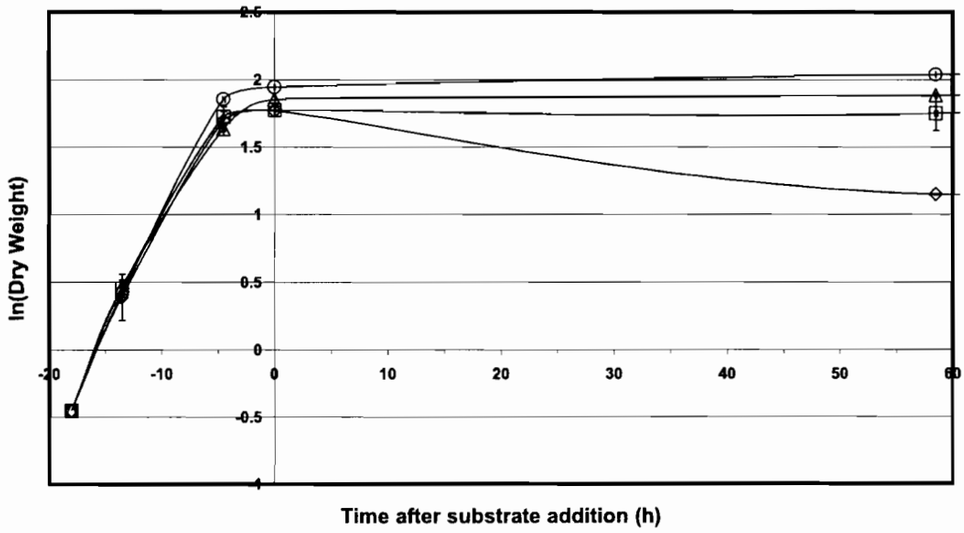

Figure 5.10: Logarithmic Growth curves for Candida tropicalis in high-glucose media

Flask 1: -◇-; **Flask 3**: -△-; **Flask 4**; **Flask 5**: -□-

Table 5.7: Growth rates in Flasks 1A, 3A, 4A and 5A

	Flask 1	Flask 2	Flask 3	Flask 4	Flask 5A
Specific Growth Rate (h^{-1})	0.21	0.2	0.19	0.22	
	Flask 1A		**Flask 3A**	**Flask 4A**	**Flask 5A**
Specific Growth Rate (h^{-1})	0.16		0.16	0.17	0.16
R^2 of linear fit	0.994		0.980	0.997	0.988

The specific growth rate results for Flasks 1A to 5A do not appear consistent with the results Flasks 1 to 4 from Section 5.3. The specific growth rate results of the former consistently lower than the latter. Slight differences in the specific growth rates between the two sets of experiments would be expected as slight inoculum and incubation temperature differences could affect the overall results. The inoculum used in this set of experiments contained more cells and less glucose than the experiments detailed in Section 5.3. Flask 4A, with the highest nitrogen content (both organic and inorganic) had the highest growth rate, while the other flasks with lower nitrogen content or only organic nitrogen content had lower specific growth rates. Flask 4A also produced the most biomass.

The important issue of interest in this section is, however, the production of dicarboxylic acid from alkane in these various media. The alkane and dicarboxylic acid concentrations in the various flasks are summarised in Figure 5.11 and the mass yields are shown in Table 5.8.

Table 5.8: Dodecanedioic acid mass yields in large shake flasks

Flask	1A	3A	4A	5A
	Medium 1	Medium 3	Medium 4	Medium 5
Dioic Acid Product (g/l)	0.03	0.47	0.33	0.71
Yield (g/g)	0.2 ± 0.07 %	2.5 ± 0.5 %	1.8 ± 0.02 %	3.8 ± 0.4 %

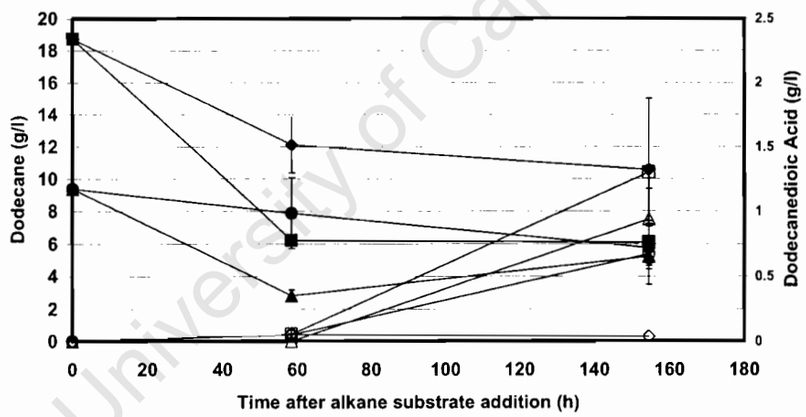

Figure 5.11: Dicarboxylic acid production in large shake flasks

Flask 1A: --◆-- Dodecane; --◇-- Dioic Acid; Flask 3A: --▲-- Dodecane; --△-- Dioic Acid;

Flask 4A: --●-- Dodecane; --○-- Dioic Acid; Flask 5A: --■-- Dodecane; --□-- Dioic Acid

The curves in Figure 5.11 show the consumption of dodecane decreasing and production of dodecanedioic acid increasing. This behaviour is in accordance with expected results in such a system, unlike the findings in Sections 5.1 and 5.2. This is suggests that samples taken less frequently and accounting for a smaller fraction of the total medium improved representative samples. Flasks 3A and 5A showed the highest levels of dioic acid production. These flasks contained organic nitrogen in the form of peptone.

While these results show less dicarboxylic acid production than in the smaller flasks, they are of the same order of magnitude, except for Flask 1A. This flask contained the exact medium developed by Picataggio *et al.* (1992), who modified *Candida tropicalis* ATCC 20962 to produce dicarboxylic acids, and as used in Section 5.2. It therefore shows surprisingly low levels of dicarboxylic acid production, even compared with the results of Section 5.2. This could well be a scale-up or sampling effect, due to the relatively low level of mixing that can be attained in unbaffled shake flasks. In addition, the levels of dicarboxylic acid production obtained in these experiments are two orders of magnitude smaller than the 120 g/l production obtained by Picataggio *et al.* (1992) as shown in Table 3.1. The author obtained these results in a 5l stirred, aerated fermentation vessel with pH control and substrate addition in a fed-batch mode. The following section will therefore summarise and discuss the results of the shake flask experiments and propose considerations for scale-up of the biological dicarboxylic acid production process.

5.5 Selection of Optimal Conditions for Dicarboxylic Acid Production in Bioreactors

The results show that the genetically modified yeast, *Candida tropicalis* ATCC 20962, is capable of producing dodecanedioic acid from dodecane substrate. The core concern is, however, to optimise this production. There are a number of parameters that can be varied in order to achieve this, namely cell concentration and growth time, alkane substrate level, richness of aqueous medium, pH and mixing and emulsification issues. The key results are summarised in Table 5.9.

Table 5.9: Summary of Biomass and Dicarboxylic Acid Production in Various Flasks

	Flask A(A)	**Flask B(B)**	**Flask C(C)**		
Biomass at alkane addition (g/l)	13.3	15.0	13.3		
	Flask A	**Flask B**	**Flask C**		
Dioic Acid Mass Yield (g/g)	5.9 %	2.7 %	5.3 %		
	YNB Medium				
Dioic Acid Mass Yield (g/g)	1.4 %				
	Flask 1	**Flask 2**	**Flask 3**	**Flask 4**	**Flask 5A**
Biomass after 18h (g/l)	6.2	4.7	5.0	7.0	
Specific Growth Rate (h^{-1})	0.21	0.2	0.19	0.22	
	Flask 1A		**Flask 3A**	**Flask 4A**	**Flask 5A**
Biomass after 18h (g/l)	6.0		6.2	7.0	5.8
Specific Growth Rate (h^{-1})	0.16		0.16	0.17	0.16
Dioic Acid Mass Yield (g/g)	0.2 ± 0.07 %		2.5 ± 0.5 %	1.8 ± 0.02 %	3.8 ± 0.4 %

A general trend in the results is that cell concentration is not necessarily a measure of good dicarboxylic acid production capability. In Section 5.1 where cell growth time before alkane substrate addition was varied, it was clearly seen in the experiments with dodecane substrate that the flasks with younger yeast batches at the time of dodecane addition, produced more dodecanedioic acid. Subsequent experiments were therefore performed adding dodecane after less than 24 hours of growth, rather than after 48 hours. This was consistent with literature as Picataggio *et al.* (1992), Uchio & Shiio (1971-1972), Jiao *et al.* (2001) and Green *et al.* (2000). The researchers all used *Candida* species to produce dicarboxylic acids and initiated the acid production stage between 16 and 24 hours after inoculation.

Analysis of the growth patterns of the *Candida tropicalis* was performed and presented in Section 5.3. After a sterile medium is inoculated with live cells, there will be a period in which little observable growth occurs. This is known as the *lag phase*. The length of this lag phase can depend on a number of factors, such as the amount of fresh cells added, the age of the cells and the type of adjustments that the cells will have to make in their new environment. The cell growth patterns observed in Section 5.3, and 5.4, showed very short lag phases (less than 4.5 hours). This could be due to the large size of the inoculum (10% of the volume of the medium), and the metabolic activity of the cells in the inoculum.

In addition, the carbon source of the inoculum was similar to the carbon source of the medium for the growth experiments. The cells were grown in a buffered medium containing glucose and yeast extract as carbon source, and Yeast Nitrogen Base (YNB) with ammonium sulphate as an inorganic nitrogen source, and then transferred to a fresh medium containing glucose, yeast extract and the same buffering salts. The only difference is that the nitrogen source was different in the case Flasks 3, 3A, and 5A, as these flasks contained Peptone as an organic nitrogen source. A lag phase can also result if cells are put into a medium richer in a limiting nutrient, as the cells will then spend a period of time utilising nutrients for creating more enzymes to metabolise the nutrient, instead of for growth (Bailey and Ollis, 1986). This change in nitrogen source did not appear to affect the lag phase.

The *exponential growth phase* follows, and is characterised by a linear increase in cell mass on a logarithmic scale, as shown in Figures 5.7 and 5.10. In the case of *Candida tropicalis* ATCC 20962 under these growth conditions, the *exponential growth phase* ended about 18 hours after inoculation, when the *stationary phase* is reached and the cell population reaches maximum size. The experiments in Section 5.3 and Section 5.4 showed that the richest medium, containing the highest levels of both glucose and yeast extract, and with inorganic nitrogen, produced the highest level of biomass with the fastest specific growth rate.

In contrast, the flask with the lowest levels of glucose and yeast extract produced the lowest level of biomass after 18 hours, which was considered the length of the exponential growth phase. This flask with dilute medium also showed signs of nutrient limitation. The glucose levels were exhausted after only 13.5 hours and the growth rate appears to diminish at about this time.

The biomass does continue to increase after this time in the presence of minimal glucose, but at a slower rate. One explanation for this is diauxic growth (Bailey and Ollis, 1986), whereby the cells metabolise carbon from another source, in this case carbon compounds in the yeast extract (Appendix I).

However, the key outcome required for these experiments is to determine the optimum conditions required for the production of dicarboxylic acid. It was noted in Section 5.1 that, in general, dicarboxylic acid production was higher when alkane was added after 24 hours rather than after 48 hours of cell growth. As recommended by Picataggio *et al.* (1992), who modified *Candida tropicalis* ATCC 20962 to produce dicarboxylic acids, it was decided to add alkane substrate after 18 hours, at end of exponential growth phase, before the cells began to enter the *stationary phase*.

From the last set of shake flask experiments performed, outlined in Section 5.4, the optimum medium for dicarboxylic acid production contains organic nitrogen in peptone, and high concentrations of yeast extract and glucose, as shown in Flask 5A. It would appear that inorganic nitrogen is more effective for producing high cell biomass, as in Flasks 4 and 4A. A direct comparison between concentration of cells and dicarboxylic acid production was not found.

On closer inspection of Figure 5.11, Flasks 3A and 5A, containing organic nitrogen, show no detectable dicarboxylic acid production. 60 hours after alkane addition, Flasks 1A and 4A show low, yet detectable, levels of dicarboxylic acid. However, after 156 hours, Flasks 3A and 5A show the highest dicarboxylic acid levels. Less complex inorganic nitrogen may be easier to metabolise than organic nitrogen. This may account for the faster cell growth and initial dicarboxylic acid production is exhibited in inorganic nitrogen-grown cells, while organic nitrogen allows the cells to remain more productive for longer.

Hill *et al.* (1986), Picataggio *et al.* (1992) and Jiao *et al.* (2001) used substantial amounts of inorganic nitrogen sources mixed with organic low-level nitrogen sources such as yeast extract and corn steep liquor for dicarboxylic acid production by *Candida* species (Table 3.1), but did not compare organic to inorganic nitrogen sources. Shiio and Uchio (1971) compared the effect of different inorganic nitrogen sources, with $(NH_4)_2HPO_4$

producing the most dicarboxylic acid from *n*-dodecane. This study concluded that other inorganic nitrogen sources, such as ammonium sulphate (as used in YNB medium) were well utilised for growth, but less desirable for dicarboxylic acid production, in accordance with the findings of this study.

In a later study (Uchio and Shiio, 1972b), these same authors experimented with resting cells and various organic nutrient sources. These were not classified according to nitrogen, carbon or any other elemental content, but were merely compared on a basis of dicarboxylic acid production per gross mass of complex nutrient source. Yeast extract, and peptone were compared as complex nutrient sources, but were not compared with inorganic nutrient sources. There is therefore a distinct absence of literature comparing the use of inorganic nitrogen sources with organic nitrogen sources.

pH control is another important factor in the biological production of dicarboxylic acids. As observed in Section 5.1, no dicarboxylic acid was detectable before the pH was maintained close to pH 8. Hill *et al.* (1986), Picataggio *et al.* (1992), Jiao *et al.* (2001) and Uchio and Shiio (1972c) all produced dicarboxylic acid at a pH of about this level. In accordance with this study, Lin *et al.* (2000) also claimed that high pH is necessary for cells to secrete acid, for the H^+ to neutralise excess OH^- in the medium. However, these authors also proposed that product feedback inhibition is involved in the conversion of intracellular alkane. High extracellular levels of dioate^{2-} ions will inhibit the secretion of acid and reduce alkane conversion. Scheller *et al.* (1998) and Chan *et al.* (1997 a, b) also noted product inhibition in the biological production of dicarboxylic acids, at product concentrations as low as 8 g/l. Lin and Chan therefore advocate continuous culture operation or *in situ* removal in a batch process in order to prevent excessive product accumulation.

The dicarboxylic acid concentrations obtained across the sets of experiments in Sections 5.1, 5.2 and 5.4 do not show consistent levels of dicarboxylic acid yield. More detailed kinetic experiments are required to determine if product or substrate inhibition exists. It is postulated that these inconsistencies result from miscibility problems. The smaller flask experiments in Sections 5.1 and 5.2 show yields as high as 5.3 – 7.7% mass yield. The highest yield obtained in large flasks (with higher nutrient levels) in Section 5.4 is 3.8 %. The difficulty in representative sampling due to miscibility issues is supported by recording of alkane concentrations above the original alkane concentration added. The calibration curves in Appendix II show a linear relationship

between alkane standards and peak area, validating alkane analytical procedure.

In a larger flask, the presence of an alkane layer on top of the aqueous medium was clearly observable. This indicates that substrate was not being dispersed sufficiently due to insufficient mixing. One negative implication is the possibility of inadequate oxygen transfer for bio-catalysed oxidation of alkanes to dicarboxylic acid.

It is clear that the alkane is not uniformly dispersed within the medium, hence the location of the cells within the medium, and the contact between the cells and the alkane could affect dicarboxylic acid production. Figure 5.12 shows micrographs of cells with alkane, taken during the experiments in large shake flasks. The image on the left shows oval-shaped yeast cells in the plane of focus. Upon refocusing on the two large masses, it becomes apparent that the masses consist of cells adhering to spherical alkane droplets. This is supported in the right hand image.

This is consistent with the observation of Mimura *et al.* (1973), who noted that hydrocarbon-assimilating yeasts attach themselves to droplets of hydrocarbon. If these "flocs" were fairly stable, this could further account for non-uniform distribution of the alkane in the medium. There are two methods that could enable good alkane dispersion in the medium – mechanical agitation and antifoam. Mimura *et al.* (1973) observed that antifoam caused cell dispersion, however, it is unknown at this stage if this would have adverse effects on the ability of *Candida* cells to adsorb oxygen from the hydrocarbon "flocs" during the growth phase. Uchio and Shiio (1972c) however, noted that the addition of antifoam stimulated the production of dicarboxylic acid in *Candida cloacae*.

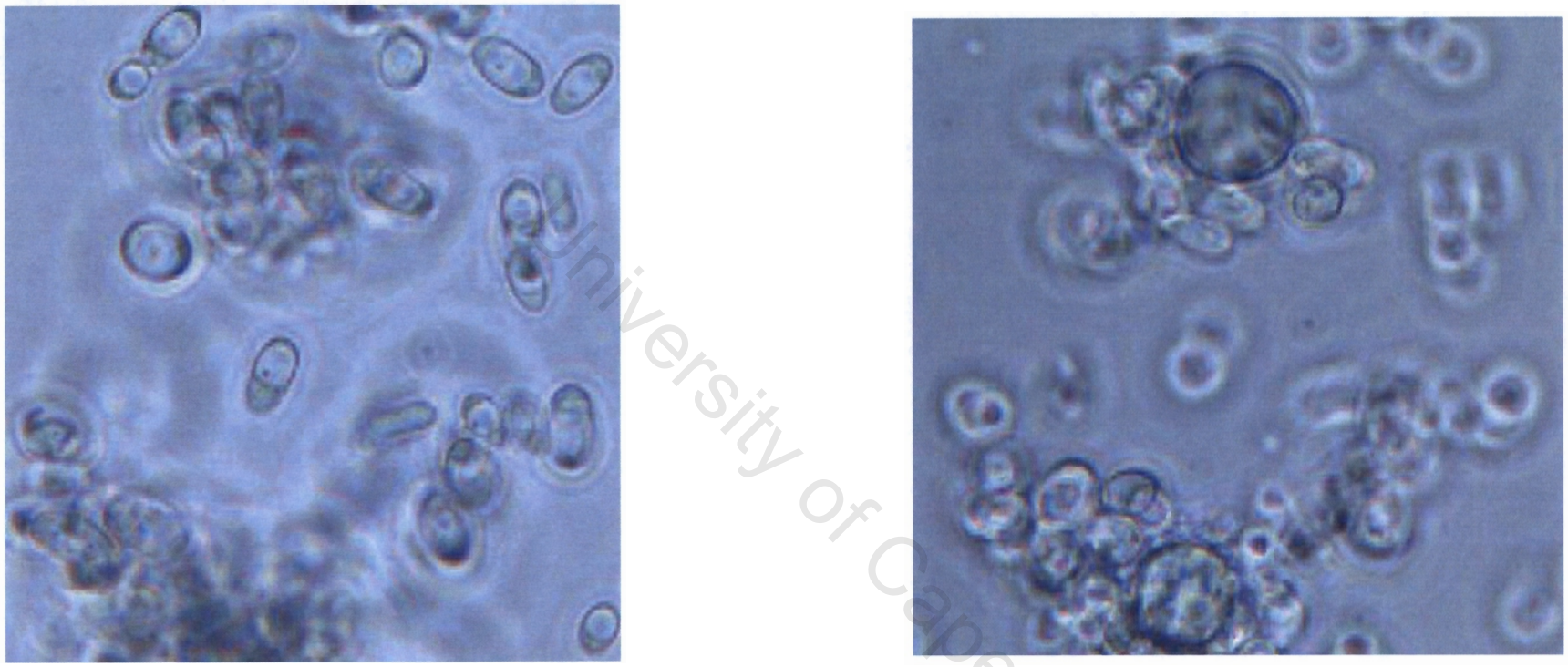

Figure 5.12: Candida tropicalis cell "flocs" with alkane droplets

The production level of dicarboxylic acid obtained in these shake flask experiments was much lower than reported in the literature. Attempting to reproduce the conditions employed by Picataggio *et al.* (1992) only resulted in a maximum concentration obtained of 1.8 g/l dicarboxylic acid, low compared to the 120 g/l obtained by the author in bioreactor studies. In addition, Jiao *et al.* (2001), Hill *et al.* (1986) and Uchio and Shiio (1972c) obtained dicarboxylic acid concentrations in the order of 22 to 64 g/l, depending on the type of alkane substrate employed. This is also far above the dicarboxylic acid product inhibition level reported by Chan *et al.* (1997 a, b). It must be noted, however, that these researchers used bioreactor systems in which optimum conditions are more readily achieved. In addition, many of these authors employed a fed-batch system, thus, while the alkane concentration was maintained at 15 volume % or less, the volume of alkane added constituted a much larger fraction of the overall fermentation. The advantage of fed-batch culture is that substrate inhibition is reduced, while substrate added is increased. However, Picataggio *et al.* (1992) and Jiao *et al.* (2001) do not report the total amount of alkane added or report the extent of alkane conversion to dicarboxylic acid, limiting the meaningful comparison to the results of the shake flask experiments performed in this project. Hill *et al.* (1986) report a molar conversion of tridecane to tridecanedioic acid of 45%. This was the highest conversion across C_{11} to C_{16} substrates. Uchio and Shiio (1972c) report a conversion of 36% for dodecane to dodecanedioic acid, and 40% for tridecane to tridecanedioic acid. This is at least an order of magnitude higher than the yields obtained in the shake flask experiments presented in this chapter.

The key difference between the work of these authors and the results presented in this project is that all these authors used automated controlled bioreactor systems with spargers for aeration, impellers for mixing, and pH control. Duplicating these dicarboxylic acid production experiments in a large volume in a well-mixed bioreactor could alleviate immiscibility problems and allow for more representative sampling. In addition, automated pH control would also provide and maintain the ideal conditions to induce dicarboxylic acid production. Sparging air could also alleviate any oxygen limitation for the alkane oxidation. It would also be advisable to employ a two-stage inoculum for a large-scale fermentation in order to allow for a more consistently reproducible initial cell concentration in a large volume.

However, the physical characteristics of the large agitated alkane-water-air system need to be characterised prior to selecting operating conditions.

According to the information summarised in Table 3.1, Picataggio *et al*. (1992) and Uchio and Shiio (1972c) used agitation rates as high as 1300 and 1400 rpm respectively. The higher the agitation rate, the greater the risk of cell damage due to shear forces. The next step in this study is therefore to determine the mixing and dispersion behaviour of alkane in a water-air system in a standard laboratory bioreactor, in order to quantify the optimum agitation and aeration rates that could be used in the biological production of dicarboxylic acids from alkanes, and give insight into the factors that would ultimately affect most hydrocarbon fermentations containing immiscible liquid phases.

6. Results and Discussion II: Transfer in Immiscible-Phase Bioreactor Systems

In Section 2.4, the potential process challenges in alkane bioprocesses were identified and discussed. Many of these challenges are common to all hydrocarbon fermentations, regardless of the product formed, and include flammability, volatility and inhibition of cell growth (Schmid *et al.*, 1998) (notably at low carbon chain lengths), insolubility (Rothen *et al.*, 1998) (notably at high carbon chain lengths) and mass transfer limitations, with respect to both oxygen (Preusting *et al.*, 1993) and hydrocarbon substrate (Schmid *et al.*, 1998). After consideration of the results of Chapter 5, it became apparent that miscibility and mixing problems are quite pronounced and would most likely affect alkane substrate and oxygen supply, hence affecting the ability of the organism to assimilate and oxidise alkane it to produce dicarboxylic acid.

Stoichiometrically, it has been shown that an increase in oxygen supply of approximately 3-fold is required during growth of yeast on hydrocarbon relative to growth on carbohydrate (Moo-Young, 1975). Experimentally, a 2.9-fold increase in oxygen was required during yeast growth on hydrocarbon relative to carbohydrate (Shennan and Levi 1974). Consequently, the oxygen transfer rate (OTR) has been mooted as a likely major process limitation, leading to a process which is transport- rather than kinetically-controlled and, correspondingly, a sub-optimal yield and productivity.

In view of the importance of an adequate OTR in the optimisation of the hydrocarbon-based bioprocess, the results of this section focus on the quantification of OTR through the evaluation of the overall mass transfer coefficient (K_La) and saturation oxygen concentration (C^*) in an air-water and an air-water-alkane system. The effect of variation of agitation, aeration and alkane level on these factors will be examined. While the values of K_La and C^* are likely to be different from those in an actual bioprocess and further, will depend on the particular bioprocess through the ionic media components, dissolved products and suspended solids, the trends in these values will be comparable to those in a bioprocess. Thus this system provides a convenient generic base for the evaluation of K_La and C^*, their corresponding influence on the OTR in hydrocarbon-based bioprocesses and the establishment of conditions for optimum operation of bioprocesses based on a hydrocarbon feedstock.

6.1 *Influence of Agitation and Aeration on K_La and OTR in an Air-Water System*

The influence of agitation and aeration on K_La (and hence OTR as a function of K_La) was examined in an aqueous system at 5 aeration rates from 0.5 to 1.5 vvm, and at 6 agitation rates from 200 to 1200 rpm. According to "Two-Film Theory", as discussed in Section 2.5, it is expected that increasing agitation and aeration would reduce stagnant boundary layers, reduce bubble size and consequently improve mass transfer, characterised numerically by an increase in K_La.

6.1.1 Effect on K_La in an air-water system

Figure 6.1 shows K_La in pure water at 30°C as a function of agitation at different aeration rates. K_La increases 6 to 10-fold as agitation is increased from 200 to 1000 rpm. As agitation is increased to 1200rpm, a decline in K_La is observed. This decline varies from 0% at 1.5 vvm, to approximately 30% at 0.5vvm. This suppression of K_La at high agitation rates is therefore more evident at lower aeration rates. This suppression was unexpected according to "Two-Film Theory", but may be due to the unique geometry of the system. During the experiments, the upper surface of the agitated liquid became unstable as the agitation rates increased from 1000 to 1200 rpm, exhibiting vortex formation and splashing.

K_La is plotted as a function of aeration, using the same experimental data, is plotted in Figure 6.2. K_La increases by a factor of only 2 or less with an increase in aeration from 0.5 to 1.5vvm. It is clear, by comparing the results in Figures 6.1 and 6.2, that increasing aeration has less effect on K_La than increasing agitation. The data also suggests that the effect of aeration on K_La is further reduced at lower agitation rates (200 to 800rpm), as depicted by the gradients of these curves approaching zero at low agitation rates.

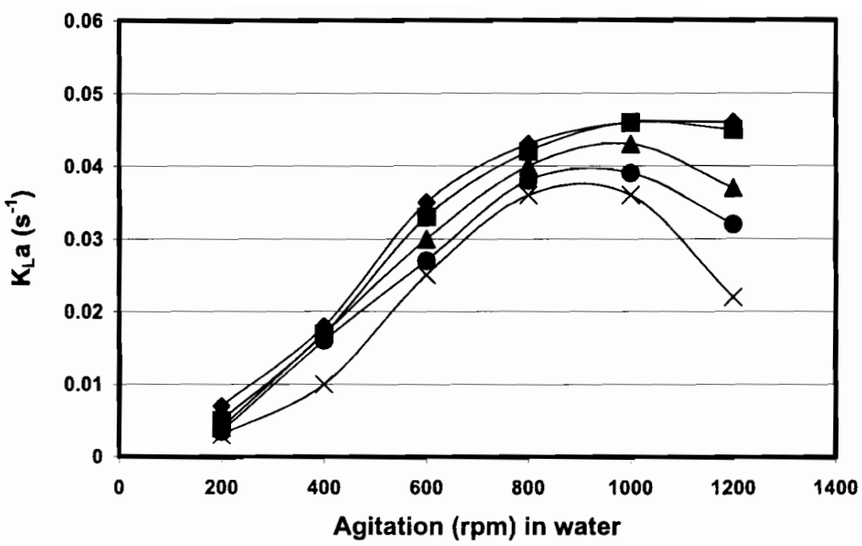

Figure 6.1: Influence of agitation on K_La in an aqueous system at different aeration rates

♦ 1.5 vvm; ■ 1.25 vvm; ▲1.0 vvm; ● 0.75 vvm; x 0.5 vvm

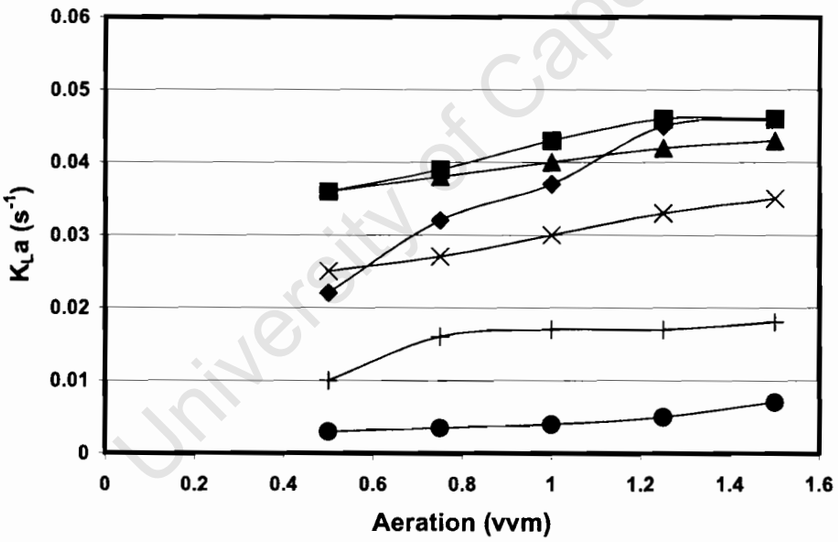

Figure 6.2: Influence of aeration on K_La in an aqueous system at different agitation rates

♦ 1200 rpm; ■ 1000 rpm; ▲800 rpm; x 600 rpm; + 400 rpm; ● 200 rpm

6.1.2 Effect on OTR in an air-water system

Since OTR varies with the instantaneous concentration of oxygen in the mixture, as according to equation 2.22, the maximum attainable OTR was determined according to equation 4.3 and is used for all comparative purposes in the analysis of the variation of OTR:

$$OTR_{max} = K_L a \,.\, C^* \tag{4.3}$$

The changes in the OTR with variation in agitation and aeration rates therefore mirrored the changes in the corresponding $K_L a$ values, as seen in Figures 6.3 and 6.4. This is a consequence of the dependence of the maximum OTR on $K_L a$ alone at a constant C*, as is the case in an air-water system at constant temperature and pressure.

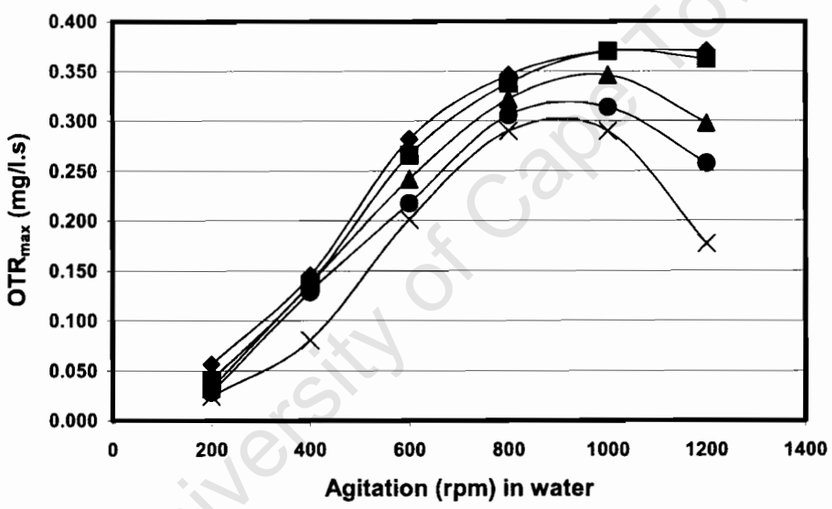

Figure 6.3: Influence of agitation on OTR in an aqueous system

♦ 1.5 vvm; ■ 1.25 vvm; ▲1.0 vvm; ● 0.75 vvm; x 0.5 vvm

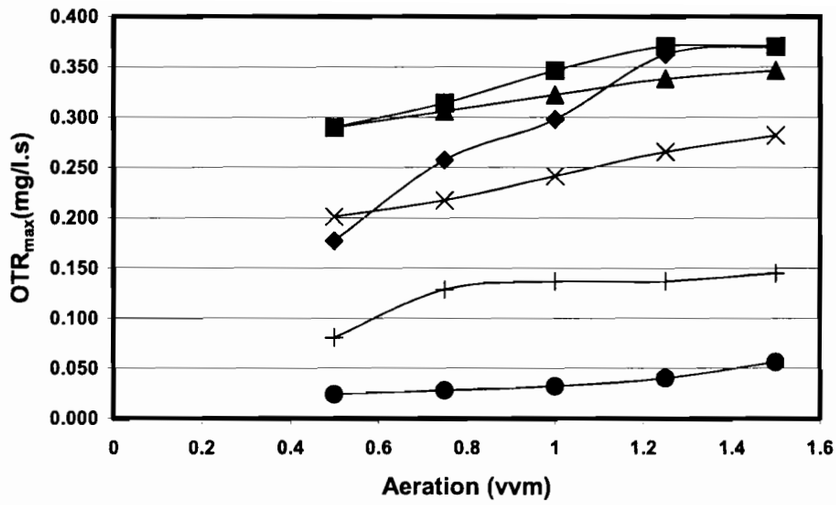

Figure 6.4: Influence of aeration on OTR in an aqueous system

♦ 1200 rpm; ■ 1000 rpm; ▲800 rpm; x 600 rpm; + 400 rpm; ● 200 rpm

6.2 Influence of Agitation, Aeration and Alkane Concentration on K_La and OTR in an Air-Water-Alkane System

The influence of agitation and aeration on K_La was examined at each of the following alkane concentrations in % (v/v): 2,5; 5; 10; 15; 20. The alkane used was the Sasol C_{12-13} cut, characterised in Section 4.1.3. The ranges of agitation and aeration rates investigated were similar to those in the air-water system. It was not possible to obtain as many data points in alkane-water mixtures, since adequate mixing was not attained at low agitation rates. This also became more pronounced in combination with reduced aeration rates. Poor miscibility was observed at agitation rates of 200 rpm at all aeration rates, and at 400 rpm and 600 rpm at aeration rates of less than 1.5 vvm and 1.0 vvm respectively. Under these conditions, both air bubbles and alkane droplets were large compared to those at the higher agitation and aeration rates; the bubbles were observed to predominate in the centre of the bioreactor while the droplets migrated to the surface. Nielson *et al.* (2003) reported similar findings on agitation of an immiscible mixture of water and hexadecane at a low agitation rate.

6.2.1 Effect on K_La in an air-water-alkane system

In a 10% alkane/ 90% water system, similar trends with regard to the effect of agitation and aeration on K_La were expected. Figure 6.5 shows the values of K_La as a function of agitation in various alkane-water mixtures at 30°C.

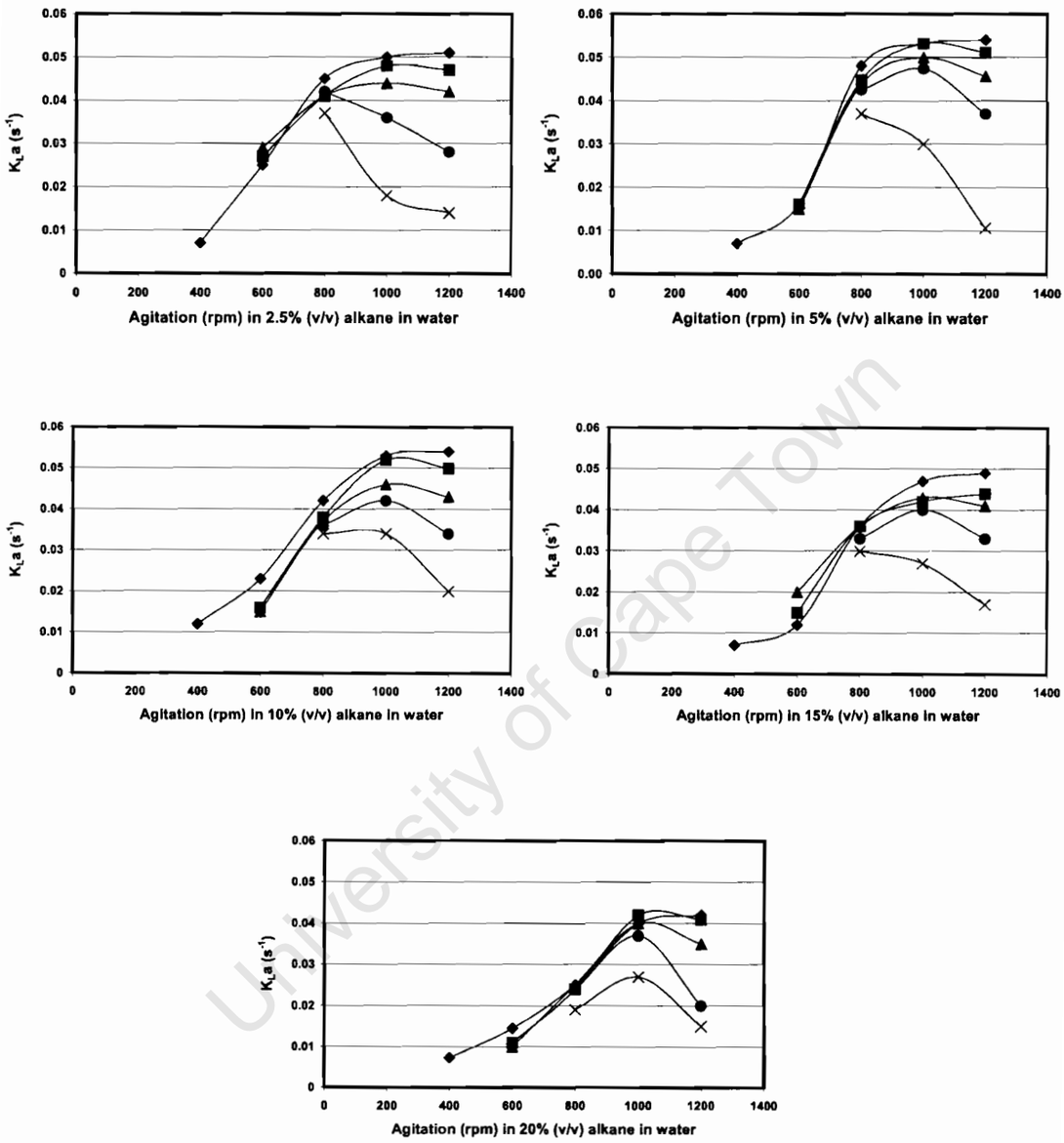

Figure 6.5: K_La versus agitation in various mixtures at 30°C

♦ 1.5 vvm; ■ 1.25 vvm; ▲1.0 vvm; ● 0.75 vvm; x 0.5 vvm

In a 10% alkane/90% water system K_La increases by a factor of 4.5 as agitation is increased from 400 to 1000 rpm at 1.5vvm. The corresponding increase in pure water was a factor of 2.5. K_La enhancement via increased agitation in the 400 to 1000rpm range is therefore more pronounced in 10% alkane than in pure water. Similar trends are observed at lower aeration rates, but fewer data points were attainable. As agitation is increased from 1000rpm to 1200rpm, a decline in K_La is observed at all aeration rates. This decline varies from approximately 0% at 1.5 vvm, to approximately 40% at 0.5vvm. This suppression of K_La at high agitation rates is once again more evident at lower aeration rates and is more pronounced than that observed in water.

In a 20% alkane / 80% water system, similar trends with regard to the effect of agitation and aeration on K_La were expected, once again. It was also of interest to determine if further alkane addition produced a more pronounced enhancement of K_La as agitation rate is increased to 1000rpm, or a more pronounced suppression of K_La at high agitation rates. In this case, K_La increases by a factor of 3 as agitation is increased from 400 to 1000 rpm at 1.5vvm. This value lies in-between that for the corresponding conditions in pure water and that in 10% alkane. As expected, similar trends are observed at lower aeration rates. This points towards there being an optimum level of alkane and therefore increased alkane levels do not necessarily continue to benefit process conditions. As agitation is increased from 1000rpm to 1200rpm, a decline in K_La is observed at all aeration rates below 1.5vvm. This decline varies from approximately 0% at 1.5vvm, to approximately 45% at 0.5vvm. These trends in K_La suppression at high agitation are very similar to the trends observed at the 10% alkane concentration.

Somewhat different behaviour was observed at very low alkane concentrations, namely, 2.5% alkane / 97.5% water. The graphs of K_La as a function of agitation for 2.5% (v/v) alkane in water have a different shape to those for 10% (v/v) or 20% (v/v) in Figure 6.5. In the case of 2.5% (v/v), K_La increased by a factor of 7 as agitation was increased from 400 to 1000 rpm at 1.5vvm. Similar trends are observed at aeration rates of 1.0 and 1.25vvm, as observed at other alkane concentrations. However, specifically at 1.5vvm, this increase is larger than the increase observed in pure water, 10% to 20% (v/v) alkane under similar conditions. As agitation is increased from 1000rpm to 1200rpm, a decline in K_La is observed at all aeration rates below 1.5vvm. However, at low aeration rates of 0.5 and 0.75 vvm, this characteristic decline begins at a lower agitation of 800rpm in the presence of 2.5% (v/v) alkane.

This is the lowest agitation rate at which reasonable miscibility is attained and reproducible data can be collected at an aeration rate of 0.5vvm. At 0.5vvm, K_La decreases by 50% as agitation increases from 800 to 1000rpm, and then levels from 1000 to 1200rpm.

The behaviour at 5% (v/v) alkane lies in-between that of 2.5 and 10% (v/v) alkane. In the case of 5% (v/v) the decline in K_La begins at 800rpm only at 0.5vvm, while the data at 0.75vvm shows the decline only as agitation is increased from 1000 to 1200rpm, as is the case for 10 to 20% (v/v) alkane.

The effect of the addition of alkane on K_La as a function of aeration, compared to the trends observed in pure water, is observed in Figure 6.6, using the same data as Figure 6.5. The curves each correspond to a constant agitation rate. For 20% (v/v) alkane in Figure 6.6, K_La increases by a factor of less than 2 as aeration is increased from 0.5 to 1.5vvm at 800 rpm. This increases to a factor of 2.7 as aeration is increased from 0.5 to 1.5vvm at 1200rpm. In the results shown in Figure 6.2 for the effect of aeration in pure water, this factor was less than 2 in all cases. This indicates that increasing aeration has a more significant effect on K_La in the case of alkane-water mixtures, than in the case for pure water. Even at very low alkane concentrations, this observation holds. For 2.5% (v/v) alkane (Figure 6.6), K_La increases by a factor of less than 1 as aeration is increased from 0.5 to 1.5vvm at 800 rpm. The largest effect is at the highest agitation rates, namely 1000 and 1200rpm, where K_La increases by a factor of approximately 3.6.

In general, the K_La value increased as agitation increased from 200 to 1000rpm, but then declined at 1200rpm. As in the case of the pure water system, this can most likely be explained by the geometry of the system, unique to the specific bioreactor conformation. Visually, jetting and vortexing was observed on the surface of the medium at 1200rpm. This turbulence would seem to suppress K_La. At 1000rpm this effect was less pronounced, while at 800rpm the surface of the medium was almost entirely flat. At speeds of 600rpm and below, large air bubbles and alkane droplets were observed, and at 200rpm, the air bubbles were mostly in the centre of the bioreactor while alkane droplets mostly migrated to the surface. Recall that, at low agitation rates, such as 200 to 400rpm, it was difficult to attain reproducible results with alkane water mixture, due to poor mixing, while at agitation rates of 400 to 1000rpm, K_La increased with increased agitation. This mixing

phenomenon can most likely explain the substantial difference in the trends obtained at high agitation rates, when compared with those obtained at low agitation rates, as shown in Figure 6.6.

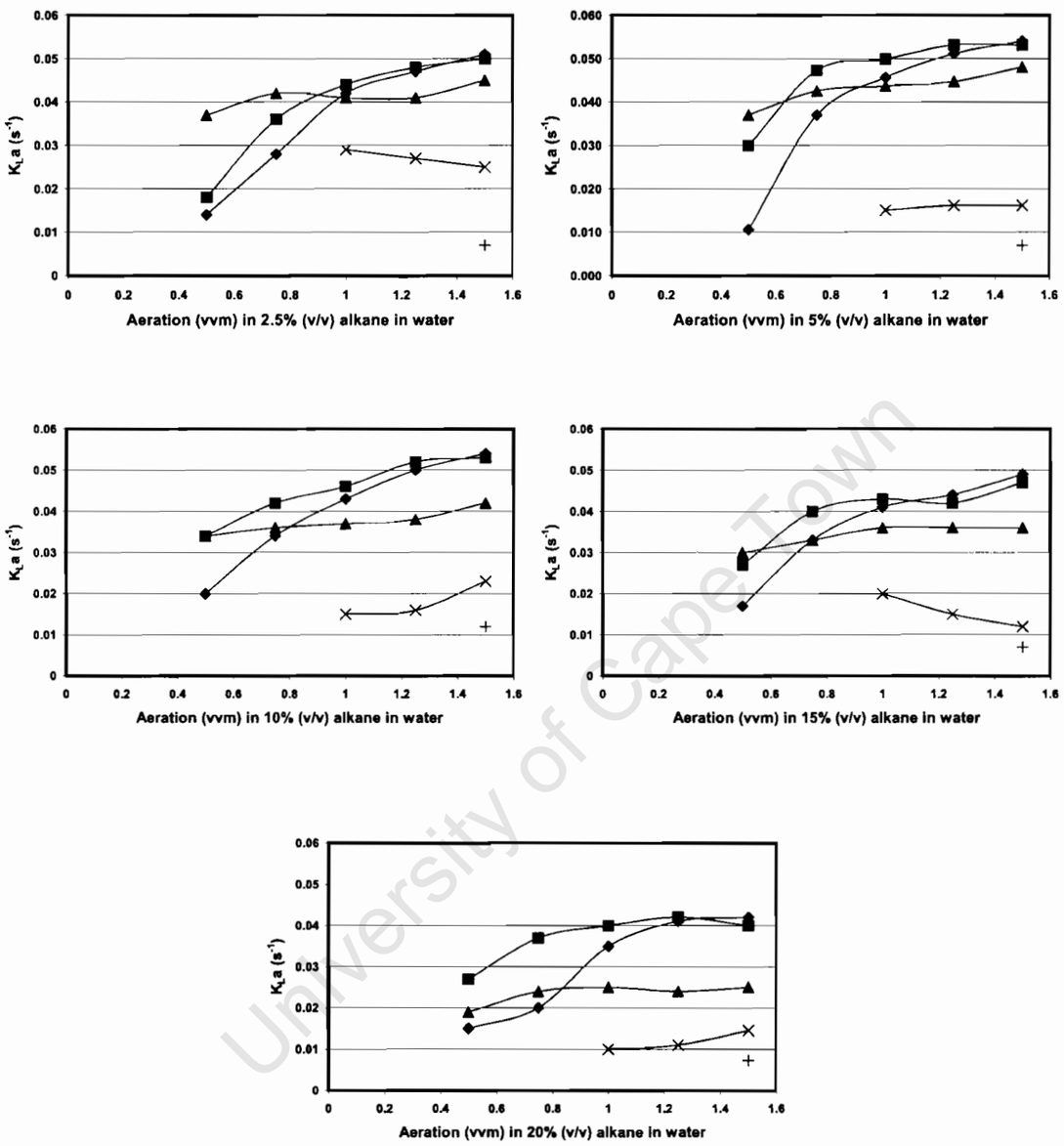

Figure 6.6: K_La versus aeration in various mixtures at 30°C

♦ 1200 rpm; ■ 1000 rpm; ▲800 rpm; x 600 rpm

In summary, an increase in agitation from 400 to 1000 rpm resulted in K_La enhancement at each aeration rate, with a subsequent decrease above 1000 rpm, at alkane concentrations of 10, 15 and 20 % (v/v). The influence of agitation rate at these alkane concentrations shown at 1.25vvm (in Figure 6.7) is typical of the trends observed at other aeration rates. At the lower alkane concentrations of less than 10%, similar trends in K_La with increasing agitation were observed at the higher aeration rates while at aeration rates of less than 1 vvm, the characteristic decline began at a comparatively lower agitation rate of 800 rpm, possibly as a consequence of decreased miscibility. Alternatively, an increase in aeration to 1.5 vvm resulted in K_La enhancement at each agitation rate.

In addition, the influence of aeration rate on the enhancement of K_La was less pronounced than that of the agitation rate, though not as insignificant as that observed in the air-water system. The influence of aeration rate at various alkane concentrations shown at 1000rpm (Figure 6.8) is typical of the trends observed at other agitation rates. The results presented indicate that the inclusion of alkane to the liquid medium affects the degree of change in K_La with respect to agitation and aeration, suggesting that an optimum alkane concentration for maximizing K_La existed. It is therefore important to examine the effect of adding alkane, with all other variables kept constant.

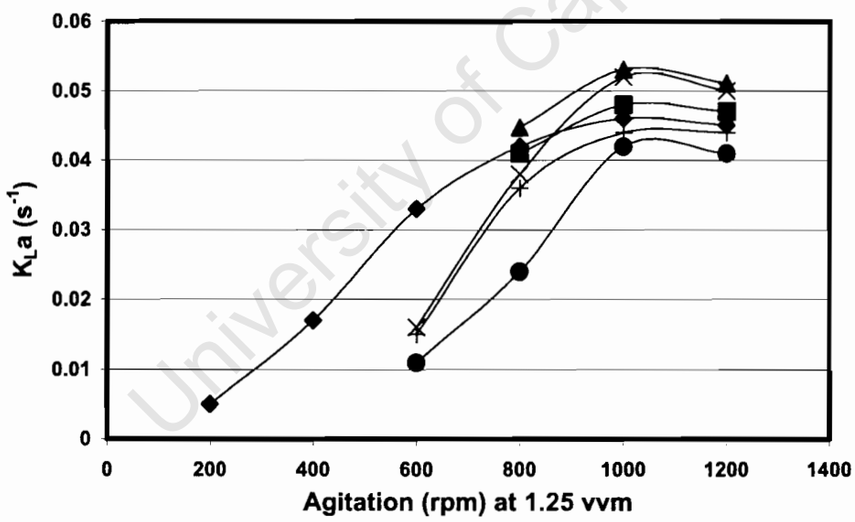

Figure 6.7: Influence of Agitation on K_La at various alkane concentrations and 1.25vvm

♦ Pure Water; ■2.5% vol Alkane; ▲5% vol Alkane; x 10% vol Alkane; + 15% vol Alkane; ● 20% vol Alkane

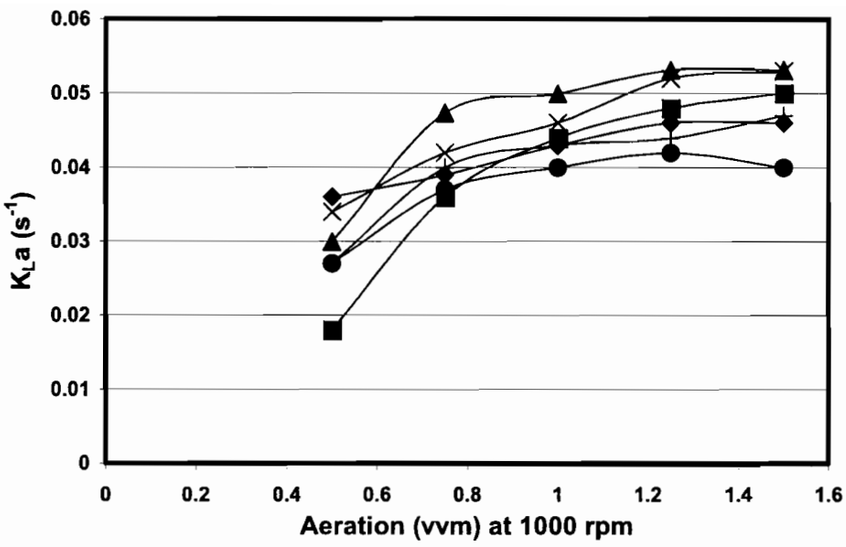

Figure 6.8: Influence of Aeration on K_La at various alkane concentrations and 1000rpm

♦ Pure Water; ■2.5% vol Alkane; ▲5% vol Alkane; x 10% vol Alkane; + 15% vol Alkane; ● 20% vol Alkane

Since the optimum aeration rate in the air-water system was 1.25 vvm and in general the increase in K_La with increasing aeration rate had reached a plateau across all alkane concentrations studied (as seen in Figure 6.8), the variation of K_La with alkane concentration was studied at this constant aeration rate over the range of agitation rates from 400 to 1200 rpm (Figure 6.9).

A marked difference in the influence of alkane concentration on K_La was observed at the low agitation rates of 600 rpm and below when compared with that observed at the high agitation rates of 800 rpm and above. At the low agitation rates, K_La was suppressed throughout with increasing alkane concentration. Conversely, at the high agitation rates, alkane addition initially resulted in K_La enhancement above that attained in water, with depression only becoming evident as alkane concentrations increased above 5 to 10% (v/v) alkane. These trends gave rise to an optimum K_La, at an agitation rate between 800 and 1000 rpm and an alkane concentration between 5 and 10% (v/v) (Figure 6.10) for constant aeration rates of 0.75 vvm and above. However, at the lowest aeration rate of 0.5 vvm, data obtained at alkane

levels below 10% (v/v) were not easily quantifiable, most likely due to inadequate mixing.

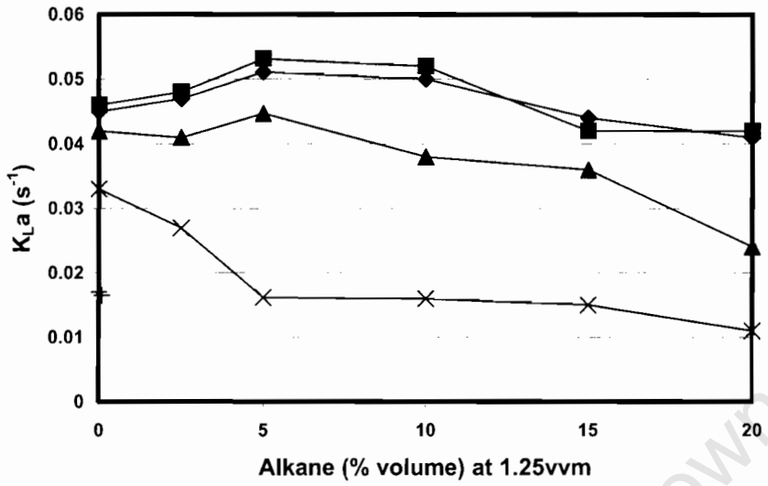

Figure 6.9: Influence of alkane concentration on K_La in an aqueous-alkane system at 1.25 vvm.

♦ 1200 rpm; ■ 1000 rpm; ▲800 rpm; x 600 rpm; + 400 rpm

Closer analysis of the results presented in Figures 6.9 and 6.10 would seem to support the concept of there being two zones of different behaviour. It is possible that at speeds of above 800 rpm, interfacial area between the alkane droplets and the water is greatly increased, resulting in alkane becoming a more effective oxygen vector, thus increasing K_La. At low agitation rates, the viscosity of the alkane could be controlling the behaviour and creating stagnant zones that cause resistance to mass transfer due to the presence of undispersed alkane.

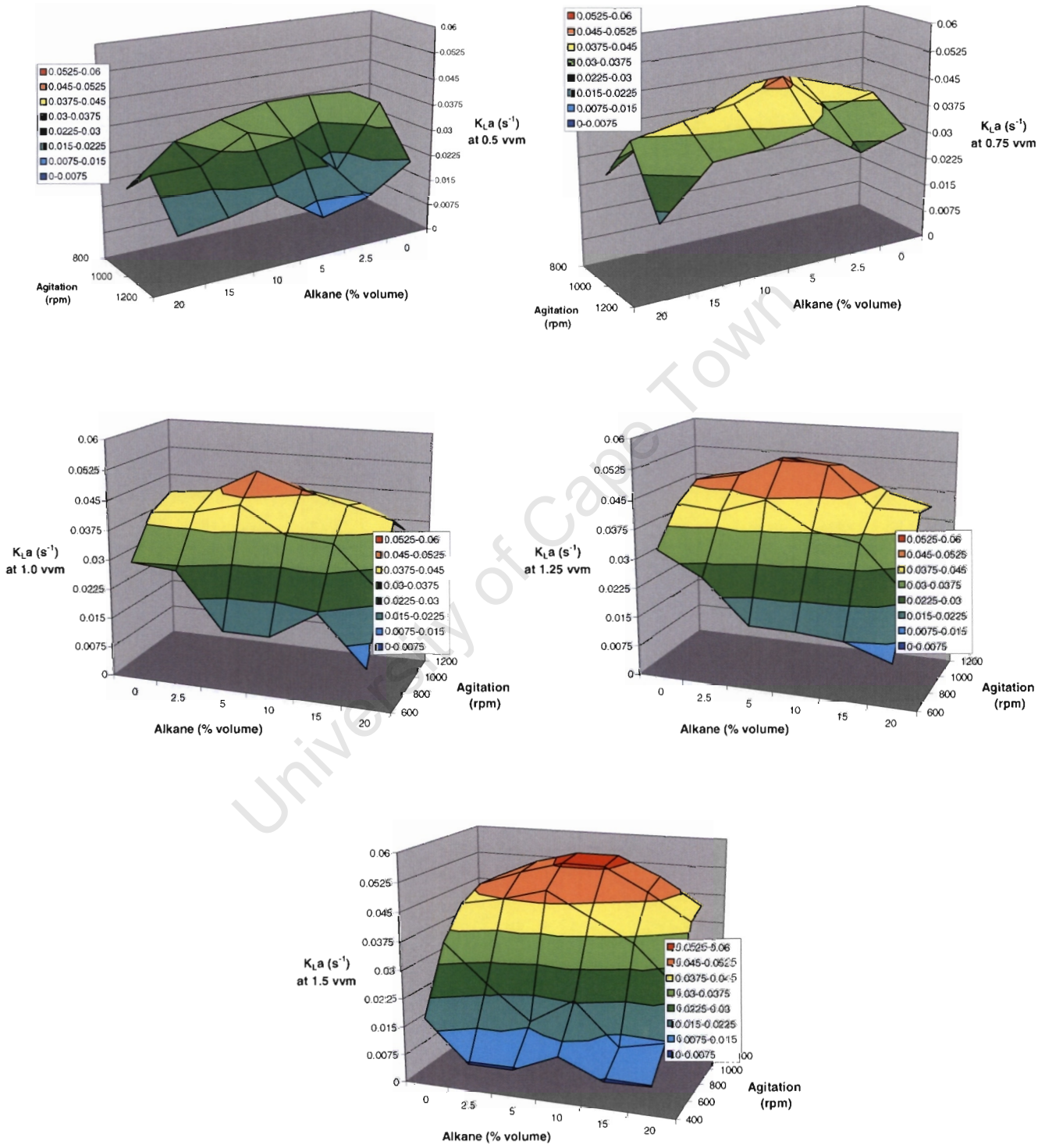

Figure 6.10: Optimum agitation, aeration and alkane concentration for K_La in an aqueous-alkane system

6.2.2 Effect on OTR in an air-water-alkane System

In addition to the influence of alkane concentration on K_La, this component will also affect the oxygen solubility in the liquid (Ju and Ho, 1989). This means that, contrary to the air-water system, the K_La cannot be directly related to the OTR but that the influence of C*, as well as that of K_La needs to be taken into account. Oxygen is approximately 6-fold more soluble in this C_{12-13} linear alkane fraction than in water, resulting in a corresponding increase in C* with increasing alkane fraction as shown in Figure 6.11. Hence, at 800 rpm and 1.25 vvm, the OTR was increased with increasing alkane concentration even though the K_La was suppressed at levels of 10% (v/v) and above.

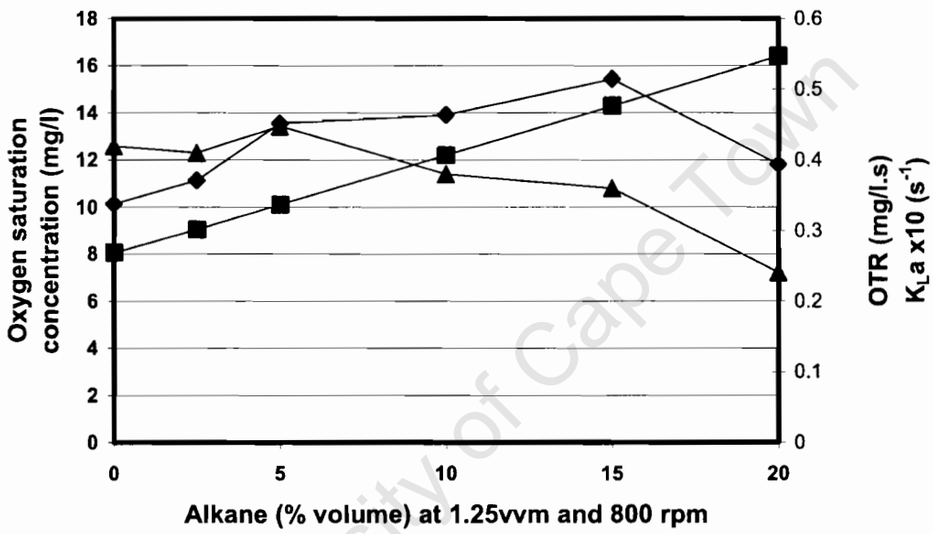

Figure 6.11: Dependence of OTR on C, K_La and alkane concentration at 1000 rpm and 1.25 vvm*

♦ OTR; ■ C*; ▲K_La x 10

When considering the OTR at various aeration rates over the range of agitation rates (Figure 6.12), it is evident that, with respect to the OTR maximum, the optimum agitation rate remains the same as for the K_La maximum, but that the optimum alkane concentration increases to between 15 and 20 %. This holds true over all the aeration rates.

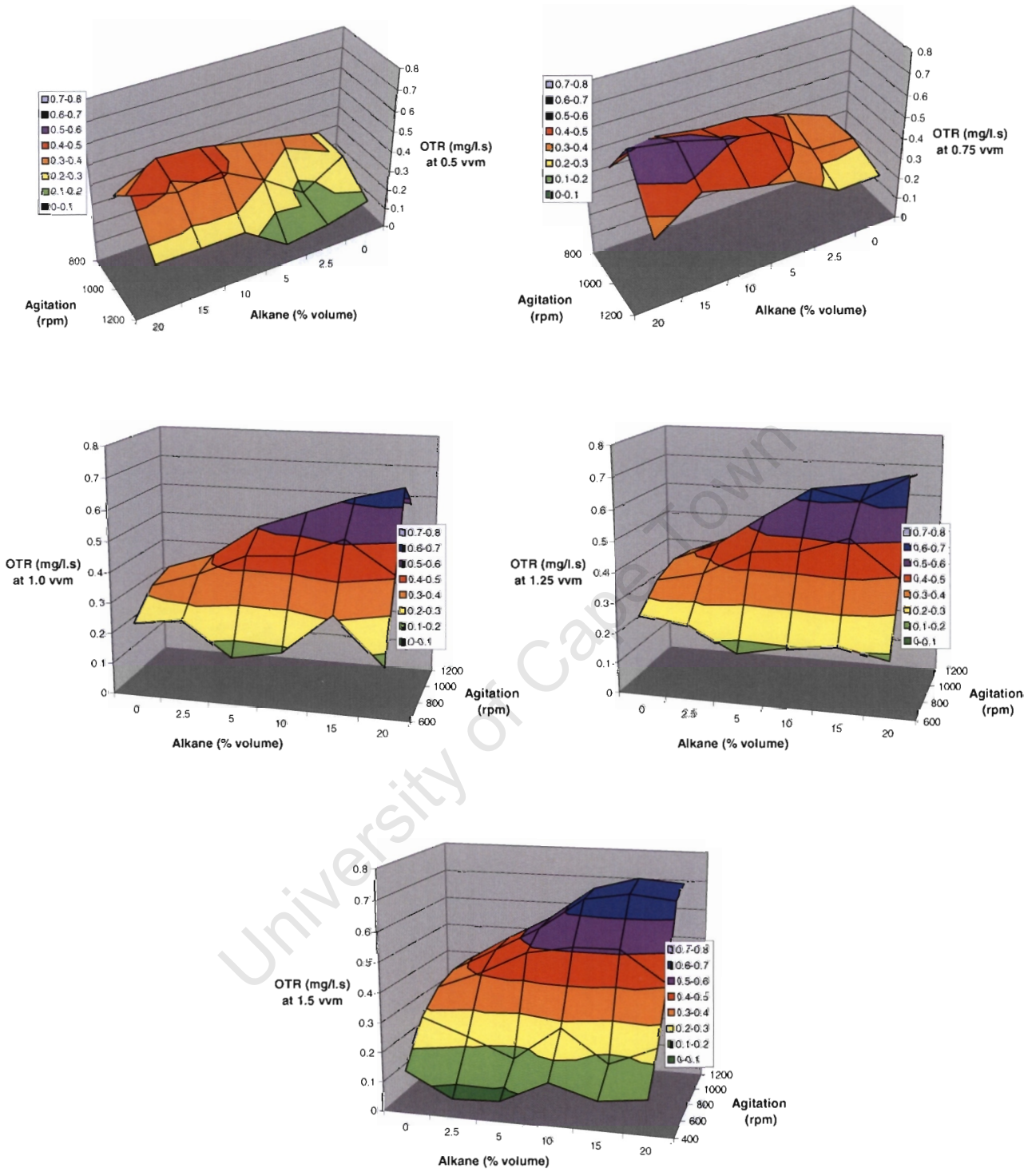

Figure 6.12: Optimum agitation, aeration and alkane concentration for OTR in an aqueous-alkane system

6.3 Modelling of Data

In order to model the data, a suitable general expression was required. As described in Section 2.5.2.3, Doran (1997) reports the following expression for stirred bioreactors containing non-coalescing non-viscous media:

$$k_L a = \delta \left(\frac{P}{V}\right)^{\alpha} u_G^{\beta} \tag{2.28}$$

where P/V = stirrer power per liquid volume [W/m^3]

u_G = superficial gas velocity [m/s]

and δ, α and β were empirical constants with the values 2.0x10^{-3}, 0.7 and 0.2 respectively.

As discussed in Section 2.5.2.3, this equation would not be suitable for an medium containing alkane. Alternatively, Nielsen *et al.* (2003) worked with an air-hexadecane-aqueous salt solution system and proposed and equation of the form:

$$k_L a = \delta \left(\frac{P}{V}\right)^{\alpha} u_s^{\beta} (1 - X)^{\gamma} \tag{6.1}$$

where P/V = specific power input [W/m^3]

u_s = superficial air velocity [m/s]

X = volumetric fraction of alkane

and δ, α, β and γ were empirical constants with the values 650, 0.31, 0.70 and 1.70 respectively.

A number of variations of equations of this format were investigated, but the following correlation was obtained using R statistical computing package (as described in Section 4.2.4) with the data presented in Section 6.1 and 6.2:

$$K_L a = 7.8 \cdot 10^{-5} Q_G^{0.45} N^{0.91} (1 - X)^{1.1} \tag{6.2}$$

where Q_G = volumetric air flowrate [vvm]

N = shear rate [rpm]

X = volumetric fraction of alkane in liquid medium.

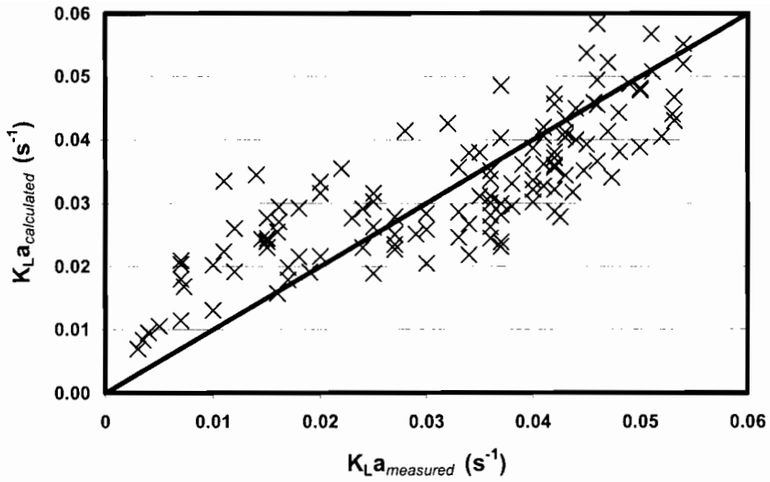

Figure 6.13: Comparison of Measured versus Calculated Values of K_La

This correlation appears similar to that developed by Nielsen *et al.* (2003), but aeration was quantified as Q_G rather than u_s, and agitation was quantified as N rather than P/V. The exponents for the variables representing agitation, aeration are positive and less than 1.0, while the exponent for (1-alkane fraction) is slightly more than 1.0. The constant coefficient for the expression is of a completely different order of magnitude, but this will be due to the different units used for the variables. The K_La values calculated according to this expression are plotted against the measured values for K_La obtained during the air-water and air-water-alkane experiments and shown in Figure 6.13.

In spite of the correlation having an R^2 value of 0.95 (R^2=1 indicating perfect fit) the data shows some deviation from the parity line. In general, the largest percentage error appears in low $K_La_{measured}$ values. Those measured values of less than $0.02s^{-1}$, are over-predicted by calculation according to Equation 6.2. $K_La_{measured}$ values of greater than $0.02s^{-1}$ tend to be under predicted via calculation, but the relative error is smaller. The data in Figure 6.13 was re-plotted to show which variable ranges (with respect to agitation, aeration or alkane concentration) were poorly predicted by equation 6.2. Figure 6.14 compares the deviation at different aeration rates, Figure 6.15 compares the deviation at different agitation rates and Figure 6.16 compares the deviation at different alkane concentrations.

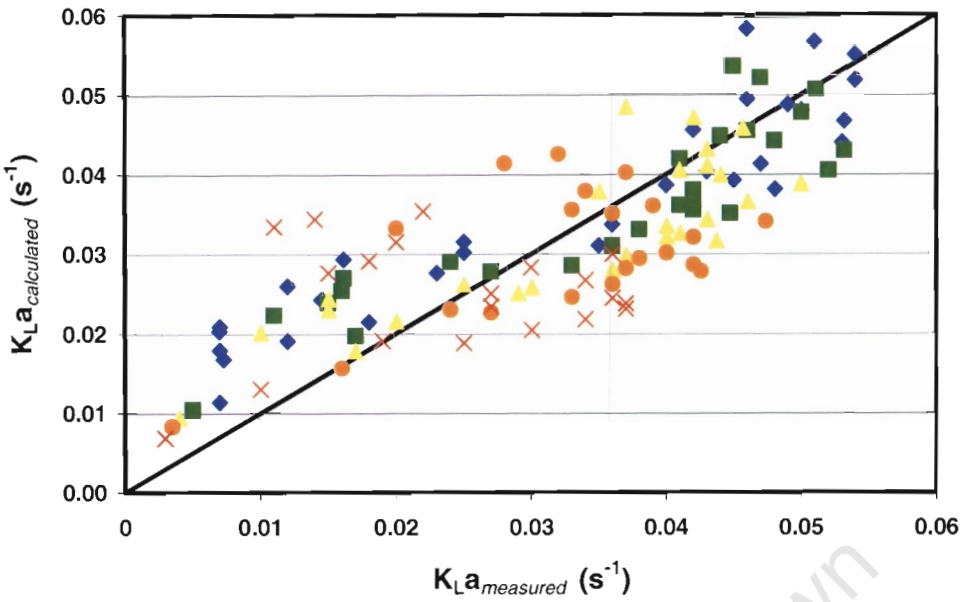

Figure 6.14: Comparison of Measured versus Calculated Values of K_La differentiated by aeration rates

♦ 1.5 vvm; ■ 1.25 vvm; ▲ 1.0 vvm; ● 0.75 vvm; x 0.5 vvm

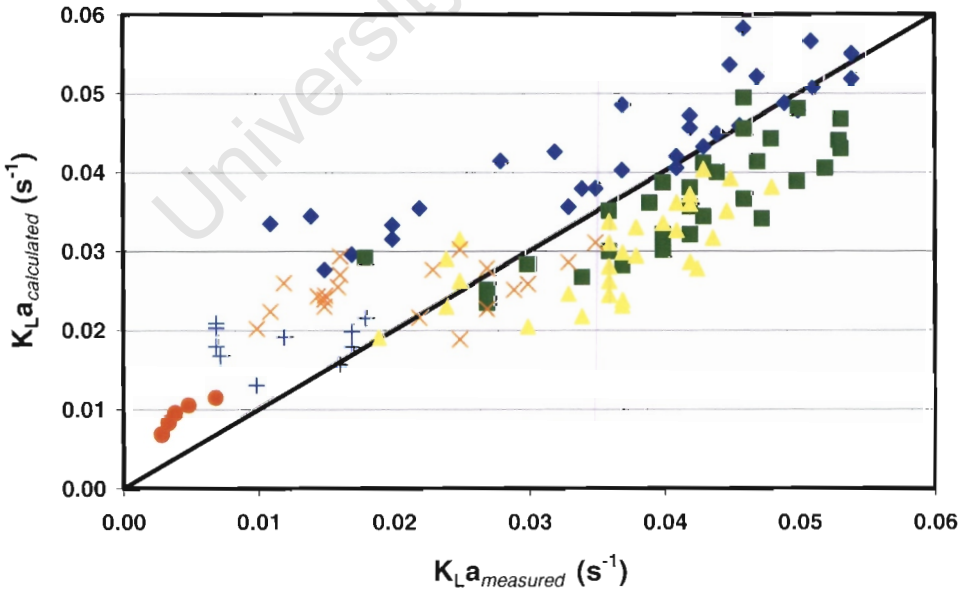

Figure 6.15: Comparison of Measured versus Calculated Values of K_La differentiated by agitation rates

♦ 1200 rpm; ■ 1000 rpm; ▲ 800 rpm; x 600 rpm; + 400 rpm; ● 200rpm

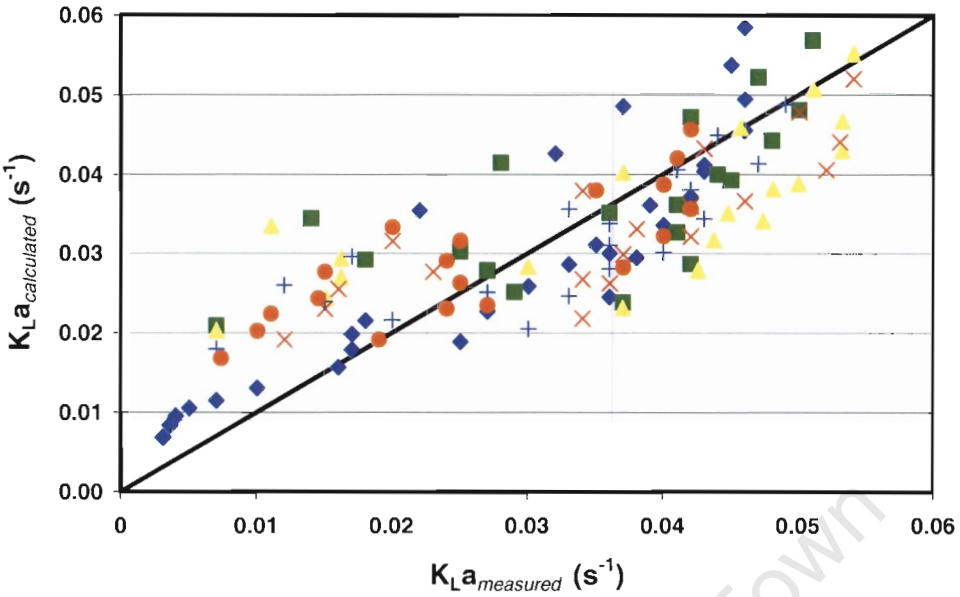

Figure 6.16: Comparison of Measured versus Calculated Values of K_La differentiated by alkane concentrations

♦ Pure Water; ■2.5% vol Alkane; ▲5% vol Alkane; x 10% vol Alkane; + 15% vol Alkane; ● 20% vol Alkane

Figure 6.14 shows each aeration rate distributed with a similar spread on either side of the parity line. However, the datum points with the largest absolute deviation from parity were those for 0.5 vvm. Since the values of K_La at 0.5 vvm tend to be at the lower end of the measured range, the percentage error in these predicted K_La values was also the highest, indicating that equation 6.2 predicted low aeration rates poorly. Figure 6.15 shows that correlation developed over-predicted the highest agitation rate (1200 rpm) and the lowest agitation rates (200 to 400 rpm). The datum points for the intermediate range of agitation rates (600 rpm) were distributed on both sides of the parity line but tended towards under-prediction in the case of 800 to 1000 rpm. The datum points showing the largest deviations from parity were for 1200 rpm. In Figure 6.16, no clear trend with respect to under- or over-predict of K_La was visible for any specific alkane concentration. Hence, equation 6.2 is best applied for prediction of K_La at intermediate agitation rates (600 to 1000 rpm) and at aeration rates above 0.5 vvm.

6.4 *Achieving Suitable Miscibility and Oxygen Transfer for Fermentation using Hydrocarbons*

Oxygen transfer and its dependence on K_La have been extensively reported and much attention has been directed towards improving OTR through K_La enhancement. K_La is a function of process parameters such as aeration and agitation rates (Doran, 1997) as well as physiological parameters of the medium, notably ionic strength (Robinson and Wilke, 1973) and viscosity (Aiba *et al.,* 1965). However, it is more difficult to alter physiological parameters during a bioprocess and therefore, in practice, K_La is increased by increasing the agitation or aeration rates or both. The increase in K_La by means of increased agitation or aeration rates is a consequence of improved turbulence. This reduces the resistance to mass transfer in stagnant boundary layers. In addition, it increases the interfacial area of the gas bubble per unit volume owing to bubble break up.

While the improvement in K_La through increased agitation or aeration or both is extensively documented, the relative effectiveness of the agitation and aeration rates in increasing the K_La is less well known. Since an increased agitation or aeration rate can sometimes result in adverse effects such as shear damage and foaming (Bailey and Ollis, 1986) an understanding of their relative effectiveness is an essential consideration in the judicious choice of the mode of operation in order to maximise the OTR without undue adverse effect on the process.

The results of this study clearly show that proportionately, relatively little improvement can be effected through an increase in the aeration rate across the range 0.5 to 1.5 vvm in this system when compared with that through an increase in the agitation rate across the range 200 to 1000 rpm, except at very high agitation and aeration rates. The variation in K_La over the full aeration range at 1000 and 1200rpm shows a variation of the same order of magnitude as the variation in K_La over the full agitation range at 1.5vvm. Therefore, the effect on K_La is more pronounced at higher agitation and aeration rates. Nielsen *et al.* (2003) also reported increased K_La with increased agitation from 200 to 800 rpm and aeration rates from 0.5 to 2 vvm. K_La was affected very little by change in aeration at agitation rates below 400rpm, and K_La was affected very little by change in agitation at aeration rates below 1.0vvm. Alternatively, a nearly 10-fold increase in the K_La, was observed when increasing aeration from 0.5 to 1 vvm at agitation rates of 400rpm to 800rpm, but at agitation rates of 400 to 800 rpm and aeration rates from 1 to 2 vvm, the

increase due to agitation appeared to be more significant than that due to aeration, at least in the system without alkane and, therefore, is in agreement with the results in our study.

The greater effect of agitation when compared with aeration suggests that the agitation rate will be the controlling parameter for enhancement of an inadequate K_La, in both carbohydrate- and hydrocarbon-based bioprocesses. In addition, the results reveal a threshold aeration rate above which a further increase in aeration had a negligible effect on K_La. This threshold value occurred progressively earlier at correspondingly lower agitation rates, confirming that the adverse effects on the process through increased aeration, especially at low agitation rates, may outweigh the benefit to the K_La. Therefore, an increase in agitation should rather be investigated under these conditions. Moreover, it is likely that an increase in the aeration rate instead of the agitation rate at low agitation would also be less cost effective since large amounts of air would be required to effect comparatively little improvement in K_La. In addition to the influence of agitation and aeration rate, the alkane concentration had a significant influence on K_La in the air-water-alkane system. Further, this influence was dependent on the agitation rates. At the higher rates of 800 rpm and above, the K_La increased above that in water, exhibiting an optimum at 5 to 10 % alkane, while contrarily at the rates below 800 rpm, the K_La declined steadily below that in water and no optimum was observed.

Several authors have observed an increase in K_La to a value above that in water resulting from hydrocarbon addition. K_La was reported to increase with increasing *n*-hexadecane levels up to 10 % in an air-water-alkane system at several agitation rates and 4 aeration rates (Hassan and Robinson, 1977). No K_La peak was observed in this study but this may have been a consequence of their alkane concentration limit of 10 %. An increase in K_La with increasing *n*-hexadecane levels was also reported in a fermentation broth at an agitation rate of 400 rpm and aeration rate of 0.21 vvm (Rols *et al.*, 1990). These authors report maximum K_La between 15 and 25 %. A peak in K_La was also observed in a tower reactor at 4 % $C_{12\text{-}16}$ alkanes at each of 7 aeration rates (Jia *et al.*, 1996) and at 3 % *n*-dodecane at a fixed aeration rate (Jia *et al.*, 1997). Galaction *et al.* (2004) also observed a peak in K_La at approximately 10% *n*-dodecane with mechanical agitation between 100 and 500 W/m^3.

This study suggests that the K_La peak as a function of alkane concentration at high agitation rates is a consequence of the relative prominence of two

system properties, namely the droplet interfacial area and liquid viscosity. Photo images presented by Galindo *et al.* (2000) show the reduction in gas bubble diameter in the presence of alkane, contact between the gas bubble and oil droplet as well as gas bubbles incorporated into castor oil droplets. This corresponds to Scenario B (Figure 6.17) proposed by Linek and Benes (1976) (Figure 2.3) as a possible mechanism for gas transfer into an oil-water emulsion.

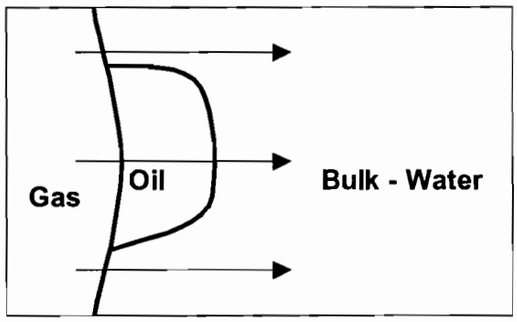

Figure 6.17: Mechanism for Gas Transfer into an Oil-Water Emulsion

A greater droplet interfacial area will result directly from an increased alkane concentration (Galindo *et al.* 2000). According to the mechanism of oxygen transfer proposed for an immiscible phase system, the greater interfacial area will improve oxygen transfer rates through the action of the alkane droplet as an active intermediate between the gas and the water in the transfer process (Rols and Goma, 1989; Rols *et al.*, 1990). These potentially lead to very efficient transfer of oxygen from air to oil. On the other hand, an increase in alkane concentration will also result in an increased viscosity with a concomitant increase in stagnant zones and increased resistance to oxygen transfer. Rols *et al.* (1990) proposed that an increase in viscosity could increase the thickness of the boundary layer around air bubbles and alkane droplets, thereby slowing the rate of drainage of the liquid film between the bubbles and droplets and in turn decreasing the rate of coalescence. Rols *et al.* (1990) postulated that the observed peak in K_La is, therefore, a likely result of the competing influences of an increased oxygen diffusion resulting from alkane droplets acting as active oxygen transfer intermediates and an inhibition of convective oxygen transfer due to increased liquid viscosity.

Conversely, a steady decline in K_La from that in water with increasing alkane concentration remains almost exclusively unreported, with the notable

exception of Nielsen *et al.* (2003) and Hassan and Robinson (1977). Nielsen *et al.* (2003) observed a decrease in K_La with increasing *n*-hexadecane from 0 to 33%. However, K_La at alkane concentrations between 0 and 10% were not reported. It is in this region that the literature data and the results presented here suggest that K_La enhancement is likely to occur with a decrease in the K_La expected at higher alkane concentrations. Further, at the highest agitation rate investigated in their system (800 rpm), there appears to be negligible difference in the magnitude of K_La at 0% and 10% and it would be interesting to know if a K_La peak would have occurred between these concentrations. The decrease in K_La observed by these authors may also be partially explained by the fact that the highest agitation rate used was 800 rpm. Increased K_La is less likely to be obtained at low agitation rates. The absence of a peak at low agitation rates is a likely consequence of the reduced turbulence at these rates. Comparatively large alkane droplets were observed and consequently, when the alkane concentration was increased, the resultant increase in the interfacial area of the alkane droplet was small relative to that at the high agitation rate. Apparently, under these conditions, the increased droplet interfacial area was not sufficient to compensate for the adverse effect of increased viscosity and the liquid viscosity became controlling with respect to oxygen transfer. This is supported by the observation of Rols *et al.* (1990) that larger droplets are less effective in enhancing oxygen transfer.

In addition to Nielsen *et al.* (2003), Hassan and Robinson (1977) also reported a decrease in the K_La with increasing *n*-dodecane addition. In this study, however, an increase in K_La with *n*-hexadecane addition was observed under identical alkane concentrations and agitation rates. The reason for the different influences of alkane carbon number on the K_La is not clear. It would appear that there is another factor that needs to be taken into account, most likely density or viscosity of the medium. Equation 6.2 developed in Section 6.3 for prediction of K_La as a function of agitation, aeration and alkane concentration had the largest error at low agitation and aeration rates, as well as at very high agitation rates. At the low agitation and aeration rates this is most likely due to diminished mixing and stagnant zones, and this error in prediction of K_La could be resolved by investigation of viscosity effects in the liquid medium. The poor prediction of K_La at high agitation rates is most likely also a consequence of abnormal mixing patterns, in this case the jetting and vortex formation observed during the experiments for measurement of K_La.

Galaction *et al.* (2004) developed an expression for k_La in an air-dodecane-carboxymethylcellulose sodium salt solution:

$$k_L a = 5.6 \cdot 10^{-3} \left[\frac{\left(\frac{P}{V}\right)^{1.54} u_s^{2.30}}{\mu^{3.78}} \right]^X \tag{6.3}$$

where P/V = specific power input [W/m^3]

u_s = superficial air velocity [m/s]

μ = apparent viscosity [Pa.s]

X = volumetric fraction of alkane.

This correlation fitted their data with an average deviation of 10%. In order to improve the predictive K_La correlation for this work, as developed in Equation 6.2, it would therefore be of interest to measure other physical parameters of the liquid medium, such as density, viscosity and surface tension. These measurements are also required to confirm the theory of "Spread Coefficients" and its effect on droplet formation, as proposed by authors such as Hassan and Robinson (1977).

While the influence of alkane addition on K_La and the increased oxygen solubility in hydrocarbons have been quantified in the literature, the resultant composite effect on OTR has generally been less explicit. Nielsen *et al.* (2003) have recognised the critical distinction between the influence of the K_La and the C* on the OTR and developed an empirical correlation for use in immiscible liquid systems which predicts an increase in OTR with increasing C* to an optimal value despite a decrease in the K_La. This is in agreement with the results presented in our study where it was found that under most operating conditions, particularly at relatively high agitation rates, the increased C* will more than compensate for the K_La suppression at higher alkane levels, resulting in a correspondingly improved OTR. On the other hand, Nielsen *et al.* (2003) reason that this predicted increase in OTR with increasing alkane concentration is insensitive to other operating conditions. This is contrary to our results where improvements in OTR were not observed at the lower agitation rates. Further, the increased K_La observed at high agitation rates and relatively low alkane levels in our study, compounded the

effect of increased C*, resulting in substantially higher rates of transfer than that which would be accomplished by increased C* alone.

The presence of hydrocarbon therefore increases the supply of oxygen invariably through an increase in C* and often, in addition, through an increase in the K_La. A high OTR during an octane-based bioprocess has been experimentally confirmed by Preusting *et al.* (1993). This increased oxygen supply may, at least in part, offset the increased oxygen requirement resulting from the deficiency of oxygen in the hydrocarbon structure. Hence, despite the increased stoichiometric requirement for oxygen when using a hydrocarbon substrate, the supply of adequate oxygen to a hydrocarbon-based bioprocess may not necessarily be more problematic than the supply to an analogous carbohydrate bioprocess.

These results also suggest a method of eliminating oxygen transfer limitation that would be applicable to both carbohydrate- and hydrocarbon-based bioprocesses. Under conditions where the oxygen demand is not satisfied, the OTR could be increased by alkane addition (in the case of a hydrocarbon-based bioprocess this could be in excess of the metabolic requirement, if necessary), specifically to introduce more oxygen into the medium. This method requires no extra energy input and would be especially attractive if a relatively cheap source of alkane was available. This is supported by the successful use of C_{12-16} alkanes as an oxygen vectors to increase the OTR during culture of *Penicillium chrysogenum* (Ju *et al.*, 1990), *Aerobacter aerogenes* (Rols *et al.*, 1990) and *Saccharomyces cerevisae* Jia *et al.* (1997).

The information presented here can be used, in combination with kinetic data relevant to the specific bioprocess, to select optimum conditions for operation and scale up of aerobic hydrocarbon-based bioprocesses such that yields and productivities are not compromised by transport limiting conditions. Clearly, the optimum parameters to achieve good oxygen transfer will be in the region of 800 to 1000 rpm, with little improvement resulting from aeration rates greater than 1 vvm. It is envisaged, however, that the optimum agitation rate will depend on the particular bioreactor and impeller geometry. The optimum alkane level would be selected preferentially in a region in which both K_La and C* are enhanced, observed to be less than 10 % for this chain length, provided that this supplied sufficient carbon to meet the metabolic needs of the microorganism. If greater levels of alkane are required for growth and/ or product formation, the process should preferably be operated with an agitation rate and alkane level at which increased C* reverses the effect of the K_La

decline on the OTR. Careful consideration, however, needs to be given to establishing the alkane concentration limit for the particular process conditions. Depending on the alkane type and the microorganism, growth inhibition may occur when further improvements in OTR will be of no use to the organism. Alkanes are well known to inhibit growth, usually at low carbon lengths (Schmid *et al.*, 1998). It is difficult, however, to predict the influence of alkanes of different carbon lengths on OTR, and more studies into the physical properties of alkane-aqueous solutions are required.

For the purposes of dicarboxylic acid production, these optimum agitation and aeration rates could be employed in a bioreactor to disperse alkane and prevent the occurrence of an immiscible alkane layer floating on top of the aqueous medium, as was observed in the experiments in shake flasks. This should allow adequate oxygen transfer for bioconversion of alkanes to dicarboxylic acid through increased OTR.

The photographs taken during the shake flask experiments are consistent with the observation of Mimura *et al.* (1973), who noted that hydrocarbon-assimilating yeasts attach themselves to droplets of hydrocarbon. The potential effect of agitation on air-alkane-yeast cell contact is however not clear at this stage, and photographic techniques could provide insight into this. Galindo *et al.* (2000) and Rocha-Valadez *et al.* (2000) employed photographic techniques to evaluate the behaviour of *Trichoderma harzianum* in a four-phase system, but it is difficult to relate their findings for physical conformation of mycelia to the potential conformation of yeast cells.

Mimura also proposed that "flocs" of alkane and cells attach themselves to air bubbles. If, in the case of dicarboxylic acid production with *Candida tropicalis*, "flocs" of alkane and cells attach themselves to air bubbles, it would further ensure that cells receive enough oxygen, either directly from the air bubble or through the hydrocarbon oxygen vector. If these "flocs" were fairly stable, however, this could account for non-uniform distribution of the alkane in the medium and limited surface renewal for mass transfer, thus allowing stagnant zones to build up. Density, viscosity and surface tension for the actual fermentation conditions should also be measured and related to those for a non-fermentative system, in order to give additional insight into the effect of these parameters on K_La, and hence OTR. If the apparent viscosity of the fermentation medium were significantly higher than the non-fermentative system, the agitation rate for maximising K_La could be nearer to 1000rpm than 800rpm, in order to ensure sufficient droplet interfacial area to overcome the

effect of increased viscosity. Alternatively, Mimura *et al.* (1973) employed antifoam to induce cell dispersion. However, it is unknown at this stage if this would have adverse effects on the ability of *Candida* cells to adsorb oxygen from the hydrocarbon "flocs" during the growth phase. Uchio and Shiio (1972c) however, noted that the addition of antifoam stimulated the production of dicarboxylic acid in *Candida cloacae*. Therefore, the antifoam did most likely not significantly affect alkane-contact, but rather prevented the formation of stagnant air-cell-alkane masses.

It is therefore most likely that the path of oxygen transfer that will occur in the biological conversion of alkanes to dicarboxylic acids by *Candida tropicalis* is that proposed by Mimura *et al.* (1973) whereby cells take up oxygen via direct absorption from the liquid film between the air bubbles and the alkane droplets, and not the bulk liquid phase. It is therefore unlikely that there will be an oxygen limitation due to the absence of oxygen in the hydrocarbon backbone. The adherence of cells to alkane droplets also has positive implications for facilitating alkane substrate uptake as discussed in Section 2.3.2. However, as discussed in Section 2.5.2, the effects of agitation and aeration cannot be ignored. The oxygen transfer mechanism would still require on a certain amount of turbulence due to air sparging or mechanical agitation in order to disperse the bubbles and "flocs" evenly throughout the bioreactor and allow for surface renewal by "floc" engagement and disengagement at the bubble interface in order to prevent the occurrence of stagnant zones. As a result, careful selection of fermentation parameters will be required in order to balance the advantage gained by using an oxygen vector with that gained by mixing. Increasing agitation may result in increased shear damage to the cells.

The optimum alkane level to employ in the biological production of dicarboxylic acid with *Candida tropicalis*, would be subject to the extent of substrate inhibition on the process. Extensive literature surveys have yielded no record of authors who have documented using more than 10 % (v/v) alkane, so while the optimum K_La lies at this level or below, and OTR is still improved at 10% (v/v) (when compared to OTR with 0% alkane). In addition, if increased dicarboxylic acid yields were achieved, product inhibition could become a factor. Chan *et al.* (1997a&b) document product inhibition of cell growth by the dicarboxylic acid product in bacteria in the presence of dicarboxylic acid concentrations of as low as 8 g/l. However, Picataggio *el al.* (1992) reported dicarboxylic acid concentrations of 120 g/l in their

fermentation. It is therefore unlikely that *Candida tropicalis* ATCC 20962 is greatly affected by product inhibition.

7. Conclusions

The following conclusions can be drawn from this work:

- *Candida tropicalis* ATCC 20962 can be used to convert C_{12} *n*-alkane to C_{12} dicarboxylic acid. Glucose is a suitable co-substrate for the completion of the respiratory cycle of the organism, and should be added in excess of the metabolic requirements of the organism. Organic nitrogen in the form of peptone gives the most sustainable dicarboxylic acid production, while inorganic nitrogen supports better biomass formation. Alkane substrate should be added before the stationary phase, and the pH of the medium should be raised to 8 in order to induce dicarboxylic acid formation.
- Due to the presence of immiscible aqueous and hydrocarbon liquid phases, fermentation with alkane can result in non-uniform medium composition and hence difficulty in obtaining representative results for process evaluation. Adequate mechanical or chemical dispersion techniques are required to avoid mass transfer limitation which can potentially affect oxygen transfer to the cells for growth and availability of alkane substrate for dicarboxylic acid production.
- The influence of agitation, aeration and alkane concentration on K_La have been quantified. K_La variation with alkane concentration up to 20% (v/v) was markedly different at different agitation rates. Comparatively little improvement can be effected through an increase in the aeration rate across the range 0.5 to 1.5 vvm in this system when compared with that through an increase in the agitation rate across the range 200 to 1000 rpm. The greater effect of agitation when compared with aeration suggests that the agitation rate will be the controlling parameter for enhancement of an inadequate K_La, in both carbohydrate- and hydrocarbon-based bioprocesses. In addition, the results reveal a threshold aeration rate above which a further increase in aeration had a negligible effect on K_La. In general, at agitation rates of below 800rpm, K_La was repressed below that of water at all alkane concentrations, while at higher agitation rates, the K_La increased initially with alkane addition, and then decreased. The optimum K_La of $0.052s^{-1}$ was found at an agitation rate of 1000 to 1200rpm and an aeration rate of 1.25vvm and an alkane concentration of 5 to 10%. It is therefore postulated that the peak in K_La results from competing influences of an increased oxygen diffusion resulting from alkane droplets acting as active oxygen transfer intermediates and an

inhibition of convective oxygen transfer due to increased liquid viscosity.

- The calculated increase in oxygen solubility in the liquid with increased alkane concentration resulted in a predicted increase in OTR at higher agitation rates, when compared with OTR in water at similar conditions. This will even occur under conditions where K_La depression is reported. Hence, the maximum OTR of 0.7mg/l.s could be reached at the same agitation and aeration rates as for maximum K_La, but with an alkane concentration of 15 to 20%. Hence, under conditions where the oxygen demand is not satisfied, the OTR could be increased by alkane addition to introduce more oxygen into the medium.
- An equation was developed to predict K_La as a function of agitation, aeration and alkane concentration. Accuracy of prediction is poorest at low agitation and aeration rates (below 600 rpm and 0.75 vvm respectively), and at very high agitation rates (above 1000rpm). In order to allow more accurate prediction of K_La and OTR, other physical parameters of the liquid medium, such as density, viscosity, surface tension and droplet size, will need to be quantified.
- These optimum agitation and aeration rates could be employed in the biological production of dicarboxylic acids to disperse alkane adequately. Addition of alkane in excess of the metabolic requirement could provide sufficient oxygen transfer for the bio-oxidation of alkanes to dicarboxylic acid through increased OTR, provided substrate inhibition was not induced.

8. Recommendations

- Further work should be performed to quantify the effect of physical parameters such as density, viscosity, surface tension and droplet size on K_La and OTR in liquid-liquid-vapour systems.
- Further investigation into improving the production of dicarboxylic acids from alkane should be conducted in a bioreactor. The medium should contain excess glucose and peptone nitrogen source. The optimum conditions for K_La and OTR in liquid-liquid-vapour systems determined in this study should be used as a base case for these experiments.
- An effort should be made of experimentally confirm the predicted increase in C* and hence OTR upon the addition of alkane to aqueous mixtures.
- Following from the base case, photographic techniques should be used to investigate the effect of process conditions on air-alkane-yeast cell. In addition, density, viscosity, surface tension and droplet size for the actual dicarboxylic acid production conditions should also be measured and related to those for a non-fermentative system, in order to optimise K_La and OTR in a fermentative system. The effect of substrate and product inhibition should be quantified to determine optimum alkane substrate level to maximise dicarboxylic acid production.

9. References

1. Abrardi, V, Rovero, G, Baldi, SS and Conti, R (1990) "Hydrodynamics of a Gas-Liquid Reactor Stirred with a Multi-Impeller System", *Trans. I. Chem. E.*, **68** (A), p 516-522.
2. Aiba, S, Humphrey, AE and Millis, N (1965) "Biochemical Engineering", Academic Press, New York.
3. Armenante, PM & Abu-Hakmeh, EA (1994) "A Novel Method for the Experimental Determination of the Minimum Agitation Speed for Complete Liquid-Liquid Dispersion in Agitated Liquid-Liquid Systems", *Trans. I. Chem. E.*, **72** (A), p 677 – 685.
4. Baburin, LA, Shvinka, JE and Viesturs, UE (1981) "Equilibrium Oxygen Concentration in Fermentation Fluids", *European J. App. Microbiol. Biotechnol.*, **13**, p 15-18.
5. Badino, AC Jr, Facciotti, MCR and Schmidell, W (2000) "Improving kLa determination in fungal fermentation, taking into account electrode response time", *J. Chem. Technol. Biotechnol.*, **75**, p 469-474.
6. Bailey, JE and Ollis, DF (1986) "Biochemical Engineering Fundamentals", McGraw-Hill, New York.
7. Blanc, C and Batiste, M (1970) "Solubility coefficient of oxygen in paraffins", *Bulletin du Centre de Recherches de Pau*, **4** (1), p 235 - 241.
8. Blasig, R, Mauersberger, S, Riege, P, Schunck, W, Jockisch, W and Franke, P (1988) "Degradation of Long-Chain n-Alkanes by the Yeast *Candida maltosa* II. Oxidation of n-Alkanes and Intermediates Using Microsomal Membrane Fractions", *Appl. Microbiol. Biotechnol.*, **28**, p 589-597.
9. Bos, P, de Bruyn, JC (1973) "The significance of hydrocarbon assimilation in yeast identification", *J. Microbiol.*, **39**, p 99 – 107.
10. Calabrese, RV, Wang, CY and Bryner, NP (1986) "Drop Breakup in Turbulent Stirred-Tank Contactors, Part III: Correlations for Mean Size and Drop Size Distribution", *AIChE Journal*, **32** (4), p 667-681.
11. Calderbank, PH and Moo-Young, M (1961) "The continuous phase heat and mass-transfer properties of dispersions", *Chem. Eng. Sci.*, **16**, p 39.
12. Chan, E-C, Cheng, C-S and Hsu, Y-H (1997 a) "Continuous Production of Dicarboxylic Acids by Immobilized *Pseudomonas aeruginosa* Cells", *J. Ferment. Bioeng.*, **83** (2), p 157-160.
13. Chan, E-C and Kuo, J (1997 b) "Biotransformation of dicarboxylic acid by immobilized *Cryptococcus* cells", *Enzyme and Microbial Technology*, **20**, p 585-589.
14. Cordova-Aguilar, MS, Sanchez, A, Serrano-Carreon, L and Galindo, E

(2001) "Oil and fungal biomass dispersion in a stirred tank containing a simulated fermentation broth", *J. Chem. Technol. Biotechnol.*, **76**, p 1101-1106.

15. Cronin, DG, Nienow, AW and Moody, GW (1994) "An Experimental Study of Mixing in a Proto-Fermenter Agitated by Dual Rushton Turbines", *Trans. I. Chem. E.*, **72** (C), p 35-40.
16. Daglas, D, Stamatoudis, M (2000) "Effect of Impeller Vertical Position on Drop Sizes in Agitated Dispersions", *Chem. Eng. Technol.*, **23** (5), p 437-440.
17. Darlington WA (1964) "Aerobic hydrocarbon fermentation. A practical evaluation", Biotechnol. Bioeng., **6**, p 241-242.
18. Doran, PM (1997) "Bioprocess Engineering Principles", Academic Press, New York.
19. Freitas, AA and Quina, FH (2000) "A Linear Free Energy Analysis of the Surface Tension of Organic Liquids", Langmuir, **16**, p 6689 – 6692.
20. Fukui, S and Tanaka, A (1980) "Production of Useful Compounds from Alkane Media in Japan", *Advances in Biochemical Engineering*, **17**, p 1-35.
21. Fukui, S and Tanaka, A (1981) "Metabolism of Alkanes by Yeasts", *Advances in Biochemical Engineering*, **19**, p 216-237.
22. Galaction, A-I, Cascaval, D, Oniscu, C, Turnea, M (2004) "Enhancement of oxygen mass transfer in stirred bioreactors using oxygen vectors. 1. Simulated fermentation broths", *Bioprocess and Biosystems Engineering*, **26**, p 231 – 238.
23. Galindo, E, Pacek, A and Nienow, AW (2000) "Study of Drop and Bubble Sizes in a Simulated Mycelial Fermentation Broth of Up to Four Phases", *Biotechol. Bioeng.*, **69** (2), p 213-221.
24. Green, KD, Turner, MK and Woodley, JM (2000) "*Candida cloacae* oxidation of long-chain fatty acids to dioic acids", *Enzyme and Microbial Technology*, **27**, p 205-211.
25. Hassan, ITM and Robinson, CW (1977) "Oxygen Transfer in Mechanically Agitated Aqeous Systems containing Dispersed Hydrocarbon", *Biotechol. Bioeng.*, **19**, p 661-682.
26. Hesse, PJ, Battino, R, Scharlin, P and Wilhelm, E (1996) "Solubility of Gases in Liquids. 20. Solubility of He, Ne, Ar, Kr, N_2, O_2, CH_4, CF_4 and SF_6 in n-Alkanes n-C_lH_{2l+2} ($6 \leq l \leq 16$) at 298.15K", *J. Chem. Eng. Data.*, **41**, p 195 – 201.
27. Hill, FF, Venn, I and Lucas, KL (1986) "Studies on the formation of long-chain dicarboxylic acids from pure n-alkanes by a mutant of *Candida tropicalis*", *Appl. Microbiol. Biotechnol.*, **24**, p 168-174.
28. Ho, CS and Ju, L (1988) "Effects of Microorganisms on Effective Oxygen Diffusion Coefficients and Solubilities in Fermentation Media",

Biotechol. Bioeng., **32**, p 313-325.

29. Ho, CS, Ju, L and Baddour, R F (1990) "Enhancing *Penicillin* Fermentations by Increased Oxygen Solubility Through the Addition of n-Hexadecane", *Biotechol. Bioeng.*, **36**, p 1110-1118.
30. Jasper, JJ and Kring, EV (1955) "The Isobaric Surface Tensions and the Thermodynamic Properties of the Surfaces of a Series of n-alkanes, C_5 to C_{18}, 1-Alkenes, C_6 to C_{16}, and of n-Decylcyclopentane, n-Decylcyclohexane and n-Decylbenzene", *Thermodynamic Properties of Surfaces of the n-Alkane Series*, **59**, p 1019 – 1021.
31. Jia, S, Li, P, Park, YS and Okabe, M (1996) "Enhanced Oxygen Transfer in Tower Bioreactor on Addition of Liquid Hydrocarbon", *J. Ferment. Bioeng.*, **82** (2), p 191-193.
32. Jia, S, Wang, M, Kahar, P, Park, Y and Okabe, M (1997) "Enhancement of Yeast Fermentation by Addition of Oxygen Vectors in Air-Lift Bioreactor", *J. Ferment. Bioeng.*, **84** (2), p 176-178.
33. Jiao, P, Huan, Y, Li, S, Hua, Y and Cao, Z (2001) "Effects and Mechanisms of H_2O_2 on Production of Dicarboxylic Acid", *Biotechol. Bioeng.*, **75** (3), p 456-462.
34. Johnson, MJ, Borkowski, J and Engblom, C (1964) "Steam Sterilizable Probes for Dissolved Oxygen Measurement", *Biotechol. Bioeng.*, **6** (4), p 457-468.
35. Ju, L, Ho, CS and Baddour, RF (1988) "Simultaneous Measurements of Oxygen Diffusion Coefficients and Solubilities in Fermentation Media with Polarographic Oxygen Electrodes", *Biotechol. Bioeng.*, **31**, p 995-1005.
36. Ju, L and Ho, CS (1989) "Oxygen Diffusion Coefficient and Solubility in n-Hexadecane", *Biotechol. Bioeng.*, **34**, p 1221-1224.
37. Jung, K, Hazenberg W, Prieto M, Witholt B (2001) "Two stage continuous process development for the production of medium-chain-length poly (3-hydroxyalkanoates)", *Biotechol. Bioeng.*, **72**, p 19-24.
38. Kappeli, O, Mueller, M and Fiecher, A (1978) "Chemical and Structural Alterations at the Cell Surface of *Candida tropicalis*, Induced by Hydrocarbon Substrate", *Journal of Bacteriology*, **133** (2), p 952-958.
39. Kappeli, O and Fiechter, A (1980) Partition of Hexadecane to the Cell Surface of Candida tropicalis: Mechanism for the Transport of Water-Insoluble Substrates, *Biotechol. Bioeng.*, **22**, p 1829-1841.
40. Keitel, G and Onken, U (1982) "The Effect of Solutes on Bubble Size in Air-Water Dispersions", *Chemical Engineering Communications*, **17**, p 85 –98.
41. Kessler, B, and Witholt, B (1999) "Poly (3-hydroxyalkanoates)". In: Flickinger MC, Drew SW (eds). *Encyclopedia of Bioprocess Technology: Fermentation, Biocatalysis and Bioseparation*, **4**, John

Wiley and Sons, New York, p 2024 - 2040.
42. Kitchener, JA, Cooper, CF (1959) "Current concepts in the theory of foaming", *Quarterly Reviews (London)*, **13**, p 71 - 97.
43. Kirk Othmer (1998) "Encyclopedia of Chemical Technology", Kroschwitz, JI, and Howe-Grant, M (eds.), 4th ed., John Wiley and Sons, New York.
44. Kosaric, N (1996) "Biosurfactants". In: Roehr M (ed.). *Biotechnology: Products of primary metabolism*, 2nd ed., VCH, Weinheim.
45. Leja, J (1982) "Surface Chemistry of Froth Flotation", Plenum Press, New York.
46. Lin, R and Cao, T, Zhang, Z (2000) "Secretion in long-chain dicarboxylic acid fermentation", *Bioproc. Eng.*, **22**, p 391-396.
47. Linek, V and Benes, P (1976) "A Study of the Mechanism of Gas Absorption into Oil-Water Emulsions", *Chem. Eng. Sci.*, **31**, p 1037-1046.
48. Linek, V, Vacek, V and Benes, P (1987) "A Critical Review and Experimental Verification of the Correct use of the Dynamic Method for the Determination of Oxygen Transfer in Aerated Agitated Vessels to Water, Electrolyte Solutions and Viscous Liquids", *Chem. Eng. J.*, **34**, p 11- 34.
49. Machon, V, Pacek, AW, Nienow, AW (1997) "Bubble Sizes in Electrolyte and Alcohol Solutions in a Turbulent Stirred Vessel", *Trans. I. Chem. E.*, **75** (A), p 339 – 348.
50. Mączyński, A, Góral, M, Wiśnewska-Gocłowska, Skrzecz, A and Shaw, D (2003) "Mutual Solubilities of Water and Alkanes", *Monatshefte für Chemie,* **134**, p 633 – 653.
51. Makranczy, J, Megyery-Balog, K, Rusz, L and Patyi, L (1976) "Solubility of Gases in Normal-Alkanes", *Hung. J. Ind. Chem.,* **4**, p 269 - 280.
52. Mattiasson, B and Adlercreutz, P (1983) *Ann. NY Acad. Sci.*, **413**, p 545 – 547.
53. Mauersberger, S, Ohkuma, M, Schunck, W-H and Takagi, M (1996) "*Candida maltosa*", In: *Non-conventional Yeasts in Biotechnology: A Handbook*, Springer.
54. McMillan, JD and Wang, DIC (1987) Ann. NY Acad. Sci, **506**, p 569 – 582.
55. Miller, G L (1959) "Dinitrosalicylic acid reagent for determination of reducing sugar", *Anal. Chem.*, **31**, p 426.
56. Mimura, A, Kawano, T and Kodaira, R (1969) "Biochemical Engineering Analysis of Hydrocarbon Fermentation: 1 – Oxygen Transfer in the Oil-Water System", *J. Ferment. Technol.*, **47**, p 229 – 236.
57. Mimura, A, Takeda, I and Wakasa, R (1973) "Some Characteristic

Phenomena of Oxygen Transfer in Hydrocarbon Fermentations", *Biotechnol. & Bioeng. Symp.,* **4**, p 467-484.

58. Montes, FJ, Catalán, J, Galán, MA (1999) "Prediction of k_La in yeast broths", *Proc. Biochem.,* **34**, p 549 – 555.
59. Moo-Young, M, Shimizu, T and Whitworth, D A (1971a) "Hydrocarbon Fermentations Using *Candida lipolytica*. I: Basic Growth Parameters for Batch and Continuous Culture Conditions", *Biotechol. Bioeng.*, **13**, p 741-760.
60. Moo-Young, M and Shimizu, T (1971b) "Hyrdocarbon Fermentations Using *Candida lipolytica*. II: A Model for Cell Growth Kinetics", *Biotechol. Bioeng.*, **13**, p 761-778.
61. Moo-Young, M (1975) "Microbial reactor design for synthetic protein production", *Can. J. Chem. Eng.,* **53**, p 113 - 118.
62. Moo-Young, M and Blanch, HW (1981) "Design of Biochemical Reactors", *Mass Transfer Criteria for Simple and Complex Systems*, p 2-61.
63. Nielsen, DR, Daugulis, J and McLellan, PJ (2003) "A Novel Method of Simulating Oxygen Mass Transfer in Two-Phase Partitioning Bioreactors", *Biotechol. Bioeng.,* **83** (6), p 735-742.
64. Paaschen, T and Lubbert, A (1997) "New Experimental Results on the Mass Transfer from Single Oxygen Bubbles into Water as the Liquid Phase", In: Proc. 4th Int. Conf. Bioreact. Bioproc. Fluid Dynam., BHR Group Conference Series, **25**, p 143 – 150.
65. Picataggio, S, Rohrer, T, Deanda, K, Lanning, D, Reynolds, R, Mielinz, J, Eirich, LD (1992) "Metabolic Engineering of *Candida tropicalis* for the Production of Long-Chain Dicarboxylic Acids", Bio/technology, **10**, p 894-898.
66. Preusting H, van Houten R, Hoefs A, van Langenberghe EK, Favre-Bulle O and Witholt B (1993) "High cell density cultivation of Pseudomonas oleovorans: growth and production of poly(3-hydroxyalkanoates) in two-liquid phase batch and fed-batch systems, *Biotechnol. Bioeng.,* **41,** p 550-556.
67. Reddy, PG, Singh, HD, Roy, PK and Baruah, JN (1982) "Predominant Role of Hydrocarbon Solubilization in the Microbial Uptake of Hydrocarbons", *Biotechol. Bioeng.*, **24**, p 1241-1269.
68. Rehm, HJ and Reiff, I (1981) "Mechanisms and Occurence of Microbial Oxidation of Long-Chain Alkanes", *Advances in Biochemical Engineering*, **19**, p 175-215.
69. Rehm, H-J (1986) "Single Cell Protein Production from Petroleum Derivatives and its Utilization as Food and Feed", In: *Perspectives in Biotechnology and Applied Microbiology*, Elsevier, London.
70. Robinson, CW and Wilke, CR (1973) "Oxygen absorption in stirred

tanks: A correlation for ionic strength effects", *Biotechnol. Bioeng.,* **15** (4), p 755 – 782.

71. Rocha-Valadez, J A, Galindo, E, Serrano-Carreon, L (2000) "Effect of the impeller-sparger configuration over *Trichoderma harzianum* growth in four-phase cultures under constant dissolved oxygen", *Bioprocess Engineering*, **23** (4), p 403 - 410.
72. Rols, JL and Goma, G (1989) "Enhancement of Oxygen Transfer Rates in Fermentation using Oxygen Vectors", *Biotech. Adv.*, **7**, p 1-14.
73. Rols, JL, Condoret, JS, Fonade, C and Goma, G (1990) "Mechanism of Enhanced Oxygen Transfer in Fermentation using Emulsified Oxygen-Vectors", *Biotechol. Bioeng.*, **35**, p 427-435.
74. Rothen SA, Sauer M, Sonnleitner B, Witholt B (1998) "Growth characteristics of *E. coli* HB101[pGEc47] on defined medium", *Biotechol. Bioeng.*, **58**, p 92 – 100.
75. Ruchti, G, Dunn, J and Bourne, JR (1981) "Comparison of Dynamic Oxygen Electrode Methods for the Measurement of K_La", *Biotechol. Bioeng.*, **23**, p 277 - 290.
76. Scheller, U, Zimmer, T, Becher, D, Schauer, F and Schunck, W-H (1998) "Oxygenation Cascade in Conversion of n-Alkanes to Dioic Acids Catalysed by Cytochrome P450 52A3", *J. Biol. Chem.*, **273** (49), p 32528 - 32534.
77. Schmid, A, Sonnleitner, B, Witholt, B (1998) Medium chain length alkane solvent-cell transfer rates in two-liquid phase Pseudomonas oleovorans cultures, Biotech Bioeng, **60**, p 10 – 23.
78. Schumpe, A, Quicker, G and Deckwer, W-D (1982) "Gas Solubilities in Microbial Culture Media", *Advances in Biochemical Engineering*, **24** (1), p 2 - 38.
79. Shennan, JL, and Levi, JD (1974) "The Growth of Yeast on Hydrocarbons", Churchill Livingstone, Edinburgh, p 1-57.
80. Shiio, I and Uchio, R (1971) "Microbial Production of Long-chain Dicarboxylic Acids from n-Alkanes: Part I. Screening and Properties of Microorganisms Producing Dicarboxylic Acids", *Agr. Biol. Chem.*, **35** (13), p 2033-2042.
81. Shuler, ML and Kargi, F (1992) "Bioprocess Engineering: Basic Concepts", 1st ed., Prentice-Hall, New Jersey.
82. Stephen, P (1991) "Method for increasing the omega-hydroxylase activity in *Candida tropicalis*", US Patent No. WO91/147.
83. Thomsen, ES and Gjaldbaek, JC (1963) "The Solubility of Hydrogen, Nitrogen, Oxygen and Ethane in Normal Hydrocarbons", *Acta Chem. Scand.,* **17**, 1, p 127-133.
84. Treybal, R (1980) "Mass-transfer operations", McGraw-Hill, Tokyo, 3rd Ed.

85. Tribe, LA, Briens, CL and Margaritis, A (1995) "Determination of the Volumetric Mass Transfer Coefficient (k_La) Using the Dynamic 'Gas Out-Gas In' Method: Analysis of Errors Caused by Dissolved Oxygen Probes", *Biotechol. Bioeng.*, **46**, p 388-392.
86. Uchio, R and Shiio, I (1972a) "Microbial Production of Long-Chain Dicarbolylic Acids from n-Alkanes. Part II. Production by Candida cloacae Mutant Unable to Assimilate Dicarboxylic Acid", *Agr. Biol. Chem.*, **36** (3), p 426-433.
87. Uchio, R and Shiio, I (1972b) Production of Dicarbolic Acids by *Candida cloacae* Mutant Unable to assimilate n-Alkane", *Agr. Biol. Chem.*, **36** (7), p 1169-1175.
88. Uchio, R and Shiio, I (1972c) "Tetradecane 1, 14-Dicarboxylic Acid Production from n-Hexadecane by *Candida cloacae*", *Agr. Biol. Chem.*, **36** (8), p 1389-1397.
89. Vadalkar, K, Singh, HD, Baruah, JN, Iyengar, J (1969) *J. Gen. Appl. Microbiol.*, **15**, p 375.
90. Wang, HJ, Le Dall, M-T, Waché, Y, Laroche, C, Belin, J-M, Gailardin, C and Nicaud, J-M (1999) "Evaluation of Acyl Coenzyme A Oxidase Isozyme Function in the n-Alkane-Assimilating Yeast *Yarrowia lipolytica*", *J. Bacteriol.*, **181** (17), p 5140-5148.
91. Welty, JR, Wicks, CE and Wilson (1984) "Fundamentals of Momentum Heat and Mass Transfer", 3rd Ed., John Wiley and Sons, New York.
92. Whitton, M, Cropper, S, and Özcan-Taşkin, NG (1997) "Mixing of liquid phasein large vessels equipped with multiple impellers", In: *Proc. 4th Int. Conf. Bioreact. Bioproc. Fluid Dynam.*, BHR Group Conference Series, **25**, p 277 -294.
93. Wiedmann, B, Wiedmann, M, Mauersberger, S, Schunck, W and Muller, H (1988) "Oxygen Limitation Induces Indirectly the Synthesis of Cytochrome P-450 mRNA in Alkane-Growing *Candida maltosa"*, *Biochemical and Biophysical Research Communications*, **150** (2), p 859-865.
94. Wilcock, RJ, Battino, R, Danforth, WF and Wilhelm, E (1978) "Solubilities of gases in liquids II. The solubilities of He, Ne, Ar, Kr, O_2, N_2, CO, CO_2, CH_4, CF_4 and SF_6 in n-octane, 1-octanol, n-decane and 1-decanol", *J. Chem. Thermodynamics*, **10**, p 817-822.
95. Wong, CW and Shiuan, JH (1986) "Effect of Additives on Mass Transfer in an Aerated Mixing Vessel", *Chemical Engineering Communications,* **43**, p 133 - 145.
96. Yamane, T, and Yoshida, F (1970) "Comments on oxygen absorption into oil-water emulsions", *J. Ferment. Technol.*, **52**, p 445 – 450.
97. Yi, ZH and Rehm, HJ (1982) "Metabolic formation of dodecanoic acid from n-dodecane by a mutant of *Candida tropicalis*", *Appl. Microbiol.*

Biotechnol., **14**, p 254 –258.

98. Yoshida, T, Tokohama, K, Chen, KC, Sunouchi, T and Taguchi, H (1977) "Oxygen transfer in hydrocarbon fermentation by *Candida rugosa*", *J. Ferment. Technol.*, **55**, p 76 – 83.
99. Zieminski, SA, Caron, MM and Blackombe, RB (1967) "Behaviour of air bubbles in dilute aqueous solutions", *Ind. Eng. Chem. Fund.*, **6**, p 233 – 242.

Internet Reference

1. R 1.9.1 (2004) In: "The Comprehensive R Archive Network", http://www.r-project.org.

Appendix I: Media for Storage and Culture Maintenance

Medium for Liquid Nitrogen Storage of Microorganisms

(courtesy of University of the Free State)

Medium Components	**g/l00ml water**
Glucose	4
Triptone	1
YNB	1

- Autoclave the Glucose and Triptone in 85ml distilled water.
- Mix 6.7g YNB in 100ml distilled water.
- Filter-sterilise and add 15ml to the autoclaved mixture.
- Add 3.5ml of medium to sterilised test-tubes.
- Add 2-3 pure colonies to each test-tube.
- Grow for 72hr on shaker.
- Prepare and sterilise 70% glycerol in distilled water.
- Add 0.5ml glycerol mixture to each test-tube.
- Sterilise straws or micro centrifuge tubes.
- Aseptically add medium. (If Pasteur pipettes are used, plug top with cotton wool and dry-sterilise at 160oC for 2 hours in oven.)
- Freeze overnight in –5°C freezer.
- Transfer to –70°C freezer or Liquid Nitrogen Storage.

YNB Medium for Storage and Maintenance of Candida tropicalis

(adapted from Picataggio *et al*., 1992)

Medium Components	**g/l water**
Difco® YNB (with amino acids/$(NH_4)_2SO_4$)	6.7
Yeast Extract	3
$(NH_4)_2SO_4$	3
KH_2PO_4	1
K_2HPO_4	1
Agar	15-18
Glucose (2%)	20
OR	
Hexadecane (1% @ 0.773 g/ml)	10

YNB and Hexadecane should be filter sterilised, while other ingredients can be autoclaved.

Detailed Composition of Bulk Components of Culture Media

Nitrogen Sources

YNB:	$(NH_4)_2SO_4$	75 wt%
	KH_2PO_4	15 wt %
	$MgSO_4.7H_2O$	0.75 wt %
	NaCl	1.5 wt %
	$CaCl_2$	1.5 wt %
Peptone: Nitrogen		11 wt %

Carbon/Nitrogen Sources

Yeast Extract:	Organic C	32 wt %
	Organic N	18.5 wt %
	Organic O	21 wt %
	$MgSO_4.7H_2O$	6 wt %
	NaCl	8 wt %
	Na_2MoO_4	0.2 wt %
	K_2HPO_4	8 wt %

Appendix II: Analytical Standard calibrations

GC Calibration Curves and Response Factors

Known amounts of dodecanedioic acid and dodecane in solution with trimethylsulphonium hydroxide and internal standards were injected into the GC column. Calibration curves were then obtained by comparing the peak areas obtained in the chromatogram with the known amount of dodecanedioic acid or dodecane in the sample.

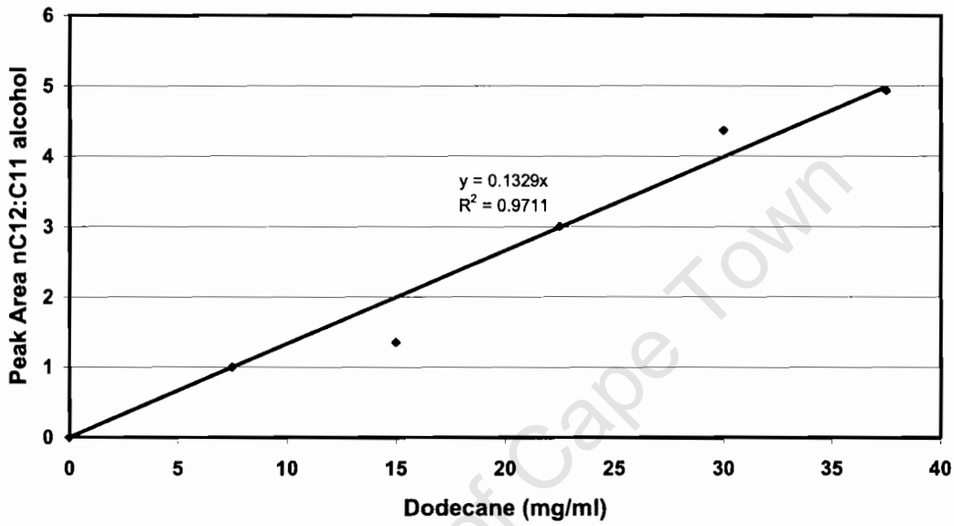

Figure A1: Calibration Curve for Calculating Dodecane concentration with reference to C11 alcohol internal standard peak area

Figure A1, shows how to calculate the concentration of dodecane in a sample by using the ratio of the dodecane response peak area and the C11 alcohol internal standard peak area. A flame ionization detector (FID) response is generally proportional to the mass of carbon present, however, various functional groups, such as oxygen affect the response to varying degrees. This response is measured by a response factor given by:

$$f = \frac{N_C}{N_{C,-O} + N_{C,+O}} \qquad \text{(A.1)}$$

where

f = response factor
N_C = number of carbon atoms in the molecule
$N_{C,-O}$ = number of carbon atoms not connected to oxygen
$N_{C,+O}$ = number of carbon atoms connected to oxygen

Therefore, any alkane will have a response factor of 1. Hence, the detector response to the presence of carbon from tridecane will be the same as the response to the equivalent amount of carbon in dodecane. Calculation of the amount of tridecane present can be performed in using the same calibration equation with a correction for carbon content as a fraction of total molecular mass, M.

Hence, the concentration of tridecane, C_{nC13} in mg/ml can be given by:

$$C_{nC13} = \frac{Area_{nC13}}{Area_{C11alcohol}} \cdot \frac{1}{0.1329} \cdot \frac{12}{M_{nC12}} \cdot \frac{M_{nC13}}{13} \qquad \text{(A.2)}$$

Figure A.2 shows how to calculate the concentration of dodecanedioic acid by using the ratio of the peak area of dodecanedioic acid and the peak area of tetradecanioic acid.

Figure A.3 shows how to calculate the glucose concentration in a solution by reading the absorbance at 510nm.

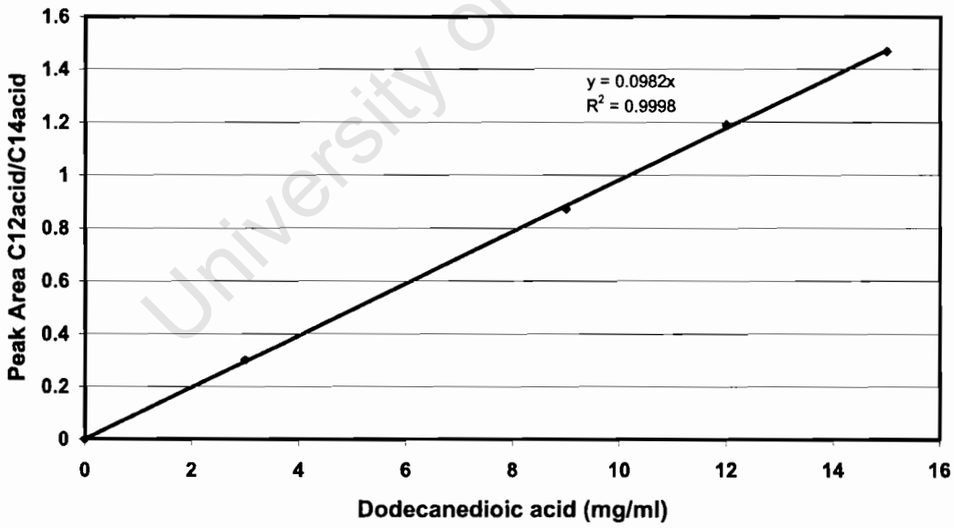

Figure A2: Calibration Curve for Calculating Dodecanedioic acid concentration with reference to tetradecane dioic acid internal standard peak area

DNS

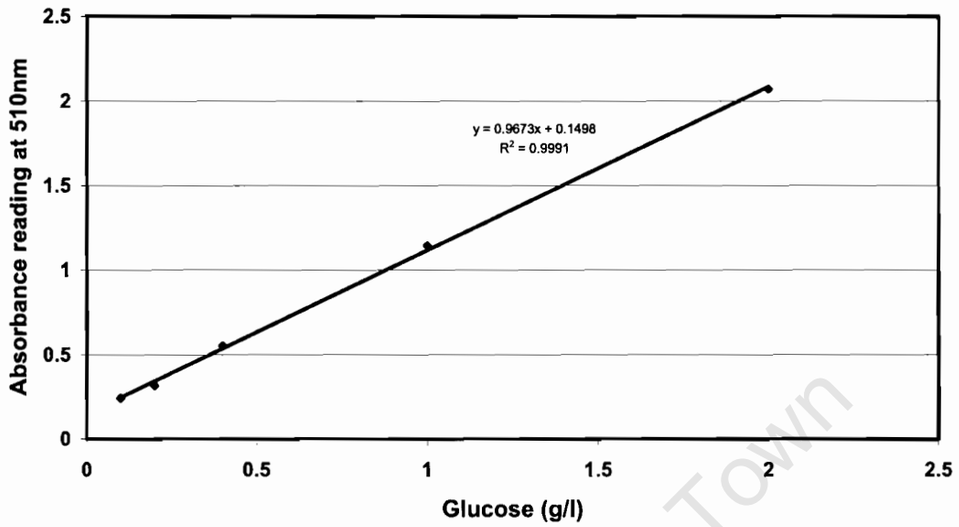

Figure A3: Calibration Curve for glucose sample concentration with reference to the absorbance reading obtained at 510nm

Appendix III: Cell Growth Data (for Chapter 5)

Table A.1: GC Data for Section 5.1

Flask A			
	C12DA	**nC12**	**nC13**
Time			
[h]	[mg/ml]	[mg/ml]	[mg/ml]
1	0	3.549053	3.49
11	0	5.234569	11.17
24	0	9.286762	9.70
48	0	2.680739	2.78
72	0.178886	5.569107	6.04
96	0.504119	10.73489	10.90
Flask B			
	C12DA	**nC12**	**nC13**
Time			
[h]	[mg/ml]	[mg/ml]	[mg/ml]
1	0	3.419477	3.36
11	0	2.148278	5.25
24	0.172311	7.521886	7.51
48	0.1868	6.615068	6.37
72	0.198461	8.025583	8.16
96	0.232065	10.43533	11.66
Flask C			
	C12DA	**nC12**	**nC13**
Time			
[h]	[mg/ml]	[mg/ml]	[mg/ml]
1	0	0.75365	1.35
11	0	5.042493	4.85
24	0	14.08005	11.88
48	0	4.188539	4.87
72	0.209017	2.873521	3.04
96	0.306732	11.52784	11.75

Flask AA		
	C12DA	**nC12**
Time		
[h]	[mg/ml]	[mg/ml]
1	0	15.88929
11	0.16209	4.405438
24	0.101537	11.54482
48	0.169447	9.658474
72	0.19939	18.97205
96	0.306752	19.84141
Flask BB		
	C12DA	**nC12**
Time		
[h]	[mg/ml]	[mg/ml]
1	0	25.66198
11	0.278521	11.1626
24	0.170757	12.08381
48	0.164156	8.358214
72	0.198758	17.68026
96	0.307649	22.95505
Flask CC		
	C12DA	**nC12**
Time		
[h]	[mg/ml]	[mg/ml]
1	0	12.66364
11	0.174803	11.34041
24	0.2429	26.20576
48	0.307914	16.54682
72	0.39678	17.79411
96	1.723125	22.86136

Table A.2: Optical Density Data for Section 5.1

Time	Flask A	Flask B	Flask C	Flask AA	Flask BB	Flask CC
(h)	Relative OD					
-24	0.20	0.30	0.39	0.20	0.27	0.27
0	5.56	5.69	6.27	6.18	6.44	6.38
0	6.70	7.25	5.07	6.95	6.45	5.98
11	6.15	5.20	3.46	6.50	6.65	6.94
24	6.55	5.80	6.30	6.75	6.10	6.00
48	6.55	5.65	5.70	5.95	5.80	5.35
72	6.20	5.80	4.85	5.60	5.75	3.40
96	6.90	6.90	3.15	6.90	5.25	2.40
120	3.70	7.70	3.90	5.60	5.25	2.35

Table A.3: GC Data for Section 5.2

	(a)		(b)		Average			
	Concentration							
	C12DA	nC12	C12DA	nC12	C12DA	Error	nC12	Error
Time								
[h]	[mg/ml]	[mg/ml]	[mg/ml]	[mg/ml]	[mg/ml]		[mg/ml]	
1	0.00	1.14	0.00	1.62	0.00	0.00	1.38	0.34
24	0.18	1.96	0.00	3.55	0.09	0.13	2.75	1.12
48	0.32	3.47	0.34	4.08	0.33	0.01	3.77	0.43
72	1.65	11.81	1.30	6.69	1.47	0.25	9.25	3.62
96	1.55	15.18	1.82	12.06	1.69	0.19	13.62	2.21
120	1.94	4.57	1.76	9.22	1.85	0.13	6.89	3.28

Table A.4: Optical Density Data for Section 5.2

Time	(a	(b)		
(h)	Relative OD		Average	Error
-18	0.66	0.57	0.62	0.06
0	3.08	2.98	3.03	0.07
0	3.62	3.65	3.64	0.02
24	6.15	6.38	6.27	0.16
48	8.35	7.24	7.80	0.78
120	8.34	7.6	7.97	0.52

Table A.5: Data for Section 5.3

Flask 1: YNB 75g/l glucose

Time	(a) Dry Weight Paper	Gross	Net	OD Reading	Dilution	Rel OD	(b) Dry Weight Paper	Gross	Net	OD Reading	Dilution	Rel OD	Average Dry Weight	Rel Error	Rel OD	Rel Error	Glucose
(h)	(g)	(g)	(g/l)				(g)	(g)	(g/l)				(g/l)				(g/l)
0													0.50		0.16		80.1
4.5	0.5088	0.5145	1.425	0.49	1	0.49	0.4478	0.4535	1.425	0.514	1	0.514	1.43	0.00	0.50	0.05	71.2
9			0	0.714	1	0.714	0.527	0.5402	3.3	0.74	1	0.74	1.65		0.73	0.04	53.0
13.5	0.4154	0.4388	4.68	0.157	10	1.57	0.4605	0.4783	4.45	0.154	10	1.54	4.57	0.05	1.56	0.02	35.0
18	0.514	0.5368	5.7	0.182	10	1.82	0.5383	0.5665	7.05	0.182	10	1.82	6.38	0.21	1.82	0.00	9.3
27	0.4359	0.4585	5.65	0.178	10	1.78	0.5439	0.5657	5.45	0.175	10	1.75	5.55	0.04	1.77	0.02	2.0
36	0.5924	0.6152	5.7	0.155	10	1.55	0.549	0.5707	5.425	0.157	10	1.57	5.56	0.05	1.56	0.01	2.2
48	0.4586	0.4782	4.9	0.157	10	1.57	0.493	0.5132	5.05	0.151	10	1.51	4.98	0.03	1.54	0.04	2.2
96	0.3795	0.4028	5.825	0.144	10	1.44	0.5469	0.5676	5.175	0.144	10	1.44	5.50	0.12	1.44	0.00	1.9

Flask 2: YNB 40g/l glucose

Time	(a) Dry Weight Paper	Gross	Net	OD Reading	Dilution	Rel OD	(b) Dry Weight Paper	Gross	Net	OD Reading	Dilution	Rel OD	Average Dry Weight	Rel Error	Rel OD	Rel Error	Glucose
(h)	(g)	(g)	(g/l)				(g)	(g)	(g/l)				(g/l)				(g/l)
0													0.50		0.16		46.0
4.5	0.7308	0.7367	1.475	0.645	1	0.645	0.5572	0.563	1.45	0.505	1	0.505	1.46	0.02	0.58	0.24	39.1
9	0.5169	0.5304	3.375	0.773	1	0.773	0.5024	0.5161	3.425	0.756	1	0.756	3.40	0.01	0.76	0.02	16.2
13.5	0.4605	0.4783	4.45	0.149	10	1.49	0.465	0.4819	4.225	0.144	10	1.44	4.34	0.05	1.47	0.03	1.3
18	0.485	0.5039	4.725	0.154	10	1.54	0.5085	0.5272	4.675	0.157	10	1.57	4.70	0.01	1.56	0.02	1.2
27	0.5061	0.5251	4.75	0.165	10	1.65	0.4029	0.421	4.525	0.143	10	1.43	4.64	0.05	1.54	0.14	1.2
36				0.165	10	1.65	0.529	0.5488	4.95	0.168	10	1.68	4.95		1.67	0.02	1.3
48	0.44	0.4606	5.15	0.201	10	2.01	0.5719	0.5929	5.25	0.187	10	1.87	5.20	0.02	1.94	0.07	1.2
96	0.622	0.6447	5.675	0.165	10	1.65	0.4957	0.516	5.075	0.19	10	1.9	5.38	0.11	1.78	0.14	1.9

Flask 3: YNB out 9.64g/l peptone

Time	(a) Dry Weight Paper	Gross	Net	OD Reading	Dilution	Rel OD	(b) Dry Weight Paper	Gross	Net	OD Reading	Dilution	Rel OD	Average Dry Weight	Rel Error	Rel OD	Rel Error	Glucose
(h)	(g)	(g)	(g/l)				(g)	(g)	(g/l)				(g/l)				(g/l)
0													0.50		0.16		74.2
4.5	0.3952	0.3999	1.175	0.489	1	0.489	0.4385	0.4432	1.175	0.409	1	0.409	1.18	0.00	0.45	0.18	72.2
9	0.5963	0.6074	2.775	0.656	1	0.656	0.5705	0.5809	2.6	0.71	1	0.71	2.69	0.07	0.68	0.08	55.5
13.5	0.5165	0.5301	3.4	0.14	10	1.4	0.5742	0.5882	3.5	0.139	10	1.39	3.45	0.03	1.40	0.01	35.0
18	0.4478	0.467	4.8	0.164	10	1.64	0.5024	0.5225	5.025	0.184	10	1.84	4.91	0.05	1.74	0.11	16.2
27	0.4696	0.4902	5.15	0.185	10	1.85	0.3606	0.3808	5.05	0.181	10	1.81	5.10	0.02	1.83	0.02	2.2
36	0.4666	0.4881	5.375	0.17	10	1.7	0.4343	0.4489	3.65	0.168	10	1.68	4.51	0.38	1.69	0.01	2.4
48	0.4363	0.4526	4.075	0.16	10	1.6	0.4165	0.4318	3.825	0.168	10	1.68	3.95	0.06	1.64	0.05	2.4
96	0.3942	0.4097	3.875	0.142	10	1.42	0.5164	0.534	4.4	0.136	10	1.36	4.14	0.13	1.39	0.04	2.3

Flask 4: YNB +16g/l YE + 75g/l glucose

Time	(a) Dry Weight Paper	Gross	Net	OD Reading	Dilution	Rel OD	(b) Dry Weight Paper	Gross	Net	OD Reading	Dilution	Rel OD	Average Dry Weight	Rel Error	Rel OD	Rel Error	Glucose
(h)	(g)	(g)	(g/l)				(g)	(g)	(g/l)				(g/l)				(g/l)
0													0.50		0.16		78.0
4.5	0.5259	0.5314	1.375	0.645	1	0.645	0.4171	0.4231	1.5	0.623	1	0.623	1.44	0.09	0.63	0.03	73.7
9	0.4965	0.5096	3.275	0.737	1	0.737	0.4793	0.495	3.925	0.801	1	0.801	3.60	0.18	0.77	0.08	49.0
13.5	0.5293	0.5595	7.55	0.215	10	2.15	0.5435	0.5678	6.075	0.234	10	2.34	6.81	0.22	2.25	0.08	14.5
18	0.5497	0.5774	6.925	0.235	10	2.35	0.4424	0.4714	7.25	0.239	10	2.39	7.09	0.05	2.37	0.02	3.0
27	0.4018	0.4296	6.95	0.248	10	2.48	0.4513	0.478	6.675	0.266	10	2.66	6.81	0.04	2.57	0.07	2.5
36	0.4224	0.4489	6.625	0.234	10	2.34	0.4568	0.4804	5.9	0.233	10	2.33	6.26	0.12	2.34	0.00	2.6
48	0.4602	0.485	6.2	0.222	10	2.22	0.3785	0.4023	5.95	0.216	10	2.16	6.08	0.04	2.19	0.03	2.6
96	0.4515	0.4771	6.4	0.223	10	2.23	0.5283	0.5563	7	0.216	10	2.16	6.70	0.09	2.20	0.03	2.6

Table A.6: Cell Growth Data for Section 5.4

Flask 1: YNB 75g/l glucose

Time	(a) Dry Weight			(b) Dry Weight					Average				
	Paper	Gross	Net	Cell Count	Paper	Gross	Net	Cell Count	Dry Weight	Rel Error	Cell Count	Glucose	Error
(h)	(g)	(g)	(g/l)	cell/ml	(g)	(g)	(g/l)	cell/ml	(g/l)		cell/ml	(g/l)	
-18				2.27E+06				2.27E+06	0.50		1.61E-01	78.3	0.01
-13.5	0.5438	0.5486	1.200	8.13E+07	0.5155	0.5225	1.75	1.38E+08	1.48	0.37	1.09E+08		
-4.5	0.4143	0.4385	4.840	2.91E+08	0.5739	0.5982	6.075	2.38E+08	5.46	0.23	2.64E+08		
0	0.4397	0.4622	5.625	5.68E+08	0.5691	0.5936	6.125	3.05E+08	5.88	0.09	4.36E+08	2.8	0.00
58.5	0.4643	0.477	3.175		0.4635	0.4761	3.15		3.16	0.01			
154.5	0.4509	0.4675	4.150	3.85E+08	0.6409	0.6567	3.95	4.98E+08	4.05	0.05	4.41E+08		

Flask 3: YNB out 9.64g/l peptone

Time	(a) Dry Weight			(b) Dry Weight					Average				
	Paper	Gross	Net	Cell Count	Paper	Gross	Net	Cell Count	Dry Weight	Rel Error	Cell Count	Glucose	Error
(h)	(g)	(g)	(g/l)	cell/ml	(g)	(g)	(g/l)	cell/ml	(g/l)		cell/ml		
-18				2.27E+06				2.27E+06	0.50		0.16	72.4	0.01
-13.5	0.5348	0.5413	1.625	8.13E+07	0.5141	0.5203	1.55	6.25E+07	1.59	0.05	7.19E+07		
-4.5	0.4214	0.4439	4.500	2.93E+08	0.501	0.5241	5.775	3.88E+08	5.14	0.25	3.40E+08		
0	0.4784	0.5037	6.325	3.20E+08	0.5284	0.5541	6.425	3.75E+08	6.38	0.02	3.48E+08	7.9	0.42
58.5	0.4962	0.5246	7.100		0.6038	0.6282	6.1		6.60	0.15			
154.5	0.47	0.4981	7.025	4.40E+08	0.4516	0.4803	7.175	3.45E+08	7.10	0.02	3.93E+08		

Flask 4: YNB +16g/l YE + 75g/l glucose

Time	(a) Dry Weight			(b) Dry Weight					Average				
	Paper	Gross	Net	Cell Count	Paper	Gross	Net	Cell Count	Dry Weight	Rel Error	Cell Count	Glucose	Error
(h)	(g)	(g)	(g/l)	cell/ml	(g)	(g)	(g/l)	cell/ml	(g/l)		cell/ml	(g/l)	
-18				2.27E+06				2.27E+06	0.50		0.16	76.3	0.01
-13.5	0.4239	0.4293	1.350	1.13E+08	0.4013	0.408	1.675	1.15E+08	1.51	0.21	1.14E+08		
-4.5	0.3596	0.3879	5.660	3.60E+08	0.486	0.5146	7.15	2.60E+08	6.41	0.23	3.10E+08		
0	0.4837	0.5108	6.775	3.05E+08	0.5959	0.6248	7.225	4.33E+08	7.00	0.06	3.69E+08	1.9	0.03
58.5	0.3781	0.4085	7.600		0.5584	0.5895	7.775		7.69	0.02			
154.5	0.5896	0.6221	8.125	4.98E+08	0.5925	0.6253	8.2	5.43E+08	8.16	0.01	5.20E+08		

Flask 5: Peptone +16g/l YE + 75g/l glucose

Time	(a) Dry Weight			(b) Dry Weight					Average				
	Paper	Gross	Net	Cell Count	Paper	Gross	Net	Cell Count	Dry Weight	Rel Error	Cell Count	Glucose	Error
(h)	(g)	(g)	(g/l)	cell/ml	(g)	(g)	(g/l)	cell/ml	(g/l)		cell/ml	(g/l)	
-18				2.27E+06				2.27E+06	0.50		0.16	75.6	0.01
-13.5	0.5348	0.5413	1.625	7.50E+07	0.5141	0.5203	1.55	7.50E+07	1.59	0.05	7.50E+07	71.2	1.07
-4.5	0.4214	0.4439	4.500	3.15E+08	0.501	0.5241	5.775	4.08E+08	5.14	0.25	3.61E+08	7.7	0.54
0	0.4784	0.5037	6.325	5.08E+08	0.5284	0.5541	6.425	3.38E+08	6.38	0.02	4.23E+08	3.1	0.01
58.5	0.4962	0.5246	7.100		0.6038	0.6282	6.1		6.60	0.15		2.5	0.03
154.5	0.47	0.4981	7.025	3.45E+08	0.4516	0.4803	7.175	4.40E+08	7.10	0.02	3.93E+08	2.6	0.03

Table A.7: pH Data for Section 5.4

pH	Flask 1				Flask 3				Flask4				Flask 5			
Time	(a)	(b)			(a)	(b)			(a)	(b)			(a)	(b)		
	pH	pH	Ave pH	Rel Error	pH	pH	Ave pH	Rel Error	pH	pH	Ave pH	Rel Error	pH	pH	Ave pH	Rel Error
(h)																
-18	6	6	6		6	6	6		6	6	6		6	6	6	
-13.5	4.22	4.17	4.195	0.04	4.93	4.93	4.93	0	5.01	5.01	5.01	0	5.33	5.32	5.325	0.007071
-4.5	2.4	2.35	2.375	0.04	3.32	3.29	3.305	0.021213	3.79	3.72	3.755	0.049497	3.94	3.92	3.93	0.014142
0	2.3	2.25	2.275	0.04	3.01	3	3.005	0.007071	3.22	3.17	3.195	0.035355	3.9	3.9	3.9	0
0	8	8	8	-	8	8	8	0	8	8	8	0	8	8	8	0
16.5	5	5	5	-	6	6	6	0	6	6	6	0	6	6	6	0
16.5	8	8	8	-	8	8	8	0	8	8	8	0	8	8	8	0
58.5	6.96	6.85	6.905	0.08	6.61	6.59	6.6	0.014142	6	6	6	0	6.58	6.58	6.58	0
58.5	8	8	8	-	8	8	8	0	8	8	8	0	8	8	8	0
115.5	7	7	7	-	7	7	7	0	7	7	7	0	7	7	7	0
115.5	8.5	8.5	8.5	-	8.5	8.5	8.5	0	8.5	8.5	8.5	0	8.5	8.5	8.5	0
154.5	8.56	8.58	8.57	0.01	8.09	7.63	7.86	0.325269	7.96	8.16	8.06	0.141421	8.38	8.4	8.39	0.014142

Table A.8: GC Data for Section 5.4

	Flask 1						Flask 3					
Time	(a)		(b)		Average		(a)		(b)		Average	
	nC12	C12DA	C12	C12DA	C12	C12DA	C12	C12DA	C12	C12DA	C12	C12DA
(h)	g/l	g/l	g/l	g/l	g/l	g/l	g/l	g/l	g/l	g/l	g/l	g/l
0.00	18.75	0.00	18.75	0.00	18.75	0.00	18.75	0.00	0.02	0.00	18.75	0.00
58.50	13.35	0.06	10.88	0.05	12.12	0.05	3.07	0.00	2.58	0.00	2.83	0.00
154.50	10.58		10.57	0.04	10.58	0.04	5.61	0.61	4.82	0.33	5.22	0.47

	Flask 4						Flask 5					
Time	(a)		(b)		Average		(a)		(b)		Average	
	C12	C12DA	C12	C12DA	C12	C12DA	C12	C12DA	C12	C12DA	C12	C12DA
(h)	g/l	g/l	g/l	g/l	g/l	g/l	g/l	g/l	g/l	g/l	g/l	g/l
0.00	18.75	0.00	0.02	0.00	18.75	0.00	18.75	0.00	18.75	0.00	18.75	0.00
58.50	9.43	0.10	6.34	0.00	7.89	0.05	6.25	0.00	6.17	0.00	6.21	0.00
154.50	6.69	0.34	4.82	0.33	5.75	0.34	5.18	0.61	7.02	0.81	6.10	0.71

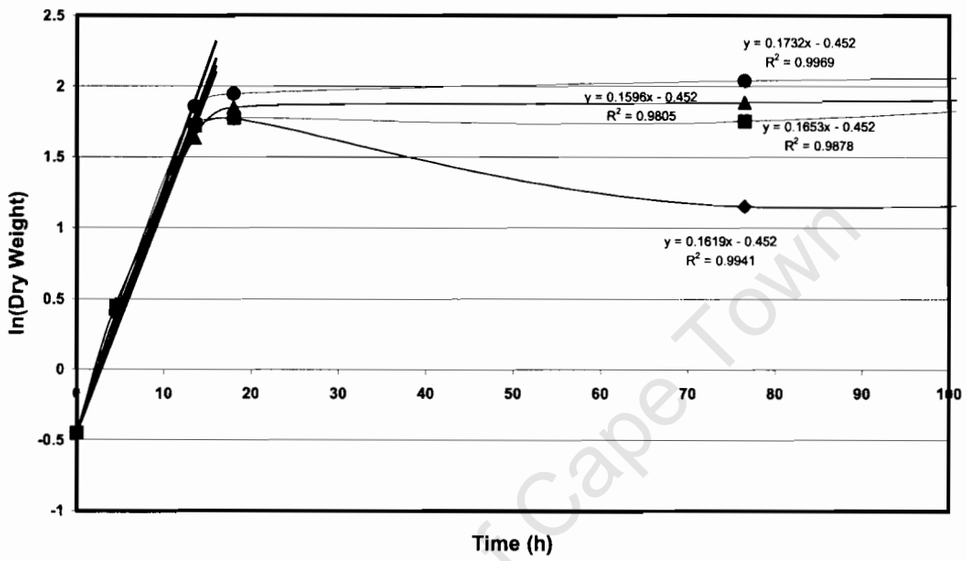

Figure A4: Logarithmic Growth curve for Candida tropicalis showing determination of specific growth rates as listed in Table 5.6

Flask 1A: -◆-; Flask 3A: -▲-; Flask 4A: -●-; Flask 5A: -■-

Appendix IV: K_La data

Table A.8: K_La and OTR Values

Pure water

K_La (/s)

Agitation (rpm)	Aeration (vvm) 1.5	1.25	1	0.75	0.5
1200	0.046	0.045	0.037	0.032	0.022
1000	0.046	0.046	0.043	0.039	0.036
800	0.043	0.042	0.04	0.038	0.036
600	0.035	0.033	0.03	0.027	0.025
400	0.018	0.017	0.017	0.016	0.01
200	0.007	0.005	0.004	0.0035	0.003

Pure water

OTR max (mg/l.s)

Agitation (rpm)	Aeration (vvm) 1.5	1.25	1	0.75	0.5
1200	0.370	0.362	0.298	0.258	0.177
1000	0.370	0.370	0.346	0.314	0.290
800	0.346	0.338	0.322	0.306	0.290
600	0.282	0.266	0.242	0.217	0.201
400	0.145	0.137	0.137	0.129	0.081
200	0.056	0.040	0.032	0.028	0.024

2.5% alkane

K_La (/s)

Agitation (rpm)	Aeration (vvm) 1.5	1.25	1	0.75	0.5
1200	0.051	0.047	0.042	0.028	0.014
1000	0.05	0.048	0.044	0.036	0.018
800	0.045	0.041	0.041	0.042	0.037
600	0.025	0.027	0.029		
400	0.007				
200					

2.5% alkane

OTR max (mg/l.s)

Agitation (rpm)	Aeration (vvm) 1.5	1.25	1	0.75	0.5
1200	0.462	0.425	0.380	0.253	0.127
1000	0.453	0.434	0.398	0.326	0.163
800	0.407	0.371	0.371	0.380	0.335
600	0.226	0.244	0.262		
400	0.063				
200					

5% alkane

K_La (/s)

Agitation (rpm)	Aeration (vvm) 1.5	1.25	1	0.75	0.5
1200	0.054	0.051	0.046	0.037	0.011
1000	0.053	0.053	0.050	0.047	0.030
800	0.048	0.045	0.044	0.043	0.037
600	0.016				
400					
200					

5% alkane

OTR max (mg/l.s)

Agitation (rpm)	Aeration (vvm) 1.5	1.25	1	0.75	0.5
1200	0.546	0.516	0.461	0.374	0.107
1000	0.537	0.537	0.504	0.478	0.302
800	0.485	0.452	0.441	0.430	0.374
600	0.163	0.000	0.000		
400	0.000				
200					

10% alkane

K_La (/s)

Agitation (rpm)	Aeration (vvm) 1.5	1.25	1	0.75	0.5
1200	0.054	0.05	0.043	0.034	0.02
1000	0.053	0.052	0.046	0.042	0.034
800	0.042	0.038	0.037	0.036	0.034
600	0.023	0.016	0.015		
400	0.012				
200					

10% alkane

OTR max (mg/l.s)

Agitation (rpm)	Aeration (vvm) 1.5	1.25	1	0.75	0.5
1200	0.659	0.610	0.525	0.415	0.244
1000	0.647	0.634	0.561	0.512	0.415
800	0.512	0.464	0.451	0.439	0.415
600	0.281	0.195	0.183		
400	0.146				
200					

15% alkane

K_La (/s)

Agitation (rpm)	Aeration (vvm) 1.5	1.25	1	0.75	0.5
1200	0.049	0.044	0.041	0.033	0.017
1000	0.047	0.042	0.043	0.04	0.027
800	0.036	0.036	0.036	0.033	0.03
600	0.012	0.015	0.02		
400	0.007				
200					

15% alkane

OTR max (mg/l.s)

Agitation (rpm)	Aeration (vvm) 1.5	1.25	1	0.75	0.5
1200	0.701	0.629	0.586	0.472	0.243
1000	0.672	0.601	0.615	0.572	0.386
800	0.515	0.515	0.515	0.472	0.429
600	0.172	0.215	0.286		
400	0.100				
200					

20%alkane

K_La (/s)

Agitation (rpm)	Aeration (vvm) 1.5	1.25	1	0.75	0.5
1200	0.042	0.041	0.035	0.02	0.015
1000	0.04	0.042	0.04	0.037	0.027
800	0.025	0.024	0.025	0.024	0.019
600	0.0145	0.011	0.01		
400	0.0073				
200					

20%alkane

OTR max (mg/l.s)

Agitation (rpm)	Aeration (vvm) 1.5	1.25	1	0.75	0.5
1200	0.689	0.672	0.574	0.328	0.246
1000	0.656	0.689	0.656	0.607	0.443
800	0.410	0.394	0.410	0.394	0.312
600	0.238	0.180	0.164		
400	0.120				
200					

Table A9: Dissolved Oxygen Data for Probe Reproducibility Tests

KLa (/s)	0.048	0.046	0.046	0.047	0.047
Time(s)	6-May-03	1-Jun-03	18-Jun-03	23-Jun-03	14-Jul-03
	C/C*				
0	0.10%	0.00%	0.10%	0.00%	0.00%
5	0.20%	0.50%	0.30%	0.00%	0.00%
10	6.20%	8.15%	6.30%	1.69%	3.20%
15	16.30%	23.66%	16.70%	14.98%	18.30%
20	34.00%	34.69%	28.90%	27.78%	31.00%
25	45.30%	44.83%	45.80%	45.83%	48.10%
30	54.90%	57.75%	55.20%	56.05%	57.60%
35	66.40%	64.91%	66.60%	67.96%	68.80%
40	72.40%	73.56%	72.60%	73.91%	74.60%
45	79.40%	78.03%	79.50%	80.75%	81.10%
50	84.60%	83.30%	83.10%	84.13%	84.40%
55	87.30%	86.08%	87.30%	88.00%	88.30%
60	90.60%	89.36%	89.50%	90.08%	90.30%
65	92.20%	91.15%	92.10%	92.56%	92.60%
70	94.10%	93.14%	93.40%	93.75%	93.90%
75	95.10%	94.73%	95.00%	95.24%	95.30%
80	96.30%	95.63%	95.80%	96.43%	96.10%
85	97.00%	96.62%	96.80%	96.92%	97.00%
90	97.70%	97.22%	97.40%	97.42%	97.50%
95	98.20%	97.91%	98.00%	98.02%	98.00%
100	98.60%	98.31%	98.30%	98.31%	98.30%
105	98.80%	98.71%	98.70%	98.61%	98.70%
110	99.10%	98.91%	98.90%	98.81%	98.90%
115	99.30%	99.20%	99.10%	99.01%	99.10%
120	99.50%	99.40%	99.30%	99.21%	99.30%
125	99.60%	99.50%	99.40%	99.31%	99.40%
130	99.70%	99.60%	99.50%	99.40%	99.50%
135		99.70%	99.60%	99.60%	99.60%
140		99.80%	99.70%	99.70%	

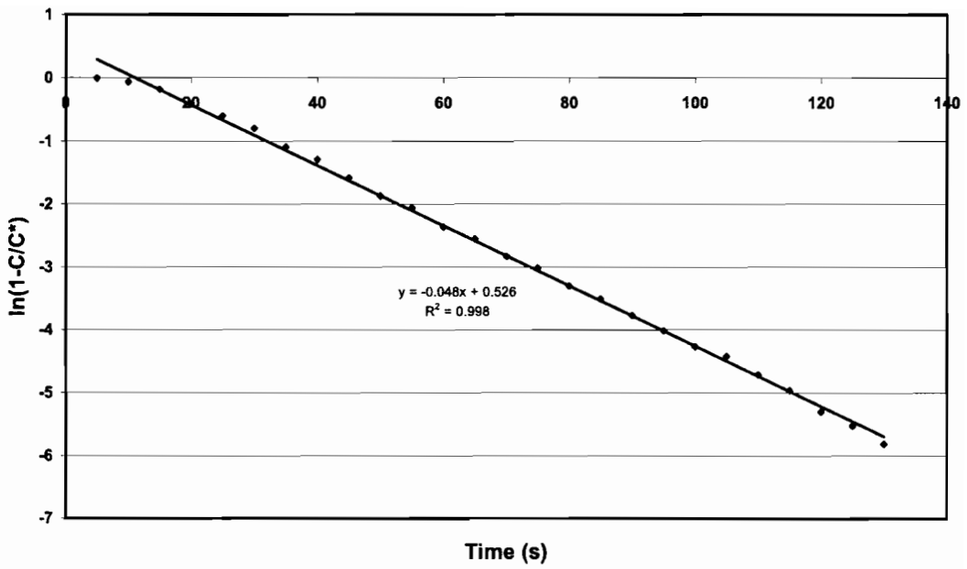

Figure A5: Sample graphical calculation of K_La for Probe 6-May-03
(K_La is given by the slope of the graph multiplied by –1, as shown in equation 4.2)

Appendix V: Statistical Analysis

R code

```
#  filename klaregfin.r
#  Created: 01/12/04 13:12:37 by williapc
#
#  $Id: R\040Script.r,v 1.1.2.2 2003/08/13 00:38:45 neum
Exp $
#

options(digits = 22)
kladata <- read.table("KLARDATA.csv",
sep=",",header=TRUE)
klastart <- c(a=1, b=1, c=1, d=1)

klamod <- nls(kLa ~ a * Aeration^b * Agitation^c * (1-
Alkane)^d, data=kladata, start=klastart,trace=F)

print(klamod)

1-deviance(klamod)/sum(kladata$kLa*kladata$kLa)
```

Output

```
> source("C:/My Documents/Mthesis/klaregfin.r")
Nonlinear regression model
  model:  kLa ~ a * Aeration^b * Agitation^c * (1 -
Alkane)^d
   data:  kladata
          a                      b
0.0000777499260395255 0.4547065089385651800
          c                      d
0.9078461875219788800 1.1026901221374035000

 residual sum-of-squares:  0.0083477419508851593
> 1-deviance(klamod)/sum(kladata$kLa*kladata$kLa)
[1] 0.9452478269046101
>
```

KLARDATA.csv

Alkane	Agitation	Aeration	kLa
0	1200	1.5	0.046
0	1000	1.5	0.046
0	800	1.5	0.043
0	600	1.5	0.035
0	400	1.5	0.018
0	200	1.5	0.007
0	1200	1.25	0.045
0	1000	1.25	0.046
0	800	1.25	0.042
0	600	1.25	0.033
0	400	1.25	0.017
0	200	1.25	0.005
0	1200	1	0.037
0	1000	1	0.043
0	800	1	0.04
0	600	1	0.03
0	400	1	0.017
0	200	1	0.004
0	1200	0.75	0.032
0	1000	0.75	0.039
0	800	0.75	0.038
0	600	0.75	0.027
0	400	0.75	0.016
0	200	0.75	0.0035
0	1200	0.5	0.022
0	1000	0.5	0.036
0	800	0.5	0.036
0	600	0.5	0.025
0	400	0.5	0.01
0	200	0.5	0.003
0.025	1200	1.5	0.051
0.025	1000	1.5	0.05
0.025	800	1.5	0.045
0.025	600	1.5	0.025
0.025	400	1.5	0.007
0.025	1200	1.25	0.047
0.025	1000	1.25	0.048
0.025	800	1.25	0.041
0.025	600	1.25	0.027
0.025	1200	1	0.042
0.025	1000	1	0.044
0.025	800	1	0.041
0.025	600	1	0.029
0.025	1200	0.75	0.028
0.025	1000	0.75	0.036
0.025	800	0.75	0.042
0.025	1200	0.5	0.014
0.025	1000	0.5	0.018
0.025	800	0.5	0.037

0.05	1200	1.5	0.054010027
0.05	1000	1.5	0.05316
0.05	800	1.5	0.048052211
0.05	600	1.5	0.016142158
0.05	400	1.5	0.00698909
0.05	1200	1.25	0.051113811
0.05	1000	1.25	0.05316
0.05	800	1.25	0.044727955
0.05	600	1.25	0.016142158
0.05	1200	1	0.045678787
0.05	1000	1	0.049934687
0.05	800	1	0.043685027
0.05	600	1	0.015054506
0.05	1200	0.75	0.036984307
0.05	1000	0.75	0.047331819
0.05	800	0.75	0.042545267
0.05	1200	0.5	0.011
0.05	1000	0.5	0.029948979
0.05	800	0.5	0.036984307
0.1	1200	1.5	0.054
0.1	1000	1.5	0.053
0.1	800	1.5	0.042
0.1	600	1.5	0.023
0.1	400	1.5	0.012
0.1	1200	1.25	0.05
0.1	1000	1.25	0.052
0.1	800	1.25	0.038
0.1	600	1.25	0.016
0.1	1200	1	0.043
0.1	1000	1	0.046
0.1	800	1	0.037
0.1	600	1	0.015
0.1	1200	0.75	0.034
0.1	1000	0.75	0.042
0.1	800	0.75	0.036
0.1	1200	0.5	0.02
0.1	1000	0.5	0.034
0.1	800	0.5	0.034
0.15	1200	1.5	0.049
0.15	1000	1.5	0.047
0.15	800	1.5	0.036
0.15	600	1.5	0.012
0.15	400	1.5	0.007
0.15	1200	1.25	0.044
0.15	1000	1.25	0.042
0.15	800	1.25	0.036
0.15	600	1.25	0.015
0.15	1200	1	0.041
0.15	1000	1	0.043
0.15	800	1	0.036
0.15	600	1	0.02

0.15	1200	0.75	0.033
0.15	1000	0.75	0.04
0.15	800	0.75	0.033
0.15	1200	0.5	0.017
0.15	1000	0.5	0.027
0.15	800	0.5	0.03
0.2	1200	1.5	0.042
0.2	1000	1.5	0.04
0.2	800	1.5	0.025
0.2	600	1.5	0.0145
0.2	400	1.5	0.0073
0.2	1200	1.25	0.041
0.2	1000	1.25	0.042
0.2	800	1.25	0.024
0.2	600	1.25	0.011
0.2	1200	1	0.035
0.2	1000	1	0.04
0.2	800	1	0.025
0.2	600	1	0.01
0.2	1200	0.75	0.02
0.2	1000	0.75	0.037
0.2	800	0.75	0.024
0.2	1200	0.5	0.015
0.2	1000	0.5	0.027
0.2	800	0.5	0.019